TECHNISCHE UNIVERSITÄT DARMSTADT

DNA breaks regulate neuronal activity: NMDA-receptor and ionizing radiation-mediated DNA double-strand breaks govern activity regulating early-response gene expression.

Vom Fachbereich Biologie
der Technischen Universität Darmstadt
zur Erlangung des Grades
Doctor rerum naturalium
genehmigte Dissertation

von
Rajvinder Kaur
geboren am 22.01.1992
in Ambala Cantt

Erstgutachter: Prof. Dr. Bodo Laube
Zweitgutachter: Prof. Dr. Alexander Löwer

Tag der Einreichung: 26.07.2021
Tag der mündlichen Prüfung: 09.09.2021

Darmstadt 2021

Kaur, Rajvinder: DNA breaks regulate neuronal activity: NMDA-receptor and ionizing radiation-mediated DNA double-strand breaks govern activity regulating early-response gene expression.
Darmstadt, Technische Universität Darmstadt,
Jahr der Veröffentlichung der Dissertation auf TUprints: 2021
URN: urn:nbn:de:tuda-tuprints-196556
Tag der mündlichen Prüfung: 09.09.2021

Ehrenwörtliche Erklärung

Ich erkläre hiermit ehrenwörtlich, dass ich die vorliegende Arbeit entsprechend den Regeln guter wissenschaftlicher Praxis selbstständig und ohne unzulässige Hilfe Dritter angefertigt habe.

Sämtliche aus fremden Quellen direkt oder indirekt übernommenen Gedanken sowie sämtliche von Anderen direkt oder indirekt übernommenen Daten, Techniken und Materialien sind als solche kenntlich gemacht. Die Arbeit wurde bisher bei keiner anderen Hochschule zu Prüfungszwecken eingereicht.

Darmstadt, den.…21.07.2021

…….

Contents

1. Summary

DNA (Deoxyribonucleic acid) double-strand breaks (DSBs) are the hazardous form of DNA damage endured on multiple occasions by both proliferating and post-mitotic cells. Unlike replicating cells, which can employ sister chromatids as a repair template, post-mitotic cells such as adult neurons could suffer lethal effects from error-prone repair of non-homologous end-joining (NHEJ) machinery. Hence, until recently, DSBs were considered only the results of pathological activity in post-mitotic cells. However, recent shreds of evidence also show the presence of neuronal activity-induced and type 2 topoisomerase beta (Top2β) generated transient physiological DSBs, which regulate the expression of multi-functional early response or immediate early genes (IEGs). Till yet, these DSBs driven gene regulations have only been studied in cortical cultures. Among many, one of the functions of effectors IEGs is the regulation of neuronal activity by activation of secondary response genes. Therefore, hypothesizing that neuronal activity induced DSB promotes certain IEGs expression and further these genes could regulate the activity, we aimed to, i) first validate the correlation of neuronal activity generated DSBs with IEGs expression in neuronal model systems other than cortical cultures ii) investigate the effects of altering DNA DSB's status on neuronal network activity.

As a model system for our analysis, we employed 14 days-in-vitro (DIV) mice hippocampal cultures (HCs), where the expression of IEGs has been reported before. As only specific neuronal activity could lead to induction of physiological DSBs, we primarily focused on the DNA breaks generated by N-Methyl-D-aspartate receptors (NMDARs) dependent cAMP (Cyclic adenosine monophosphate) response element-binding protein (CREB) activity. For our investigation, we employed a combination of Microelectrode arrays recordings (MEA) for neuronal network activity measurements, Gamma-H2AX staining to monitor DSBs' presence and messenger Ribonucleic acid (mRNA) and protein analysis for IEGs expression.

Following NMDAR activation, we detected an increase in DSBs status, which correlated with the expression of IEGs- c-Fos, Egr1 and c-Jun and upregulation in neuronal activity. Additionally, the DSBs status and IEGs expression were also analyzed following the inhibition of essential synaptic plasticity-associated components, CREB and the GluN2B subunit of the NMDAR. Our results showed that the deficiency in any of these factors leads to a decrease in certain IEGs expression, likely by causing changes in DSBs status. Further, to investigate if DSBs status alteration can affect neuronal firing activity by perturbating IEGs expression, we incubated HCs with either etoposide, a chemotherapeutic agent that generates DSBs on the site of Top2β activity, Top2β (small interfering RNA) siRNA and NHEJ inhibitor (NU7441). Our data discovered that a perturbation in either the induction and repair of the DSBs following NMDAR activation contributes to both altered IEGs expression and neuronal activity.

Furthermore, the IEGs expression was also monitored in the Severe combined

immunodeficiency (SCID) mice model. Our novel results revealed that these mice models have a low level of IEGs expression, most likely due to the inherent deficiency in the components of NHEJ. This could lead to severe learning and memory problems that these mice possess. Thus, our study provides experimental evidence on the role of synaptic NMDARs mediated DSBs in mediating IEGs expression and further how a perturbation in the DSBs induction and repair could contribute to an altered pattern of neuronal activity in HCs. Furthermore, by assessing these connective links of receptor activity with gene expression and neuronal recordings, our study validates the multi-purpose use of such an in-vitro model to elucidate changes in cellular and electrophysiological levels.

In the second part of this work, we investigated the effect of low-dose radiation exposure on IEGs expression. Ionizing radiation (IR) is an effective treatment for various tumors infested in the central nervous system (CNS). Proceeding the clinical trials, multiple literature pieces have shown how even low dose exposure could alter synaptic plasticity, a basis for cognitive functioning. However, it becomes complicated to assess the connective link between irradiation and synaptic plasticity-associated components due to IR's multi targets. Therefore, to understand how irradiation can have a lethal effect on cognitive domains, we focussed on the expression of the genes that are easily activated by various stimuli and play a role in learning and memory acquisition. For this, we studied the effect of low to moderate IR doses on the expression of IEGs in 14 DIV HCs.

Results of immunostaining against Gamma-H2AX following radiation exposure revealed that a single 2 Gy dose generates many DSBs in the post-mitotic neuron post-60-minute (min) exposure. However, the expression of IEGs such as c-Fos and Egr1 as assessed by mRNA and protein analysis following the same dose radiation exposure is downregulated. As both of these genes are the regulator of neuronal activity, we next analyzed the neuronal network activity following irradiation. Our data revealed that a single dose of 2 Gy is sufficient to cause a decrease in neuronal network activity after 60 min of exposure. NMDAR plays a vital role in IEGs expression; therefore, we investigated if NMDA incubation can counteract the radiation alleviated IEGs expression level. Consequently, we further investigated the simultaneous impact of NMDAR activation and irradiation on the control of IEGs expression by DSB's and mRNA analysis. Our results revealed that 60 min of continuous NMDA treatment counteracts radiation-induced alleviation of IEGs expression.

These findings are the first to reveal changes in IEGs expression and neuronal activity in HCs following 1-hour post- single-irradiation events. Further, it hints towards the interaction radiation has with the NMDAR pathway for the gene expression changes.

2. Zusammenfassung

DNA ("Deoxyribonucleic acid")-Doppelstrangbrüche (DSB) sind eine gefährliche Form von DNA-Schäden, die sowohl proliferierende als auch post-mitotische Zellen erleiden können. Im Gegensatz zu proliferierenden Zellen, die Schwesterchromatiden als Reparaturvorlage verwenden können, post-mitotische Zellen, wie z.B. adulte Neuronen, können durch die fehleranfällige Reparatur der "non-homologous end-joining" (NHEJ) tödliche Wirkungen erleiden. Daher wurden DSB bis vor kurzem nur als Ergebnis einer pathologischen Aktivität in postmitotischen Zellen angesehen. Jedoch deuten kürzlich veröffentlicht Studien auf einen Zusammenhang von durch neuronale Aktivität induzierte und durch Typ-2-Topoisomerase beta (Top2β) erzeugte transiente physiologische DSB, welche die Expression von multifunktionalen "early response"- oder "immediate early genes" (IEGs) regulieren. Bisher wurde diese DSB-gesteuerte Genregulation nur in kortikalen Kulturen untersucht. Eine der vielen Funktionen der IEGs ist die Regulation der neuronalen Aktivität durch die Aktivierung von Sekundärantwortgenen. Daher stellten wir die Hypothese auf, dass neuronale Aktivität induzierte DSBs die Expression bestimmter IEGs fördert und dass diese Gene die Aktivität regulieren könnten. Unser Ziel war es, i) zunächst die Korrelation von neuronaler Aktivität, die DSB erzeugt, mit der Expression von IEGs in anderen neuronalen Modellsystemen als kortikalen Kulturen zu validieren und ii) die Auswirkungen der Veränderung des DNA-DSB-Status auf die neuronale Netzwerkaktivität zu untersuchen.

Als Modellsystem für unsere Analyse verwendeten wir 14 "Days-in-vitro" (DIV) Mäuse-"hippocampal cultures" (HCs), in denen bereits über die Expression von IEGs berichtet worden war. Da nur spezifische neuronale Aktivität zur Induktion physiologischer DSBs führen kann, konzentrierten wir uns primär auf die DNA-Brüche, die durch "N-Methyl-D-Aspartate-Receptors" (NMDARs) abhängige "cAMP ("Cyclic adenosine monophosphate") response element-binding protein" (CREB) Aktivität erzeugt werden. Für unsere Untersuchung verwendeten wir eine Kombination aus "Microelectrode-Array"-Aufnahmen (MEA) zur Messung der neuronalen Netzwerkaktivität, Gamma-H2AX-Färbungen zur Überwachung des Vorhandenseins von DSB und "messanger Ribonucleic acid" (mRNA) und Protein-Analyse für die IEGs-Expression.

Nach NMDAR-Aktivierung wurde ein Anstieg des DSB-Status festgestellt, der mit der Expression von IEGs- c-Fos, Egr1 und c-Jun - und einer Hochregulierung der neuronalen Aktivität korrelierte. Zusätzlich wurde der DSB-Status und die IEGs-Expression auch nach der Hemmung von essentiellen, mit synaptischer Plastizität assoziierte Komponenten, CREB und die GluN2B-Untereinheit des NMDAR, analysiert. Unsere Ergebnisse zeigten, dass der Mangel an einem dieser Faktoren zu einer Abnahme der Expression bestimmter IEGs führt, wahrscheinlich durch Veränderungen im DSB-Status. Um weiter zu untersuchen, ob eine Veränderung des DSB-Status die neuronale Feuerungsaktivität durch eine Störung der IEGs-Expression beeinflussen kann, inkubierten wir HCs entweder mit Etoposid, einem Chemotherapeutikum, das DSBs an den Stellen Top2β-Aktivität, Top2β (small interfering RNA) siRNA und NHEJ-Inhibitor (NU7441) erzeugt. Unsere Daten entdeckten, dass eine Störung in der Induktion und Reparatur der DSB nach NMDAR-Aktivierung sowohl zu einer veränderten IEGs-

Expression als auch zu einer veränderten neuronalen Aktivität beiträgt. Darüber hinaus wurde die IEGs-Expression auch im Mäusemodell der "Severe combined immunodeficiency" (SCID) überwacht. Unsere neuen Ergebnisse zeigten, dass diese Mäusemodelle eine niedrige IEGs-Expression aufweisen, was höchstwahrscheinlich auf den inhärenten Mangel an den Komponenten von NHEJ zurückzuführen ist. Dies könnte zu schweren Lern- und Gedächtnisdefiziten führen, welche diese Mäuse haben.
Somit liefert unsere Studie experimentelle Beweise für die Rolle der durch synaptische NMDARs vermittelten DSB bei der Vermittlung der IEGs-Expression und zeigt darüber hinaus, wie eine Störung der DSB-Induktion und -Reparatur zu einem veränderten Muster der neuronalen Aktivität in HCs beitragen könnte. Indem wir diese Zusammenhänge der Rezeptoraktivität mit der Genexpression und den neuronalen Ableitungen untersuchen, validiert unsere Studie außerdem die vielseitige Verwendung eines solchen In-vitro-Modells zur Aufklärung von Veränderungen auf zellulärer und elektrophysiologischer Ebene.

Im zweiten Teil dieser Arbeit untersuchten wir die Auswirkung von Strahlenbelastung auf die Expression von IEGs. Ionisierende Strahlung (IS) ist eine wirksame Behandlung für verschiedene Tumore, die das zentrale Nervensystem (ZNS) befallen. Im Anschluss an die klinischen Studien wurde in der Literatur mehrfach gezeigt, wie selbst eine niedrige Dosis die synaptische Plastizität, eine Grundlage für kognitive Funktionen, verändern kann. Allerdings wird es aufgrund der vielen Angriffspunkte der IS kompliziert, den Zusammenhang zwischen der Bestrahlung und den Komponenten der synaptischen Plastizität zu beurteilen. Um zu verstehen, wie eine Bestrahlung eine tödliche Wirkung auf kognitive Bereiche haben kann, konzentrierten wir uns auf die Expression der Gene, die leicht durch verschiedene Reize aktiviert werden und eine Rolle beim Lernen und Gedächtniserwerb spielen. Dazu untersuchten wir den Effekt einer niedrigen bis moderaten IS-Dosis auf die Expression von IEGs in 14 DIV HCs.
Die Ergebnisse der Immunfärbung gegen Gamma-H2AX nach Strahlenexposition zeigten, dass eine einzelne 2 Gy-Dosis viele DSB post-mitotischen Neuron 60 Minuten (min) nach der Exposition erzeugt. Allerdings ist die Expression von IEGs wie c-Fos und Egr1, wie durch mRNA- und Protein-Analyse ermittelt, nach der gleichen IS Dosis herunterreguliert. Da diese beiden Gene die neuronale Aktivität regulieren, analysierten wir als nächstes die neuronale Netzwerkaktivität nach der Bestrahlung. Unsere Daten zeigten, dass eine Einzeldosis von 2 Gy ausreicht, um eine Abnahme der neuronalen Netzwerkaktivität 60 min nach der Bestrahlung zu verursachen. NMDAR spielt eine wichtige Rolle bei der IEGs-Expression; daher untersuchten wir, ob die NMDA-Inkubation dem durch die Strahlung verminderten IEGs-Expressionsniveau entgegenwirken kann. Folglich untersuchten wir weiter den gleichzeitigen Einfluss von NMDAR-Aktivierung und Bestrahlung auf die Kontrolle der IEGs-Expression durch DSB und mRNA-Analyse. Unsere Ergebnisse zeigten, dass eine 60-minütige kontinuierliche NMDA-Behandlung der strahleninduzierten Verminderung der IEGs-Expression entgegenwirkt.
Diese Ergebnisse sind die ersten, die Veränderungen in der IEGs-Expression und der neuronalen

Aktivität in HCs nach 1-stündigen einzelnen Bestrahlungsereignissen aufzeigen. Außerdem weisen sie auf die Interaktion der Strahlung mit dem NMDAR-Signalweg hin, die für die Veränderungen der Genexpression verantwortlich ist.

3. Introduction

3.1. Physiological and Programmed DNA damage

DNA is the reservoir of an organism's genetic information; therefore, it becomes essential to preserve its integrity from the various type of damages generated within the cell or by external agents. DNA (Deoxyribonucleic acid) double-strand break (DSB) is arguably the most harmful damage among many lesions incurred by DNA. Even though DSBs are rare, any improper repair of such breaks can lead to genomic instability and genetic material loss, further progressing to tumor formation. Therefore, it becomes essential for cell survival to have the error-free repair of generated DSBs. Homologous recombination (HR) is one of the most accurate mechanisms for DSBs repair. This recombination repair utilizes the existing sister chromatid as a template at the break site. Therefore, such repair is most active in the S phase, followed by brief activity in G2/M and is absent in the G1 phase [1]. Another DSB repair pathway is classical non-homologous end joining (cNHEJ). In this repair mechanism, the Ku70/Ku80 dimer binds to the two broken DNA ends, followed by end processing with DNA-dependent protein kinase (DNA-PK) catalytic subunit (DNA-PK_{cs}) and further sealing by XRCC4/Ligase IV/XLF complex of damaged ends [2]. As NHEJ does not require any template, this pathway is active throughout the cycle; however, there are also chances of mutations, minor faults, or even the loss of original DNA sequence with this error-prone repair pathway [2,3]. Nevertheless, post-mitotic cells such as neurons rely on NHEJ for their DSBs repair, where a component of the DNA-PK_{cs} complex, DNA-PK, plays an essential role. Any unrepaired or faulty DSB repair in neurons has been associated with neuropathological conditions [4].

Even though DSBs are deleterious, processes such as Meiosis, V(D)J Recombination, class switch recombination (CSR), and replication rely on programmed DNA damage and repair [5,6]. One example comes from Severe combined immunodeficiency (SCID) mice, where the absence of NHEJ protein components renders the mice immunodeficient [7]. Therefore, even though physiological breaks are also needed for various cellular functions, DSBs, especially in neurons, are mostly considered damage or lethality indicators. However, in recent years, it has been shown that neuronal activity generated physiological DSBs play a crucial role in regulating the transcription of multiple genes required for synaptic plasticity [8]. These generated programmed DSBs are rapidly induced following specific neural activity and are usually transient, as they are repaired within 2 hours of activity. Using the mice model, it has also been shown that programmed breaks could be well repaired by sleep [9]. However, if not corrected, they can lead to neurodegenerative conditions such as Alzheimer's [10]. Recent evidence also suggests that DNA DSBs are also crucial in deciding the cell fate of neural progenitor cells to promote neural diversity [11]. Therefore, programmed DSBs seem to be an essential mechanism controlling transcription in both replicating and differentiated neurons. However, it is indeed surprising that post-mitotic cells, which rely on intrinsically mutagenic NHEJ for DSBs repair, would induce programmed damage to induce certain gene transcription. Further, the evidence has only come along from the studies in cortical culture. Hence, further validation in other neuronal cell types is needed to understand if this

DSBs mediated transcription is a general mechanism in the central nervous system (CNS) following neuronal activity. Additionally, it would be interesting to understand what would be the consequence when any perturbation in physiological activity generated DSBs occurs. A schematic representation of programmed DNA damage and its repair pathway in cells during various processes is presented (Figure 1) [5].

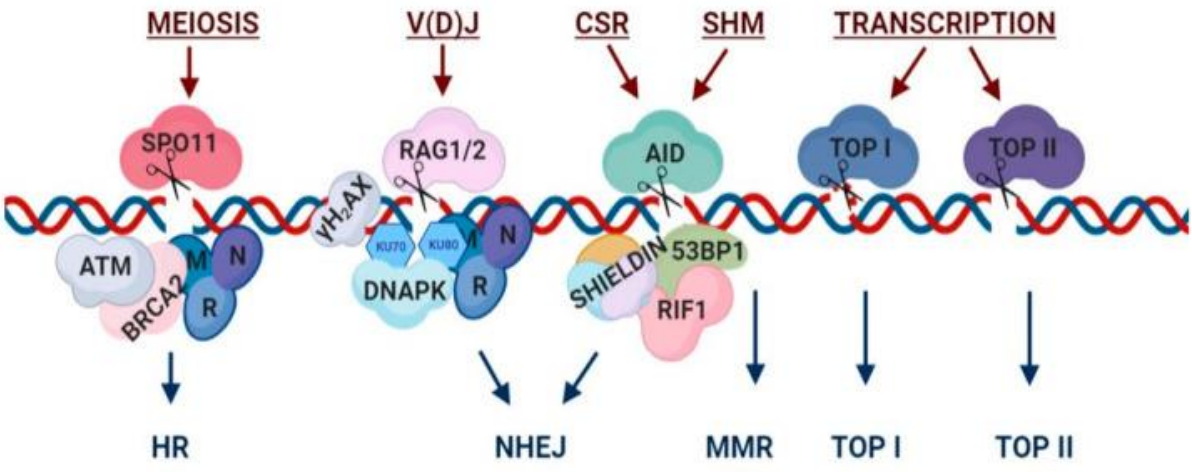

Figure 1: Representative mechanistic scheme of programmed DNA damage and its repair pathway. During meiotic recombination, SPO11 catalyzed DSBs is further repaired by recruiting HR repair factors such as Ataxia-Telangiectasia Mutated (ATM), Breast Cancer Type 2 (BRCA2) and the Mre11-Rad50-Nbs1 (MRN) complex on the sites of the damage. For V(D)J recombination, following phospho-histone H2AX (γH2AX) signaling at the site of recombination activating genes (RAG)-induced DSBs, components of NHEJ machinery- MRN complex and DNA-PK_{cs} complex factors are recruited. The process of CSR and somatic hypermutation (SHM) are initiated by Activation-Induced Cytidine Deaminase (AID). p53-binding protein 1 (53BP1), Rap1-interacting factor 1 (RIF1) and the shieldin complex, components of NHEJ, are recruited to the CSR site, and SHM breaks are repaired through mismatch repair (MMR). To relax torsional stress during transcription, topoisomerase I (TOP I) or topoisomerase II (TOP II) generates DSBs at the promoter region of various genes (adopted from Oster S, Aqeilan RI, 2020 [5]).

3.1.1. Type 2 topoisomerase beta (Top2β): A role in the generation of physiological DSBs

The physiological breaks generated by neuronal activity in the promotor region of various synaptic plasticity-associated genes are via the assistance of Top2β [8]. DNA topoisomerases are crucial enzymes needed for solving topological problems arising inside the DNA during replication, transcription and chromatin organization. To resolve supercoiled DNA structure, the type I subfamily of topoisomerases transiently cut one strand of DNA and allow another strand to pass through, leading to further reunion of the ends, whereas the member of the type II subfamily induces a breakage of both DNA strands. The activity of the type I topoisomerases is mainly required during replication and transcription elongation [12]. Top2α (Type 2 topoisomerase alpha) and Top2β are ubiquitous enzymes that belong to type II topoisomerases and share a striking 68% identity in their amino acid sequence [13]. Both Top2α and Top2β are adenosine triphosphate (ATP)-dependent homodimers that generate coordinated DSB. During the catalysis process, the DNA segment termed as 'G segment' ('G' for gate) is cleaved, and the segment of DNA that passes through the cleaved G segment is termed as 'T segment' ('T' for transported). Before the catalysis process, the ATPpase domains of the enzyme stay in a close position. The binding of the 2 ATP molecules changes conformations of the domains from open to close. During the catalysis process, in the presence of magnesium (Mg^{2+}) ions, the enzyme transiently cleaves G segment DNA by nucleophilic attack of the active tyrosine (Tyr805 and Tyr821 in human Top2α and Top2β) on the

phosphate backbone of the opposite strands. This transesterification reaction results in the formation of a 5′-phosphotyrosyl covalent bond. The scissile bonds on both strands are staggered. Further, the T segment is passed through transiently open G segments, and ATP is hydrolyzed. The release of the hydrolytic products allows the T segment to be released from the enzyme complex, and the cleaved G segment is re-united [14–16] (Figure 2a) [14].

Over the past decades, the use of human DNA topoisomerase II's as the target for cancer therapy has proven effective. Drugs targeting Top2 are classified as either Top2 poisons or catalytic inhibitors [17]. Top2 poisons, which result in the induction of DSBs, can be further sub-divided based on their DNA intercalating and non-intercalating properties. Etoposide is a widely used non-intercalating anticancer drug that leads to the stabilization of generated DSBs intermediate termed as the TOP2 cleavage complex (TOP2cc). This TOP2cc contains a covalent link between the enzyme and the 5'-terminus of the incised DNA duplex [18]. Bisdioxopiperazines belong to the class of Top2 catalytic inhibitors that block ATPase activity non-competitively and trap Top2 as a closed clamp. ICRF-193 [meso-4,4-(2,3-butanediyl)-bis(2,6-piperazinedione) is one example of bisdioxopiperazine that forms the catalytic non-cleavable complex and hence do not lead to the generation of DSBs [19] (Figure 2a) [14].

Although both Top2 have similar enzymatic properties, they exhibit differences in their expression pattern and their role in cellular processes. Such as Top2α expression has been mainly reported on replicating tissue; whereas, Top2β is ubiquitously expressed and has been detected throughout the cell cycle [13,20]. Further, the expression of Top2β has been found abundant in post-mitotic neurons, where it plays a crucial role in the transcription of various genes [8,21–23]. The study using transcriptional profiling and quantitative Polymerase Chain Reaction (qPCR) data has shown that only a few genes are affected by the knockout of Top2β in early embryonal development [23] however, defects in neural and neuromuscular development and suppression of late developmental genes with Top2β knockout are evident [24,25]. Further, knockdown of Top2β in specific brain regions has been shown to leads to abnormal cerebral cortex lamination and decreased neuron migration, further suggesting that Top2β activity is required for the transcription of particular genes [25]. It has recently been shown that specific neuronal activity leads to the generation of transient DSBs at the promoter region of synaptic plasticity-associated genes, which further helps in these genes' rapid expression [8].

Additionally, these DSBs are mediated by the Top2β activity. It is no surprise that for the immediate expression of synaptic plasticity-associated genes, Top2β activity would be required to help override the impediments. Generally, the cleavage complex formed between Top2β and DNA strands is a very short-lived intermediate because of the rapid re-ligation of the DSB. However, interestingly, in organized physiological DSBs, Top2β induces persistent DSBs and is not re-ligated by Top2β itself. Further inhibition of the repair of these physiological generated DSBs, results in constant expression [8].

Other than neuronal cells, the induction of regulatory DSBs by Top2β has also been reported in different cell lines for the expression of estrogen receptor α regulated genes and glucocorticoid receptor transcriptional activation [26–28]. Therefore, the regulated transcription mediated by Top2β further

raises two exciting questions i) what would be the consequence of the perturbation in the Top2β activity ii) what other factors contribute to Top2β induced DSBs and repair.

In the context of DSBs induction and repair by Top2β, it has been shown that in the transcription control of a subset of hormone-responsive genes, Top2β interacts with the proteins that play a role in DNA repair. On the promotor regions of insulin, estrogen and glucocorticoid-responsive genes, it has been shown that Top2β forms a complex with DNA-PK_{cs}, Ku70, and poly (ADP (adenosine diphosphate) ribose) polymerase1 (PARP-1) [29]. Further, in the transcription control of immediate early genes (IEGs) or early response genes, the number of Top2β-induced DSBs has also been shown to be increased upon inhibition of DNA-PK_{cs}, indicating how DNA repair proteins play a vital role in the regulation and repair of physiological breaks induced by Top2β activity [8]. Taken together, the coordinated induction and repair of regulatory DSBs, seems to be crucial for rapid induction of synaptic plasticity-associated genes.

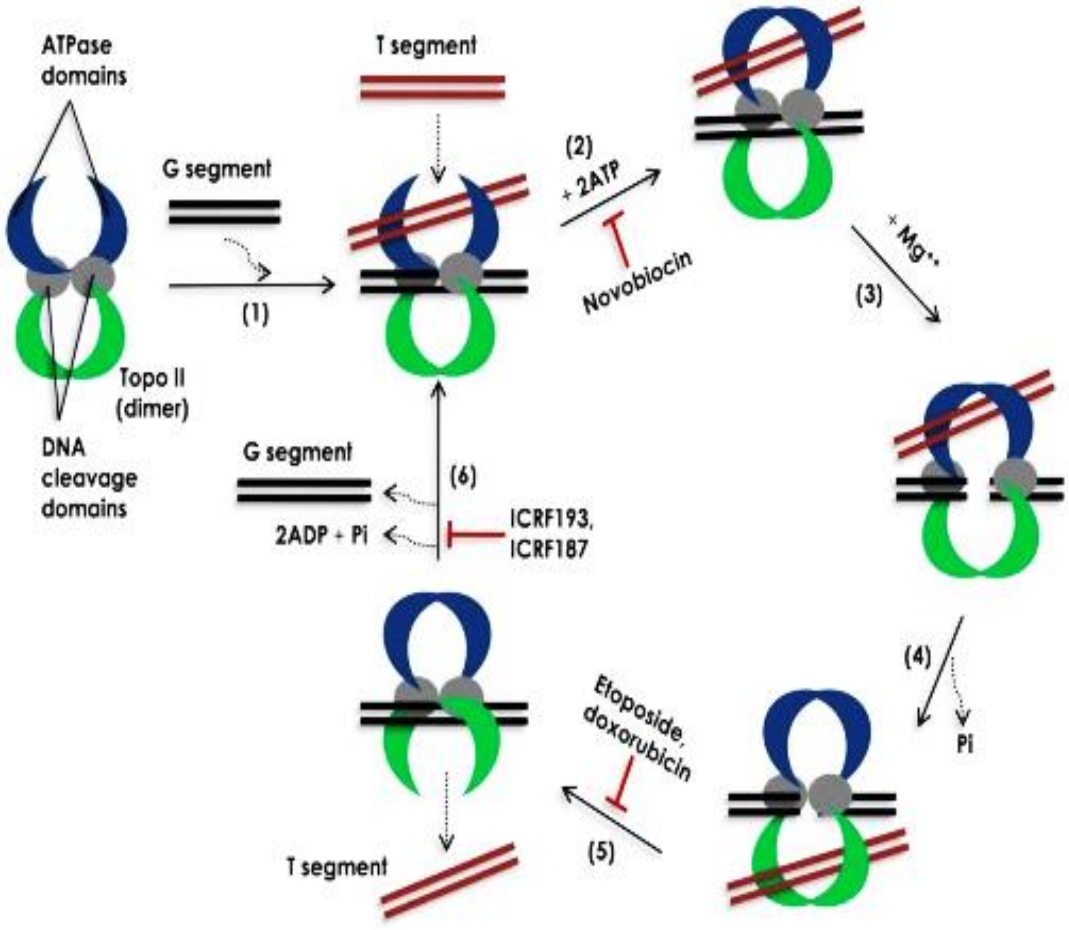

Figure 2: Top2 enzymes catalytic cycle and their activity inhibitors. The ATPase domain (shown in blue) shows the DNA-binding domain in green and the cleavage core domain represented in grey. (1) The enzyme core domain binds to the G segment; black and ATPase domain binds to T segment; red. (2) The binding of two ATP molecules to the ATPase domain leads to the change in the domain's confirmation from open to close. Novobiocin drug leads to the inhibition of ATP binding. (3) The transient G segment cleavage is Mg^{2+}-dependent and can be inhibited with the use of merbarone. (4) ATP hydrolysis is followed by the T segment's transport through the cleaved G segment. (5) The passed T segment is then released from the enzyme, and the G segment is cleaved back. G cleavage step could be inhibited by the use of etoposide and doxorubicin, which trap the enzyme with a cleaved DNA double-strand. (6) The T segment is released, and the change follows in the confirmation of the ATPase clamp from close to open by the second hydrolysis of the ATP. This enzyme gets ready for the next catalytic cycle. Inhibition of the ATPase activity of the enzyme bisdioxopiperazines such as ICRF-193 can trap the Top2 in the state of inactivity (adopted and modified from Jain C. et al. [14]).

3.1.2. NHEJ: A role in the repair of physiological DSBs

Repair of regulatory DSBs induced by Top2β activity in neurons is mainly mediated through the component of NHEJ. The c-NHEJ repair machinery is perceived to be mutagenic and error-prone. However, it has also been argued that the machinery's intrinsically mutagenic nature could be due to the flexibility and effectiveness of dealing with a broad type of DSBs [30]. Hence, NHEJ is proficient machinery for both pathological and programmed DNA DSBs repair. Such as mammalian cells lacking NHEJ are hypersensitive to etoposide-mediated DSBs [31]. Top2β induces physiological breaks are not repaired by Top2β itself and requires the attention of NHEJ, so any delay or mutation in NHEJ components can have a severe consequence on the transcription. Therefore, it becomes essential to understand the components of NHEJ.

When DSBs occur, the heterodimers of Ku70/80 bind to the two broken ends, making a scaffold to recruit other significant components of NHEJ. The Ku heterodimer directly recruits DNA-PK_{cs} to the broken ends. Upon binding, DNA-PK_{cs} get activated and phosphorylates itself and proteins like H2AX present on an adjacent nucleosome. Phosphorylation of the Ser-139 residue of the histone variant H2AX, forming γH2AX at the site of DSBs, is an early cellular response and could be visualized by appropriate staining and later counted manually. The removal of DNA-PK_{cs} is later followed by recruitment of X-ray cross-complementing protein 4 (XRCCP4), DNA Ligase IV, XRCCP4-like factor (XLF), and Aprataxin-and-PNK-like factor (APLF) to the sites of the damage, which assist in re-sealing the ends [32,33].

3.2. Synaptic plasticity associated: Immediate early genes (IEGs)/early response genes

Activity-induced neural plasticity is an essential mechanism through which the brain stores long-term memories. Neural plasticity refers to a neuron's ability to induce short and long-lasting structural changes in response to various external stimuli and cellular scenarios [34]. The expression of IEGs such as anti-cellular oncogene- c-Fos, early growth response 1 (Egr-1), proto-oncogene- c-Jun, and activity-regulated cytoskeleton (Arc) is upregulated both rapidly and selectively in certain neuronal populations of specific brain regions following various stimuli. The expression of these genes further plays an essential role in neural plasticity [35]. Recently, it has been shown that activity-induced physiological DSBs govern these genes' expression [8]. It was shown that knockdown of Top2β in cultured primary neurons inhibits the induction of specific IEGs following neuronal activity stimulation and the expression could be rescued by Cas9-generated DSBs targeted to the IEGs promoter region. Further, the involvement of NHEJ in the repair of these Top2β has also been hinted at. Hence, it becomes crucial to understand these genes' function and how their expression in basal and activity state is regulated.

The term ´Immediate-early genes´ comes from the study of viral genes transcribed rapidly when the virus integrates into the host cell. These viral genes utilize pre-existing host cell transcription factors for their expression, and their transcription occurs in the absence of de novo protein synthesis [36]. This term is also now used to describe cellular genes whose messenger Ribonucleic acid (mRNA) expression

is rapidly and transiently induced following stimulation by various extracellular signals like growth factors and neurotransmitters, such as neuronal IEGs. Considerable evidence has shown a correlation between the neuronal activity and expression of certain IEGs within a minute (min) after stimulation. This robust gene stimulation is due to already bounded RNA polymerase II (RNAPII) complex and activity-dependent transcription factors- cAMP (Cyclic adenosine monophosphate) response element-binding protein (CREB) and Serum response factor (SRF) at the promoter region of these genes even in the basal state, as well as chromatin modifications that allow active transcription to occur. However, under normal conditions, the expression of these genes is low.

As observed in the case of c-Fos expression, following neuronal activity signaling, CREB and ETS Like-1 protein (ELK1) are phosphorylated, followed parallel by recruitment of the histone acetyltransferase, CREB-binding protein (CBP) to the promotor region and then transferring of CBP and RNAPII to enhancer elements [37]. Hence, the factors needed for such gene robust transcription are already present in the basal state. Specific activity leads to rapid phosphorylation and transfer of the factors that cause mRNA of these IEGs to be transcribed within min.

Depending on the stimulus, IEGs can have either distinct or broad expression in neurons, such as following physiological activity; IEGs expression could only be found to increase in neurons' subpopulation related to that activity. In contrast, after an insult, the expression could be widely disturbed [38]. IEGs are grouped into two categories- effector and regulatory. The genes expressed directly after an initial activity stimulus are known as regulatory genes. These regulatory genes later modulate the transcription of various other gene products that directly regulate neuronal activity or synaptic plasticity [39]. One of the IEGs, c-Fos, was the first to be identified, and further, its expression was also shown to be activity-dependent. Therefore, its expression is used as an indicator of recent neuronal activity. The transcription factor codes for a 380–amino acid protein known as the Fos protein. The Fos protein structure constitutes a DNA binding region and a leucine zipper region (a leucine residue every 7 amino acids). The leucine zipper region forms an alpha helix and aligns with other proteins of the same structure to form dimers. This dimer can also bind to various DNA regions known as the activator protein 1 (AP-1) site, regulating late effector genes' expression [40,41]. Multiple studies have clearly shown an association between c-Fos expression and plasticity ([42], reviewed in [43]).

One of the primary functions of c-Fos that has recently been clearly shown is mediating neuronal excitability by regulating the expression of the kainic acid receptor Glutamate receptor 6 (GluR6) and brain-derived neurotrophic factor (BDNF) [44]. Although c-Fos carries out the transcription of various genes, it cannot regulate the transcription by itself. Following neuronal activity stimulus, the gene forms heterodimers with any of the jun family members (c-jun, junB, or junD) and creates an AP-1 complex. However, depending on the stimulus, the heterodimer's composition may vary and hence the transcription of genes downstream the cascade of effector genes [42].

Another IEG that has been proven to be rapidly regulated in both physiological and pathological conditions following activity stimulus and has been shown to be a regulator of neuronal activity and plasticity is Egr1, also known as Krox-24, Zif268, NGFI-A, and TIS8 [45,46] (reviewed in [47,48]),

owning its different names due to simultaneous identification by various groups. The Egr-1 belongs to a large group of Egr genes family that includes- EGR-1, EGR-2, EGR-3, EGR-4, EGR-alpha and the tumor suppressor, Wilms' tumor gene product (WT1). The Egr1 structure consists of a DNA binding region and three Cysteine2-Histidine2 (C2H2) zinc fingers. Further, six serum response or CC(A+T-rich) 6GG (CArG) motifs of the Egr1 sequence have been shown to be radiation-responsive [49]. Through the organization of intercellular signaling cascade, actin cytoskeleton and transcription of various downstream functioning genes, Egr1 possesses the ability to control neuronal activity in a widespread manner (reviewed in [47]).

Another recently discovered gene, Neuronal PAS domain protein 4 (Npas4), is a neuron-specific transcription factor-induced selectively by neuronal activity. This gene's role in cellular homeostasis has been well established. It has been shown to regulate the expression of many activity-dependent genes and modulate synaptic connections in response to excitatory and inhibitory signals [50,51] (reviewed in [52]). Another one of the main characterized IEG that plays a role in synaptic modulation is the Arc, also known as Arg3.1. Following activation, the mRNA of this effector gene is shifted to the dendrites, where it works to organize and maintain the new and old synapses for plasticity-related mechanisms such as long-term potentiation (LTP) and long-term depression (LTD) (reviewed in [40]).

A major problem in defining the regulation and function of these IEGs is partly due to their interconnected and complicated cascade of activation. Such as c-Fos and Npas4 have been shown to bind to each other enhancer elements, and additionally, to the same promoter region of various activity-regulated genes [53]. Even though the transcription of these IEGs seems to be complicated, their rapid activation is indeed required in response to neuronal activity. Recent evidence has pointed out that even though essential elements needed for robust transcription of these genes are present at the promoter region in the basal state, the expression of these genes following neuronal activity is restrained by the imposition of topological constraints and that the DSBs mediated by Top2β activity overpass these restraints [8]. Further, not all signals but only a specific neuronal activity could lead to the formation of these activity-induced DSBs, implying the importance of widespread increase of physiological DSBs in long-term memory formation with exploratory activity [54].

3.2.1. N-Methyl-D-aspartate-receptor (NMDAR) structure and function in synaptic plasticity

As the transcription of IEGs requires an initial stimulus, in that context, N-Methyl-D-aspartate-receptor (NMDAR) activation plays a vital role. Glutamate is the primary mediator of excitatory synaptic transmission [55]. Glutamate receptors are further divided into ligand-gated ion channels (ionotropic receptors) and G-protein coupled (metabotropic) receptors. Ionotropic receptors are also grouped based on their pharmacological properties: GluA (α-amino-3-hydroxy-5-methyl-4-isoxazole propionic acid (AMPA)), GluK (kainate), GluN (N-Methyl-D-aspartic acid (NMDA)), and GluD (δ) receptors.

Widely expressed throughout the CNS, NMDAR activation is indeed crucial for synaptic transmission. They have achieved a primary interest in the recent decades due to their role in physiological and

excitotoxicity transmission. NMDARs are heterotetrameric assemblies composed of two obligatory GluN1 subunits and varying contributions of two GluN2A-D or GluN3A-B subunits [56,57]. GluN1 assembles with either GluN2A or GluN2B subunit in the brain. GluN2A or GluN2B expression varies with development and depending on the subunit expression, different signaling pathways are activated. GluN2B has a dominant expression during early development; however, later, both GluN2A or GluN2B are expressed. It has been proposed that GluN2A expression is required for stabilization of synapse, whereas the GluN2B subunit regulates spine formation and spine retraction [58]. Further studies have hinted that the expression of GluN2B is essential for synaptic plasticity and LTP formation than GluN2A[59–61].

NMDARs are located at both pre-and post-synapse and are relatively abundant in the hippocampus and cortex. The NMDAR consists of four domains: a large extracellular amino-terminal domain (ATD), an agonist binding domain (ABD), a transmembrane domain (TMD), and an intracellular carboxyl-terminal domain (CTD). The ATD plays a crucial role in the receptor assembly, modulation, receptor activation and deactivation and could bind allosteric modulators such as GluN2B-selective antagonists- Ifenprodil (4-[2-(4-benzylpiperidin-1-yl)-1-hydroxypropyl phenol, Ro 25-6981 maleate, hence showing promising effects for certain neurodegenerative disorders [62]. The ABD domain is composed of two polypeptide sequences that form a bilobed structure with a cleft, in which the ligand can occupy the place. The TMD comprises three transmembrane helices, M1, M3, M4 segments, and an M2 reentrance loop. MK-801 (5R,10S)-(+)-5-methyl-10,11-dihydro-5H-dibenzo[a,d]cyclohepten-5,10-imine) (dizocilpine) and memantine are also promising drugs that target the TMD domain [63]. The CTD domain interacts with scaffold as well as a signaling protein such as postsynaptic density protein 95 (PSD-95), calmodulin, and neurofilament subunit NF-L. Phosphorylation of the CTD domain further regulates the trafficking and neuronal currents of NMDARs [64], (reviewed in [57,65], (Figure 3a) [57]).

The activation of NMDARs is significantly slower than AMPA receptors (AMPARs) and kainate receptors. This slow activation is due to the tight binding of Mg^{2+} to the channel pore, which does not allow any ion permeation [66]. AMPAR activation induces sodium influx through the channels, which overrides the voltage-dependent Mg^{2+} blockade of NMDA receptors. Following the glycine (Gly) binding or D-ser to the GluN1 subunit and Glutamate to GluN2 subunits, Ca^{2+} is influx through the pore [67]. In the case of NMDAR, the agonist molecule NMDA binds selectively to the channel. The increased concentration of Ca^{2+} concentration intracellularly acts as a second messenger signal for the further activation of various signaling cascades that later leads to the expression of the genes such as IEGs that play a role in the physiological adaptions of neurons. One of the critical targets of Ca^{2+} influx following NMDAR activation in the neurons is the transcription factor CREB. CREB activation is further involved in the regulation of IEGs, hence playing a significant role in behavioral adaptions in response to environmental cues [68].

However, Ca^{2+} entry mediated by NMDAR activity could also lead to excitotoxicity effects. This excitotoxic effect could be due to the overactivation of synaptic NMDARs or the aberrant signaling by the activation of extrasynaptic NMDARs. Extrasynaptic NMDARs can be defined as the ones situated

far from the PSD and are also farther away from the location of synaptic glutamate release. Although most NMDARs are synaptic located, a substantial number is located at extrasynaptic sites in the developed brain [69,70]. The first model proposed for NMDARs mediated toxicity showed that synaptic NMDARs are neuroprotective, whereas extrasynaptic promote apoptosis by triggering mitochondrial dysfunction [71] (Figure 3b) [72]. According to this model, not the Ca^{2+} overload but the flow of Ca^{2+} either through synaptic or extrasynaptic decide the cell fate. However, another model demonstrated that the extrasynaptic NMDARs activation and the bi-directional activation of synaptic NMDAR regulate cell fate. The model shows that low-dose NMDA (15 and 20 μM) activates synaptic receptors, which leads to pro-survival signaling. Conversely, higher doses lead to progressive activation of extrasynaptic and synaptic NMDARs, which trigger cell death. Therefore, according to this model, excitotoxicity depends on the magnitude and duration of synaptic and extrasynaptic NMDARs activation [73]. Taken together, for the activation of the pro-survival signaling pathway, it becomes imperative to monitor the NMDA concentration in the culture.

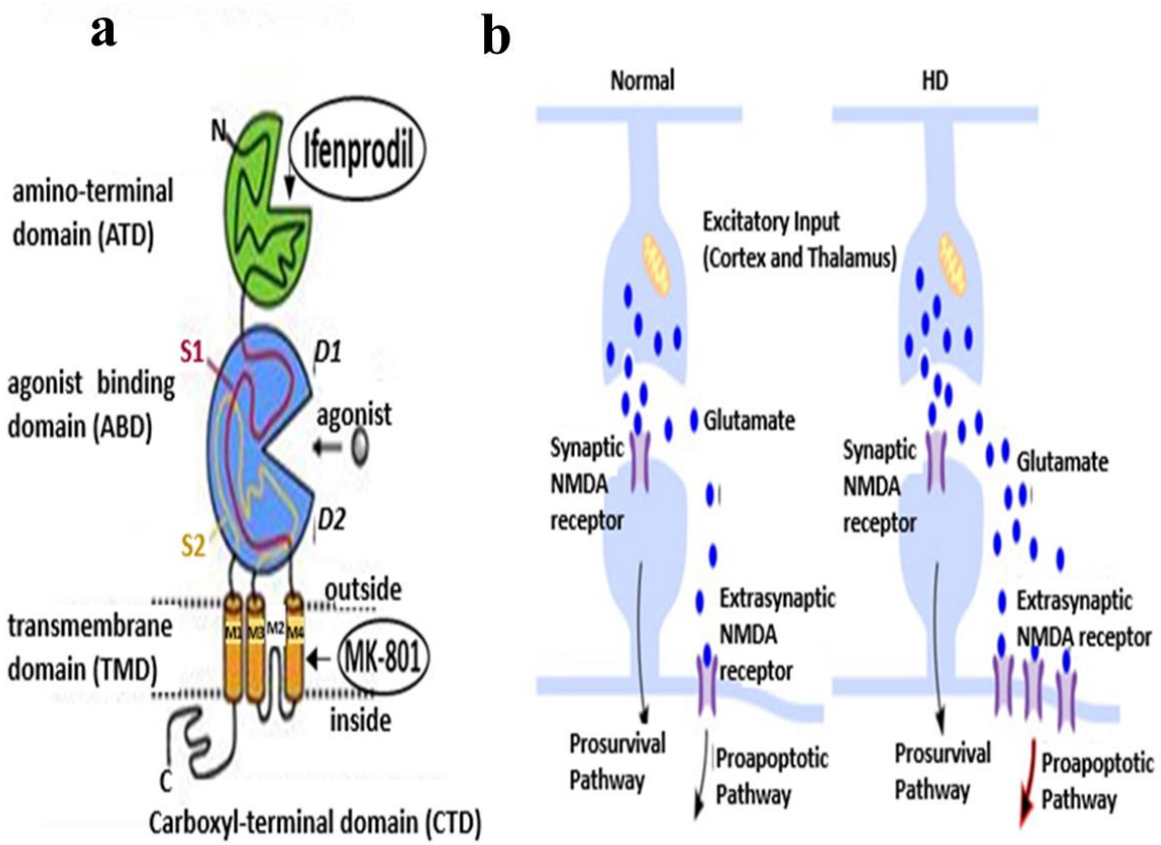

Figure 3: Structure and location of NMDARs. (a) NMDARs subunit comprises four major domains: The extracellular amino-terminal domain (green), where allosteric modulator of GluN2B subunit such as Ifenprodil can bind, leading to aberrant NMDAR activity. The agonist binding domain (blue) is formed by S1 and S2 polypeptide segments that further folds into upper-D1 and lower lobe-D2 structures. The agonist binds to the cleft, located between the lobes. The transmembrane domain (orange) consists of three transmembrane helices (M1, M2, and M4) and a membrane reentrance loop (M2). MK-801 sits in the channel pore formed by these helices. The intracellular CTD interacts with scaffold and signaling proteins (Modified figure from Hansen et al.[57]). (b) Activation of synaptic NMDARs leads to the pro-survival pathway. In contrast, extrasynaptic NMDARs activation, either due to high glutamate concentration or the increase in the number of extrasynaptic NMDARs, could further lead to proapoptotic signaling, a contributing factor to Huntington disease (HD) (adopted from Levine et al. [72]).

3.2.2. Key molecules connecting NMDARs with IEGs expression

To understand how NMDAR activation robustly mediates IEGs expression, it is imperative to understand the critical signaling molecules or components that play a role in connecting receptor activation with synaptic plasticity-associated gene expression.

In brief, the release of presynaptic glutamate or treatment with the NMDA activates the postsynaptic NMDARs, leading to the Ca^{2+} influx. The Ca^{2+} influx contributes to the rearrangement of scaffolding proteins and acts as an essential intracellular second messenger, reviewed in [67]. Once inside the postsynaptic neuron's nucleus, Ca^{2+} can bind to the calmodulin to activate the calmodulin-dependent protein kinase II (CaMK II) and protein kinases A (PKA) and C (PKC), which further leads to the activation of mitogen-activated protein kinase (MAPK). The MAPK is transported to the nucleus, where it activates and phosphorylates CREB at ser 133 positions. CREB is one of the essential transcription factors activating downstream signaling pathways, reviewed in [74,75].

CaMK II and PSD-95 are the components of the postsynaptic density. PSD-95, located at the cytoplasmic membrane, is a critical scaffold protein that directly interacts with the GluN2A and GluN2B subunits of NMDARs and plays an essential role in neuron maturation and synapse development [76]. The CaMKII autophosphorylation at the Thr286 position by binding of Ca^{2+} to the calmodulin complex is also an essential mediator of synaptic plasticity [77]. For the LTP induction, activated CaMK II binds to proteins such as PSD-95, α-actinin, synaptic adhesion molecule densin-180. Further, it also plays a role in activating microtubule-associated protein 2 (MAP-2) and NF-L, essential for structural plasticity [78] (reviewed in [75]).

PKA influences synaptic plasticity by phosphorylation of different substrates such as GluR1 of AMPAR [79], reviewed in [75]. Phosphorylation of any four subtypes of MAPK: extracellular signal-regulated protein kinase (ERK), p38 MAPK, c-jun N-terminal kinase (JNK) and ERK5 leads to the activation of many downstream target genes and proteins. Localized in the nucleus, phosphorylation of transcription factor CREB following Ca^{2+} influx is a vital regulator of neuronal network activity.

CREB plays a significant role in the activation of IEGs as when the phosphorylation of CREB is inhibited, so does IEG expression and protein synthesis (Figure 4a)[75]. Hence, the molecular components involved in the NMDAR mediated IEGs expression includes: PSD-95, CaMK II, PKA, MAPK, and CREB. Any perturbation in these components' expression or activation can alter IEGs expression, severely affecting LTP formation and synaptic plasticity.

Taken together, IEGs expression is topologically constraints by the presence of various factors such as CREB at the promoter region, and when signaling comes from a specific neuronal activity and robust transcription is needed, these constraints are resolved by induction of Top2β mediate DSBs, which further requires the help of NHEJ for their repair (Figure 4b)[8].

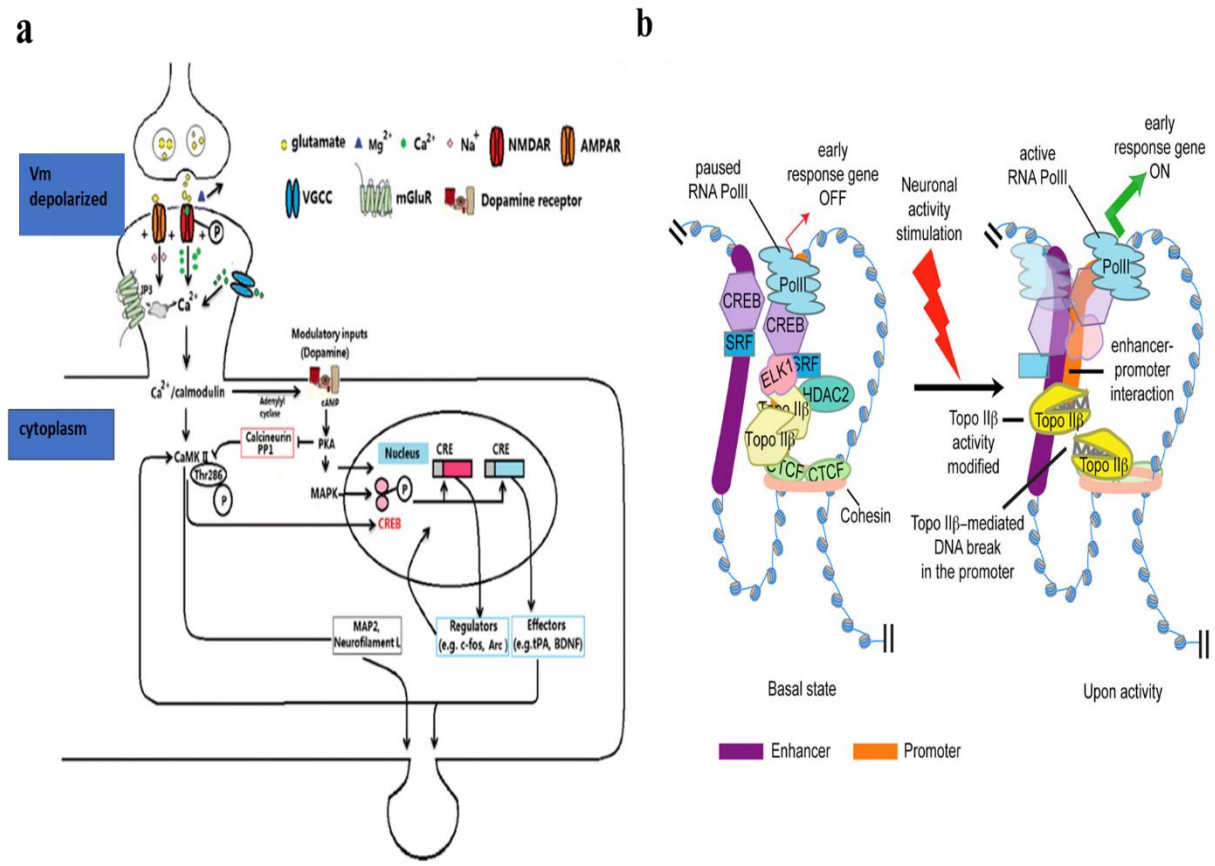

Figure 4: NMDAR signaling initiated Top2β mediated DSBs govern IEGs expression. (a) Release of presynaptic glutamate triggers activation of postsynaptically located NMDA and AMPARs. AMPAR activation causes the removal of Mg^{2+} from the NMDAR channel pore and the influx of Ca^{2+} ions. Once intracellularly, the Ca^{2+} further binds to calmodulin, which, with Adenylyl cyclase's help, leads to the activation of calmodulin-dependent PKA and PKC basis for the activation of MAPK. PKA activation counteracts protein phosphatase 1 (PP1), which leads to the phosphorylation and activation of CaMKII, which plays a role in structural plasticity by regulating MAP2 and neurofilament L. The MAPK and CaMKII further activate CREB located in the nucleus, where it regulates the expression of regulator and effector IEGs (Figure adopted from Wang and Peng, 2016 [75]). (b) In the basal state, CREB and SRF are bound to both the promoter and enhancer regions of IEGs. Further, ELKI and DNA-dependent RNA polymerase II (RNA PolII) are also attached to the IEGs promotor site. The transcriptional repressor CTCF, cohesion and histone deacetylase 2 (HDAC) are also located near the Top2β site, at the region of the transcription start site. These factors together keep IEGs in an inactive state. Following the neuronal activity such as NMDAR signaling, HDAC2 is released by activated calcineurin activity, and Top2β activity induces a DSB into the IEGs promoter region, relieving the topological constraints and enabling enhancer-promoter interaction, which allows the paused PolII to start gene transcription (Adopted from Madabhushi et al.[8]).

3.3. Ionizing radiation and its impact on cognitive function

Radiation is defined as energy that originates from the source and travels through the material in space. It has electric and magnetic fields associated, and it also possesses wave-like properties; hence, radiation is also termed electromagnetic waves.

Radiation is classified into two groups: Ionizing and non-ionizing. Both forms of radiation interact with the matter; however, unlike ionizing radiation (IR), non-IR does not remove electrons from the matter. Hence, it does not lead to the atom's ionization. IR possesses sufficient energy to remove electrons that are tightly bounded from the atom. IR is further categorized into the group of electromagnetic or particulate energy. The alpha and beta particles fall into the latter group. This IR group does not possess high penetrating power; hence the risk associated with their exposure is low, but they can still lead to adverse health effects when injected or inhaled in high quantities.

The X-rays and γ-rays fall into the first group. This type of IR can penetrate human tissue, and therefore, since its discovery, it has gained wide popularity in the diagnostics and therapeutics field of medicine [80–82]. However, exposure to IR can also lead to severe damage to organs. Previously, only high dose radiation exposure was associated with adverse health effects, however, gained popularity of radiotherapy, as well as the increase in the number of studies dealing with investigating the impact of acute and moderate IR exposure on patients, have also shown that low dose exposure, in the long run, can also induce changes in cellular activity [83,84], reviewed in [85].

The damage associated with high-dose IR exposure is mainly due to either direct nuclear damage or increased oxidative stress. Following irradiation, water molecules' radiolysis occurs that leads to the increased formation of reactive oxygen species (ROS), which further can lead to DSBs formation and, ultimately, cell death [86] (Figure 5) [87]. Even though the studies related to evaluating detrimental effects of low-dose IR are on the rise, it is still unknown how the low-dose IR could cause alteration in a cellular system. One such example comes from the effect of low-dose IR on cognitive function. Various epidemiological studies followed by primary research have hinted that low-dose IR exposure can induce cognitive defects [88,89]. However, the mechanism of such defects is still not clear and probably involves various gene and signaling pathway alterations [90].

However, as the low to moderate IR dose is widely used to treat multiple CNS tumors, it becomes imperative to examine the association that low dose IR has with cognitive function and synaptic plasticity-associated components. As the effect of low-dose IR can be complicated and can be altered based on the exposed dose, the time following irradiation when cells are analyzed, it also becomes essential to focus on a specific pathway or genes expression, which is regulated within a short time and could be activated with multiple stimuli.

3.3.1. Ionizing radiation and IEGs expression

IEGs are induced rapidly and transiently in response to various stimuli and environmental scenarios and are essential for synaptic plasticity and cognitive functions [37]. Recent evidence has also shown that induction of DSBs in the promotor region of certain IEGs, leads to their robust transcription [8]. Therefore, it is highly likely that alteration of IEGs transcription plays a vital role in the radiation-induced cognitive defects. However, it is complex to define the changes in specific IEGs expression after irradiation, as their mRNA and protein expression levels are dependent on the tissue analyzed, the time after which the expression is monitored and irradiation dose. Regardless of the complex and variable expression, various studies have reported increased IEGs expressions of c-Fos, c-Jun, c-Myc and others with either high (5-50 Gy) or low dose IR exposure (less than or 2 Gy) in their specific cell lines [91–94]. Therefore, it seems that one of the effects of IR interaction in the cell is the upregulation of particular IEGs expression. This upregulation could be a part due to the presence of the specific region at these gene promotor sites that respond to radiation exposure, such as inducibility of the Egr1 gene with IR is conferred by an area containing six serum responses or CC(A+T-rich)6GG (CArG) motifs [49]. Further, a model proposed by Weichselbaum et al. [95] suggests that products of these IEGs further regulate downstream genes that play a role in cell and tissue adaptation to radiation-induced stress.

Although various studies have shown the direct effect of different radiation doses on IEGs expression in additional tissue [96,97], only very few gene analysis reviews have been carried out in the neuronal cultures or the brain tissue. The results from Usenius et al. [98] were the first ones that detected an alteration in IEGs expression, c-Fos, Egr1 and c-Jun in scattered neuronal populations by In-situ hybridization histochemistry and immunocytochemistry with low dose irradiation exposure. However, the recent publications by Kempf et al. [99,100], with proteome/mRNA expression analysis and miRNA-quantification, have shed broad light on the effect of the low dose IR on the alteration of synaptic plasticity associated components. Further studies performed on the hippocampal section of mice brains have reported decreased c-Fos and Arc expression day or weeks after irradiation [101,102]. Hence, there seems to be an inverse correlation between irradiation exposure and IEGs expression in the brain than other tissues, a likely explanation for cognitive function deficits. However, most of these studies have been carried out days or months after irradiation exposure, and IEGs expression is rapid and transient. Various factors could influence the expression leading to altered levels depending on the monitored time. Therefore, to precisely study how low dose exposure can alter these synaptic plasticity's-related genes' expression in a short time, it becomes imperative to examine the immediate effects of low dose IR on IEGs expressions in the model system consisting mainly of neurons post-single-dose exposure. Additionally, as certain IEGs regulate the expression of proteins involved in regulating neuronal excitability [44,47,103], it is likely, that an alteration in IEGs expression could be translated to changes in neuronal activity. Further, to prevent radiotherapy's detrimental side effects, it becomes essential to elucidate the impact and interaction of low and moderate radiation doses with the receptors and components of molecular signaling pathways such as NMDAR.

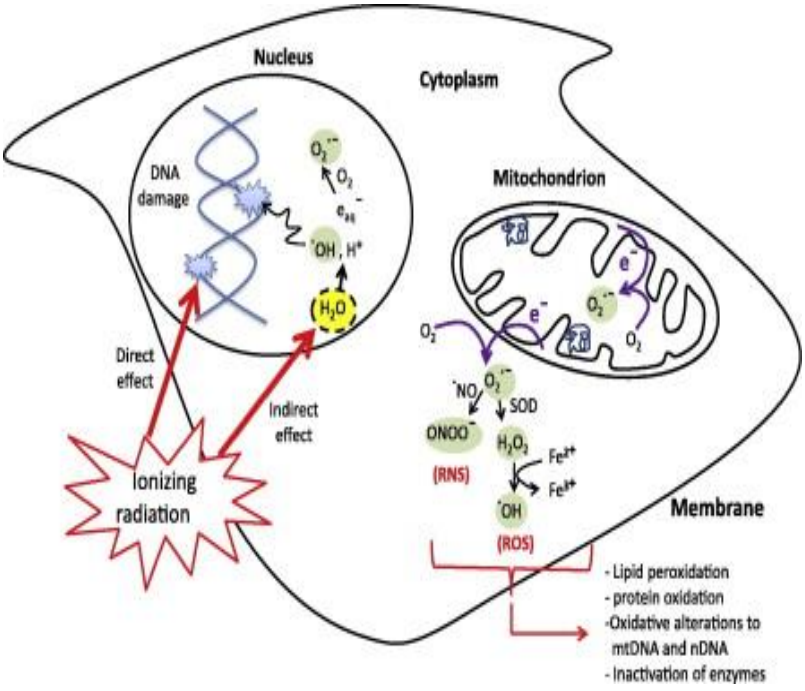

Figure 5: The direct and indirect effect of IR in the cell. IR can lead to DNA damage such as single or DNA DSBs through direct interaction with DNA or radiolysis of cellular water. Radiolysis leads to the generation of reactive chemical species by oxidases and nitric stimulation. Further, IR can also interact with normal mitochondrial function and leads to the generation of reactive oxygen, as well as reactive nitrogen species (RNS), which contributes to persistent alterations in lipids, proteins, nuclear DNA (nDNA) and mitochondrial DNA (mtDNA) (Figure adopted from Azzam et al. [87]

3.4. Aim of the study

NMDAR-mediated Ca^{2+} transients regulate the expression of IEGs in neurons which are essential for neural plasticity. In this regard, the CREB phosphorylation and activation following receptor activation plays a significant role. Further, the expression of the GLuN2B subunit of NMDAR is also crucial for LTP induction and maintenance. IEGs play a role in neural plasticity by regulating neuronal excitability, as the expression of certain IEGs is known to be one of the master mediators of neuronal activity. Although various factors needed for the rapid transcription of these genes are already bounded at the promotor as well as the enhancer site, recent evidence has also shown the role of activity-induced DNA DSBs mediated by the Top2β and NHEJ activity in the robust regulation of certain IEGs using cortical culture as a model system. Hence, the recently identified presence of programmed DSBs at the promotor site of these genes raises three interesting questions: i) is the process of activity-induced DSBs for IEGs expression also observed in another neuronal model system? ii) what role CREB and GLuN2B subunit of NMDAR have on the DSBs status and consequently on IEGs expression? iii) what effects a perturbation in the status of DNA DSBs could have on neuronal activity? Even though it is well-known that NMDAR activation is linked to IEGs expression, the investigation of the above-stated, three put-forward questions will provide a better understanding of how the receptor activity components by modulation of DSBs status regulates neuronal activity in both physiological and pathological conditions. In this aspect, a parallel investigation of DSBs/IEGs expression status followed by detecting neuronal firing rate in mice hippocampal cultures (HCs) following NMDAR activation or the incubation with agents that perturbates DSBs formation could serve as an essential tool.

While for many brain tumors, radiotherapy remains an effective treatment, exposure to even a low dose of IR has been shown to be associated with cognitive function deficits. Therefore, it raises an interesting question on the interaction IR has with components of synaptic plasticity. IEGs are induced rapidly and transiently in response to various stimuli such as NMDAR activation; further, they play a role in neural plasticity and cognitive functions. Hence, alteration in IEGs expression likely plays a vital role in radiation-induced cognitive deficits. A few existing studies have shown that IR decreases certain IEGs expression in mice brains, day or weeks after exposure. However, as IEGs activation is robust, various factors could alter expression levels depending on the monitored time. Thus, this study aims to analyze the immediate exposure effects of a single low to a moderate IR dose on the IEGs expression in a model system, where neurons are abundant. As the hippocampus is a highly radiation-sensitive brain region associated with learning and memory consolidation. Therefore, by using HCs as in vitro model system and the staining against the H2A histone variant's phosphorylated form, γ-H2AX as a marker for DSBs presence (Löbrich et al. [104], this study aimed to i) analyze the expression of c-Fos, Egr1 and c-Jun in HCs after 14 days in vitro (DIV) with 0.5 and 2 Gy dose exposure ii) examine the alteration in neuronal network activity 60 min post-radiation exposure iii) observe the combined effect of NMDA and different radiation doses on DNA DSBs count as well as on IEGs expression.

4. Material and Methods

4.1. Antibodies

Table 1: Primary antibodies

Antibody	Host	Method	Dilution	Clone number, Manufacturer
Anti-c-Fos	Rabbit	Western Blot	1:2000	PA1318, BosterBio (Pleasanton, U.S.A)
Anti-Glyceraldehyde 3-phosphate dehydrogenase (GAPDH)	Rabbit	Western Blot	1:2000	FL-335, Santa Cruz (Dallas, U.S.A)
Anti-γH2AX (Ser139), clone JBW301	Mouse	Immunostaining	1:1000	05-636, Merck (Darmstadt, Germany)
Anti-MAP2	Mouse	Immunostaining	1:500	ab11267, Abcam (Cambridge, UK)
Anti-neuronal nuclei (NeuN), clone A60	Rabbit	Immunostaining	1:300	ab177487, Abcam
Anti-GluN2B	Rabbit	Immunostaining	1:250	ab65783, Abcam
Anti-GluN1	Mouse	Immunostaining	1:250	05-432, Merck

Table 2: Secondary antibodies

Antibody	Method	Dilution	Manufacturer
Goat anti-rabbit-horseradish peroxidase (HRP)	Western Blot	1:10000	Chemicon (part of Merck, Darmstadt)
Goat anti-rabbit Alexa 488	Immunostaining	1:400	Abcam
Goat anti-mouse Alexa 594	Immunostaining	1:400	Abcam

4.2. Agonists and inhibitors

Table 3: Agonists and inhibitors

Agonist/Inhibitor	Final Concentration	Manufacturer
Etoposide	5 µM	Merck
Gly	2 µM	Carl Roth GmBH (Karlsruhe,Germany)
ICRF-193	10 µM	Santa Cruz
KG-501 (2-naphthol-AS-E-phosphate)	20 µM	Merck
Ro 25-6981 maleate	10 µM	Tocris Bioscience (Bristol, U.K.)
(+)-MK801 maleate (Dizocilpine)	20 µM	Tocris Bioscience
Ifenprodil hemitartrate	20 µM	Tocris Bioscience
NU7441 (8-(4-Dibenzothienyl)-2-(4-morpholinyl)-4H-1-benzopyran-4-one)	10 µM	Tocris Bioscience
NMDA	15 µM	Tocris Bioscience

4.3. Solution

Table 4: For Western blotting

Type of buffer	Reagents
TBS (Tris (Tris(hydroxymethyl)aminomethane) buffer saline)-T	50 mM Tris, 150 mM NaCl, 0.1% Tween20

Blocking buffer	5% milk in TBS-T with 0.1% Tween-20
Sodium dodecyl sulfate (SDS)-PAGE running-buffer	25 mM Tris, 192 mM gly, 0.1% SDS
4x Loading buffer	240 mM Tris/HCL (pH6.8), 40% glycerol, 8% SDS, 50 µM dithiothreitol (DTT), 0.04% bromophenol blue
Antibody buffer	1% milk in TBS-T with 0.1% Tween-20
RIPA (Radioimmunoprecipitation assay) Lysis buffer	25 mM Tris/HCl, pH 7.4, 140 mM NaCl, 1 mM Ethylenediaminetetraacetic acid (EDTA), 0.5 mM Ethylene glycol-bis (β-aminoethyl ether)-N, N, N′, N′-tetra acetic acid (EGTA), 2 mM Na-Fluoride (Na-F), 1 mM Sodium orthovanadate (Na_3VO_4), 1% v/v Triton X-100, 0.1%w/v Na-deoxycholate, 0.1% w/v SDS
10% SDS-gel	33% v/v Rotiphorese (37.5:1), 250 mM Tris-HCl (pH 8.8), 0.01% w/v SDS, 0.01% w/v Ammonium persulfate,0.001% v/v Tetramethyl ethylenediamine

Table 5: For Immunofluorescent staining

Type of buffer	Reagents
Phosphate-buffered saline (PBS)	137 mM NaCl, 2.7 mM KCl, 10 mM Na_2HPO_4, 1.8 mM KH_2PO_4
Blocking buffer	5% goat serum (GS) in 1X PBS
Antibody Buffer	5% GS in 1X PBS for primary antibody 2% GS in 1X PBS for secondary antibody

4.4. Primer's sequence and the publications where they are mentioned

Table 6: Primer Sequence

Gene	Sequence	Publications
c-Fos	Forward: 5' GAT GTT CTC GGG TTT CAA CG 3' Reverse: 5' GGA GAA GGA GTC GGC TGG 3'	Corbett et al., 2017 [105]
Egr1	Forward: 5' TCC TCT CCA TCA CAT GCC TG 3' Reverse: 5' CAC TCT GAC ACA TGC TCC AG 3'	Hendrickx et al., 2013 [106], Opsomer et al., 2020 [107]
Gapdh	Forward: 5' ACC CAG AAG ACT GTG GAT GG 3' Reverse: 5' ACA CAT TGG GGG TAG GAA CA 3'	Opsomer et al., 2020 [107]
c-Jun	Forward: 5' TGA AAG CTG TGT CCC CTG TC 3' Reverse: 5' ATC ACA GCA CAT GCC ACT TC 3'	Hendrickx et al., 2014 [106]
Npas4	Forward: 5'AGC ATT CCA GGC TCA TCT GAA 3′ Reverse: 5'GGC GAA GTA AGT CTT GGT AGG ATT 3′	Choy et al., 2016 [108]
Top2β	Forward: 5′ACC AGT ACC GCT AAA GAA GCA 3′ Reverse: 5′GCT GTC TCC GAT CCT CCA TAA A 3′	Primer Bank

4.5. Accell SMART pool small interfering RNA (siRNA) sequences

Table 7: siRNA sequences

siRNA	Sequences
Top2β SMARTpool siRNA (a pool of four siRNA oligos)	CGAGUAAUUAUGACGAUGA, GCAGAAUCUACAAAGCUUA, CGGUUAAGUUAUUAUGGUU, GUAGUAGAUCAAGUUGUUA
Non-targeting Control Pool (negative control pool of four siRNAs)	UGGUUUACAUGUCGACUAA, UGGUUUACAUGUUUUCUGA, UGGUUUACAUGUUUUCCUA, UGGUUUACAUGUUGUGUGA.

4.6. Primary culture of mice hippocampal neurons and treatments

4.6.1. Removal of the brain and hippocamp dissection

Primary cultures of wild type (WT)-C57Bl/6j and SCID-C57BL/6j.SCID mice hippocampal neurons were established using postnatal (P0-P1) mice of either sex. SCID mice were obtained from Jackson Laboratory (Maine, USA) and kept in a pathogen-free, well-controlled environment. Both mice's breeds were maintained in optimized room conditions-12 light/12 dark cycles, 23°C temperature with 60 % humidity. Routine monitoring was performed, and animals were provided with standard food and water ad libitum. Mouse pups were euthanized by decapitation with large scissors. Before the isolation procedure, the dissection tools (11254-20, Dumont 5 forceps, 14060-09, Iris Scissors, 10316-14, Ultra micro knife - 22.5 angles- all bought from Fine Science Tools, Heidelberg, Germany) were first sterilized with 80% ethanol and then were kept on a bench in the flask containing 80% ethanol until use. Before using them for hippocampi removal, all the tools were washed with distilled water. The bench where all the dissection procedure was performed was also wiped with Biocidal ZF (WAK-ZF-1, Tanus, Germany) and 80% ethanol. For hippocampi isolation, the heads of sacrificed mice were collected and rinsed two times in ice-cold PBS, pH 7.4. Then, the heads were transferred under the microscope to a new 60 mm dish containing ice-cold Hank's buffered saline solution (HBSS, Thermo Scientific, Massachusetts, USA), which was supplemented with the standard 1% v/v Penicillin-Streptomycin (Pen-strep) (Sigma-Aldrich, Missouri, USA) mixture. Two small incisions were made in the mouse eye's direction to keep the head in a firm and stable position. Holding the head's frontal side with forceps, a horizontal cut from the posterior to the frontal side was made to remove the skin and further the skull. The isolated brain was later transferred to a new 60 mm dish kept on ice and contained HBSS. The same procedure was repeated for all pups before moving to the steps of hippocampi dissection. For the removal of hippocampi, the two hemispheres were separated carefully using an Ultra micro knife. From the separated hemisphere, the cortex was rolled out to make the hippocampus seen clearly. First, the meninges were removed from the hemispheres, and later a small cut along the hippocampus's side was made to isolate the tissue gently. The same procedure was reported for the removal of the hippocampus from another hemisphere. For enzymatical dissociation, the isolated hippocampi were transferred to the pre-warmed Falcon tube containing 2 ml of Trypsin-EDTA (500 BAEE units' porcine trypsin and 180 µg EDTA) and DNAse (0.1%) (Sigma-Aldrich) in the water bath for 20 min at 37°C. The falcon tube was inverted every 5 min. The trypsinization was followed later by mechanical trituration under laminar culture hood with 1,000 µL filtered tip (8 up and down) in neutralization media- neurobasal with 10% Fetal bovine serum (FBS). The triturated mixture containing dispersed cells was kept for 10 min under the hood, followed later by brief centrifugation at 130xg for 5 min at room temperature. The obtained cell pellet was suspended in neurobasal media containing 1% B-27 Plus (Thermo Scientific), 2 mM GlutaMAX (Thermo Scientific) and 1% v/v Pen-Strep. The cell suspensions were counted with trypan blue exclusion.

4.6.2. Cell plating

The coverslips were first treated with 1M HCl, followed by heating at 50–60°C for 8 h with gentle agitation. Next, the coverslips were washed multiple times with distilled water. The washed coverslips were later rinsed and stored in 100% ethanol before use. On the day of the coating, coverslips were again cleaned with distilled water and dried before overnight treatment with 250 µL Poly-D-lysine (Sigma-Aldrich) (1 mg/ml in Borate buffer) at 4°C per coverslip, and Laminin (Thermo Scientific) (0.5 mg/ml in PBS) for 2 hours at 37°C in 24-well plate format. Cells were plated at a density of 90,000 cells/1.9 cm^2 in Poly-D-lysine and Laminin-coated plates.

The cell culture was maintained for 14 DIV in a 95% air and 5% CO2 atmosphere at 37°C. To prevent the growth and division of non-neuronal cell types and ensure the purity of the neuronal cultures, 1 µmol/L of 5-fluorouracil (FU) and Uridine was added to the media day after cell plating. New cell media was replenished three days later, followed by the change in half of the media every 3-4 days.

4.6.3. Culture treatments

To access the differences in NMDA and mock-treated cells regarding IEGs expression, DSBs number and firing activity, a concentration of 15 µM NMDA and 2 µM gly was applied on 14 DIV cultures to activate NMDARs. Further, to block CREB signaling, GluN2B subunit activity, or the whole NMDAR activity, cultures were pre-incubated for an hour, either with 20 µM of KG-501 dissolved in dimethyl sulfoxide (DMSO), 20 µM of Ifenprodil, 10 µM of Ro 25-6981 maleate, or 20 µM of MK-801 maleate, followed by NMDA and gly treatment. Mock cultures were treated with NMDA and gly only. For the inhibition of Top2β relegation activity, cultures were exposed to 5 µM of etoposide dissolved in DMSO. To block the Top2β DNA cleavage activity, ICRF-193 was dissolved in DMSO, and 10 µM of its concentration was used. To inhibit the activity of DNA-PK_{cs}, cultures were incubated with a 10 µM concentration of NU7026 for 1 hour. In the case of ICRF-193 and NU7026, the respective control group was treated with NMDA and gly only.

The 14 DIV neuronal cultures were irradiated in an X-ray tube equipped with a tungsten anode (Philips, Amsterdam, Netherlands), using a power of 19mA and 90 kV. The cells were placed at a distance of 30 cm from the radiation surface, with a dose rate of 1,96Gy/min as established by Ficke dosimetry. The irradiated samples were exposed with a single dose of 0.5 Gy or 2 Gy X-rays. Sham samples (irradiated with 0 Gy) were placed in the radiation chamber and shielded with a lead. The treatment time was adapted for glass coverslips or microelectrode arrays (MEA) recordings chips with radiometric calculation to prevent exposure to a higher dose due to secondary electrons' production. Both Sham and irradiated samples were transported back to the tissue incubator, and the experiments were performed 60 min post-exposure. In combined NMDA and radiation treatment, samples to be irradiated were taken to the radiation facility, a concentration of 15 µM NMDA and 2 µM gly was applied to activate NMDARs just before the cells are put into the radiation chamber, followed by irradiation with a single dose of 0.5 Gy or 2 Gy. The analysis was performed 60 min post-exposure. In the case of NMDA Sham, cells were also treated with NMDA and gly but were shielded with lead. For every treatment condition,

three independent biological replicates were included.

4.7. Immunofluorescence analysis

Cells seeded on the coverslips for 14 DIV after defined treatments were first rinsed with PBS, followed by the addition of 4% paraformaldehyde/PBS for 30 min for cell fixation. After fixation, three repetitive washing steps, each for 10 min with PBS, were performed, and cells were permeabilized with 0.4% Triton X-100 in PBS at room temperature for 5 min. The cells were washed (3x10min) with PBS and subsequently blocked using 10% GS diluted in PBS for at least 1 hour. Next, cultures were incubated overnight at 4°C with either of the following primary antibodies: anti-γH2AX, anti-NeuN, anti-GluN1, anti-GluN2B, and anti-MAP2 (for antibody dilution see table 1, 4.1).

The next day, the samples were rinsed in PBS (3x10min). One of the following secondary antibodies was used to assess visualization- Alexa-488-conjugated goat anti-rabbit and Alexa-594-conjugated goat anti-mouse (table 2, 4.1). The samples were incubated with secondary antibodies for at least 1-hour at room temperature in the dark. After repetitive PBS washing steps (3x10min), cells were incubated 2µg/ml DAPI (4′,6-diamidino-2-phenylindole) for 8 min followed by two more washing steps, each for 10 min with PBS, and one 10 min step with distilled water. After rinsing, coverslips were mounted on the microscopic slides using a Fluoromount-G medium. Coverslips were kept overnight at 4°C, and the samples were imaged the day after. Images were taken with an inverted epifluorescence microscope Axio Observer Z1 (Zeiss, Oberkochen, Germany) using a 20x or 63x oil immersion objective. Captured fluorescence images were further processed using ImageJ software. For analyzing the presence of DSBs (foci count) after varied treatments, a minimum of 60 cells from three independent experiments was analyzed, and the number of foci was counted manually. An unpaired nonparametric test- Mann–Whitney U test was applied for the foci' statistical analysis.

4.8. Western blotting

After defined treatment, cells plated at appropriate density on 24 well plates (Starlab, Hamburg) were washed twice with ice cold-PBS and lysed using chilled RIPA buffer supplemented with a 1% protease inhibitor cocktail (Merck). The collected cell lysate was centrifuged at 15,000 rpm at 4°C for 20 min, and the supernatant was collected. The protein concentrations were determined using a Pierce™ BCA (bicinchoninic acid assay) protein assay kit according to the manufacturer's protocol (Thermo Fisher Scientific). A 30 to 60 µg protein sample was mixed with 4x SDS-loading buffer containing 50mM DTT, heated to 70°C for 10 min for denaturation, and loaded onto 10% polyacrylamide gel with appropriate protein ladder. The proteins were separated in running buffer at a constant 120-130 V for 1.2 hours. Separated proteins were blotted on polyvinylidene difluoride (PVDF) membrane (Bio-Rad, California, U.S.A) using a semi-dry transfer system (Biorad) for 25 min at a constant 25 V, followed by 1 hour blocking with 5% skim milk in TBS containing 0.05% (v/v) Tween 20 (TBS-T). Blocking was followed by treatment with anti-c-FOS and anti-GAPDH antibody diluted in TBS-T with 1% skim milk buffer overnight at 4°C (table 1, 4.1).

The next day, blots were washed three times each for 10 min with TBS-T followed by one hour blocking at room temperature with HRP-conjugated goat anti-rabbit secondary antibody (table 2, 4.1). Following three-time membrane washing with TBS-T, each for 10 min, the signal was developed using the Pierce Western Blotting Substrate (Thermo Scientific). The staining was visualized with a CCD camera in the ChemiDoc MP imaging system (BioRad). Quantitative analyses were performed using Image Lab software (BioRad). Band intensities were normalized to GAPDH, and the cFOS/GAPDH ratios were normalized in the control treatment. For statistics, a parametric t-test was performed (GraphPad Prism 7.0).

4.9. RNA extraction, cDNA synthesis, and qPCR

TRIzol-chloroform extraction (Thermo scientific) was used to isolate total RNA from 14 DIV neuronal cultures. Isolation was performed under RNAse-free conditions. Further surfaces and non-disposable items were wiped with RNaseZap RNase Decontamination Solution (Cat. no. AM9780, Thermo Fisher) to remove RNase contamination. A 0.3 to 0.4 mL of TRIzol reagent per $1x10^5$-10^7 cells was used for cell lysis. The lysate was pipetted up and down multiple times for homogenization. The lysate was further passed through the 20-gauge needle and 1 mL syringe at least 10 times, followed by the addition of Cholorform to the lysate (0.2 mL of chloroform/ 1 mL of TRIzol Reagent used for initial lysis). Samples were incubated for 3 min and subsequently centrifuged for 15 min at 12,000xg and 4°C. The colorless aqueous RNA phase was transferred into a new tube. GlycoBlue coprecipitant (50 ug/ml) (glycogen covalently linked to a blue dye; Cat. No. AM9515, Thermo Fisher) and isopropanol (0.5 mL of isopropanol to the aqueous phase, per 1 mL of TRIzol reagent) were added to the RNA phase to facilitate precipitation. After 10 min centrifugation at 12,000xg at 4°C, the RNA was pelleted out. The pellet was cleaned two times with 75% ethanol, dried and further resuspended in RNase-free water. To remove residual genomic DNA contamination, extracted samples were further treated with RNase-free DNase I, followed by incubation for 30 min at 37°C, following the manufacturer's instructions (Thermo Scientific). Samples were resuspended in diethyl pyrocarbonate (DEPC) treated water. The purity and concentration of RNA were assessed with a spectrophotometer (Thermo Scientific). RNA integrity was further verified with denaturing 1% agarose gel. Reverse transcription or cDNA synthesis was performed using 1 µg of total RNA with the Revert Aid First Strand cDNA Synthesis kit (Thermo Scientific). Oligo $(dT)_{18}$ was used to yield full-length clones. The aliquotes of cDNA were stored at -20°C until further use.

To analyze the IEGs relative expression, real-time quantitative PCR (RT-qPCR) was performed with the StepOne Real-Time PCR System (Applied Biosystems, California, USA). Each reaction was carried out in triplicate in a 96-well plate (Thermo Scientific). Briefly, the PCR reaction was carried in a total volume of 20 µL, consisting of (50 ng) (around 2 µL) of cDNA, 12 µL of 2X Powerup SYBR green master mix (Thermo Fisher), 1 µL of 10 µM forward and reverses Primer, and 4 µL of DEPC treated water.

A negative control reaction was performed without cDNA. PCR amplification was carried out in the

following steps: initial denaturation at 95°C for 20 s, 40 cycles at 95°C for 3 s, annealing and elongation at 60°C for 30 s. Melt Curve Step: 3 more cycle steps to generate a melt curve. Gapdh was used as a housekeeping gene. A statistical test (such as a t-test or One-way ANOVA) was performed on raw mean ΔCt values obtained from the control and experimental groups. The graphs were plotted using $2^{-\Delta\Delta Ct}$ values.

4.10. MEA cell plating and experimental settings

The MEA2100 system with the standard MEA chips "60MEA200/10iR-Ti" from Multi Channel Systems was used to record changes in the membrane potential or voltage following various treatments. Before usage, chips were thoroughly cleaned with 70% ethanol, distilled water, and autoclaved. One day before cell plating, chips were coated with Poly-D-lysine and with Laminin. The next day, the cells were plated on chips at appropriate densities. On 14 DIV, the chips that were ready for recording were placed into the amplifier, where they were kept for at least 3-5 min without any interruption before the recordings.

After a defined treatment, spike activity was recorded for a period of 120 s from the cultures. Voltage potentials were recorded simultaneously from across 60 channels of the chip. A spike detector function was employed in the MEA software program for the spike activity's live documentation following various treatments. During the entire recording period, chips were kept on a heated stage which was maintained at a 37°C temperature. In NMDA and etoposide MEA recordings, the control condition was the electrophysiological activity observed directly after pharmacological modulators' addition, followed by recording the same chips at various time points to detect the changes in the voltage potential with treatment over time.

Two different chips were recorded in the case of spike activity analysis with Top2β siRNA and DNA-PK_{cs} inhibitor. The experimental group was incubated first either with Top2β siRNA and DNA-PK_{cs} inhibitor, followed by NMDA and gly addition. In contrast, the control MEA culture had only NMDA and gly incubation for 30 min.

4.11. MEA analysis

The MEA data was analyzed by M.Sc. Jan Wissmann from the Department of Biology, Centre for Computational Biology & Simulation. For the quantitative analysis of spike information, the MEA data was either converted to the HDF5 file format for the export in Python or .NEX format for transferring to the commercial NeuroEXplorer program (Nex Technologies, Madison, WI, USA).

Most of the recorded spike data were analyzed in Python, except the radiation spike data, edited in the NeuroEXplorer program. For the files converted to .NEX format, the data was edited in Neuroexplorer 5 version to distinguish between signal and noise and for clear spikes readout. Custom-made Microsoft Excel macro was further used to calculate the mean spikes rate over time in both Control/Sham and treated/irradiated samples.

The results from treated/irradiated samples were normalized to the recorded Control/Sham data. As not,

all the channels from the recordings were suitable for the analysis, either due to the high noise than signal ratio or less or no manually detected spikes; we only selected the channels where we could manually see a clear spike presence, and the analysis shows the presence of at least 1 spike/second (sec). In Python, the investigation was carried out using Snakemake and the NumPy/SciPy libraries [Snakemake [109], Numpy [110], SciPy [111]]. The recordings were sampled at 10 kHz (0.1ms per step), and for preprocessing, a Butterworth low-pass and a high-pass filter for 5 kHz and 100 Hz was applied. The contrast was increased for some recordings by convolution with a kernel function that approximates spike shape to find and extract unique spikes in the data. To further increase the contrast, two-pass spike detection was applied. The noise level was calculated with a custom deviation function, and a custom measure of the deviation was further evaluated to decrease the sensitivity to outliers. The noise was estimated according to the following equation, $x = [x_1, x_2 \dots x_N]\sigma_4 = \left(\frac{1}{N}\sum_i |x_i - \hat{x}|^{\frac{1}{4}}\right)^4$, where $\hat{x}$ is the mean of a time series. For the detection of local extremum in each recording, σ^4 was used as a parameter. Using the results from the first pass, a time series with increased contrast was obtained. The results from the first pass were further used in the second pass of peak finding with increased thresholds. Time points from the second pass were saved as spikes if the peak from the first pass was within 20 steps of the given peak from the second pass.

4.12. Transfection with Accell siRNA

Self-deliverable Accell SMARTpool siRNA (a pool of four siRNA oligos) against mice Top2β (Dharmacon- A horizon discovery group company, Waterbeach, UK) was used to knock down mRNA expression in neuronal cultures significantly. Accell Non-targeting Control Pool (negative control pool of four siRNAs) (Dharmacon) at the working concentration of 1 µM was used as a control. Per manufacturers' instructions, Smartpool siRNA was dissolved in 1x siRNA buffer (Dharmacon), and the cultures seeded at optimal density were incubated with 1 µM concentration of specific siRNA for 72 hours.

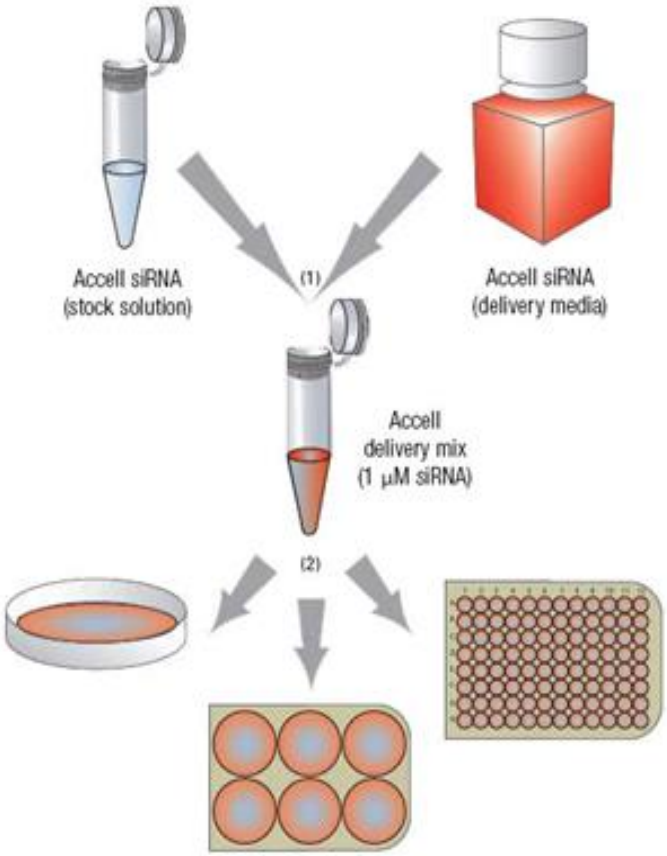

Figure 6: Schematic protocol of Accell siRNA application. Accell siRNA is mixed with Accell siRNA delivery media, and 1 µM of its concentration is applied directly to the cells plated either on Petri plate 6 or 96 well plate. The siRNA is kept for 72 hours to achieve high knockdown efficiency. Figure modified from Horizon discovery.com.

5. Results

5.1. Chapter 1: Assessment of physiological activity-induced DSBs on the regulation of IEGs expression and neuronal activity of 14 DIV HCs

5.1.1. Establishment of the model system- Primary culture of mice hippocampal neurons

To precisely analyze the role of activity-induced DNA DSBs in neuronal IEGs expression, it becomes imperative to first establish a model system that consists of predominate neuronal populations and further contains the molecular signaling pathways or components required for robust IEGs expression. Activation and expression of IEGs are involved in hippocampal synaptic plasticity and memory consolidation processes. For this reason, the primary culture of mice hippocampal neurons was established. An immunocytochemical approach with neuronal protein marker MAP2 was taken to monitor the culture's neuron purity and neurite growth dynamics. For this, cells fixed on coverslips were stained on days 3,7 and 14 following plating to investigate the culture's neuron purity and analyze when they establish their extensive neurite processes (**Figure 7a**).

The morphological method showed an enriched, extensive and intertwined network of neurites is present at almost pure 14 DIV neuronal culture. Since extensive neurite connections are the indicator of active synaptic sites, we further investigated if the synapse formed at 14 DIV was functional. Thus, the spontaneous activity was recorded from the culture using the MEA system. The raw voltage traces from MEA recording from the culture of 14 DIV shows the functional neuronal network activity (**Figure 7b)**. Hence, for assessing DSBs for regulating IEGs expression, 14 DIV hippocampal neuronal cultures were used as a model system.

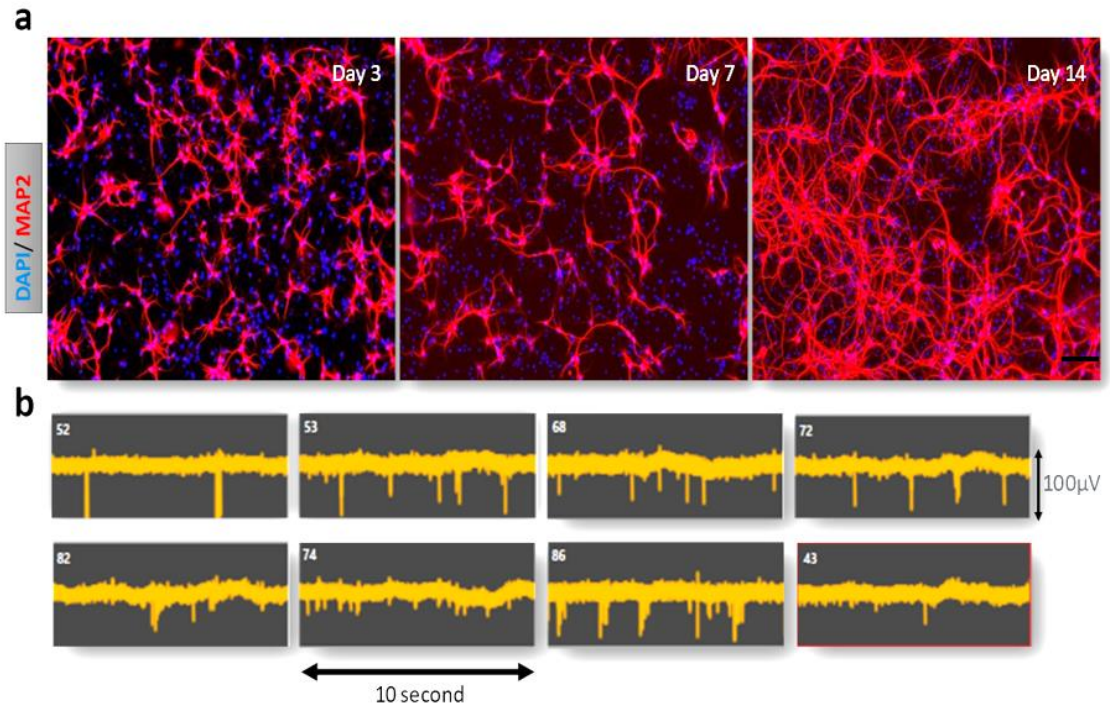

Figure 7: Primary mice hippocampal culture morphology at days 3, 7, and 14 following plating and spontaneous activity traces recorded at 14 DIV. (a) Immunostaining with neuronal protein marker MAP2 depicts the abundance of neurons in the model culture system, as well as shows that at 14 DIV, an interconnected network of neurites is formed, nucleus stained for DAPI, scale bar- 20 µm (b) An example traces of raw voltage recorded using MEA system form 14 DIV hippocampal culture without any treatment. Each panel shows 10 sec of the recording.

5.1.2. NMDA stimulates neuronal activity, IEGs expression and induces DNA DSBs in 14 DIV

5.1.2.1. NMDAR activity-mediated DNA DSBs correlates with induction of IEGs expression

The physiological function of DNA DSBs in the regulation of IEGs expression has not been discussed in other brain regions like the hippocampus. Further, the functional importance of regulatory DSBs in the mediation of neuronal activity is unclear. Therefore, for the first part, we investigated the correlation between NMDAR activity-induced DNA DSBs with the mRNA and protein levels of IEGs in primary hippocampal neurons. For this reason, the number of DSBs after 30 min of low NMDA concentrations (15 µM) application was analyzed by staining against γH2AX. We observed an increased number of γH2AX foci per cell in response to NMDA from 1.75 ± 0.09 to 4.75 ± 0.48 after 30 min ($p<0.0001$, Mann-Whitney U, n=3, **Figure 8 a, b**).

To examine whether the NMDA-induced increase in the number of DSBs was exclusively dependent on NMDAR activity, the status of DSBs in the cultures pre-treated for an hour with 10 µM MK801 followed by 30 min of 15 µM NMDA application were analyzed. Pre-incubation of cultures with MK-801 resulted in decreased γH2AX foci per cell from 6.4 ± 0.38 in exclusively NMDA treated cultures to 3.7 ± 0.22 in pre-MK801 treated cultures ($p<0.0001$, Mann-Whitney U, n=3, **Figure 8 c, d**).

Next, to determine whether the observed increase in the number of DNA DSBs could also be reflected

in the transcriptional status of IEGs such as *c-Fos*, *Egr1*, and *c-Jun*, we further performed quantitative reverse-transcription polymerase chain reaction (qRT-PCR) after 30 min of NMDA application. Post 30 min NMDA exposure, *c-Fos* and *Egr1* mRNA expression was up to 1.7 ± 0.13-fold (p=0.0127, unpaired two-tailed t-test, n=3) and 1.3 ± 0.12-fold (p=0.0421, unpaired two-tailed t-test, n=3) increased, whereas, no change in the expression level of *c-Jun* mRNA (0.98 ± 0.10-fold, p=0.9672, unpaired two-tailed t-test, n=3. **Figure 8 e**) was detected.

As we observed a correlation between NMDAR activity mediated increase in the number of DNA DSBs and the upregulation in specific IEGs expression after 30 min NMDA treatment, we also aimed to analyze the consequences of extended NMDAR activation on the number of γH2AX foci and expression level of *c-Fos*, *Egr1*, *c-Jun* and *Npas4* mRNA. Therefore, the number of γH2AX foci and IEGs expression was also analyzed after 60 min of NMDA treatment. The number of γH2AX foci per cell increased from 2.14 ± 0.15 to 5.4 ± 0.51 after 60 min of NMDA application (p<0.0001, Mann-Whitney U, n=3, **Figure 9 a, b**). Further, 60 min of treatment with NMDA resulted in a comparable increase in the expression level of *c-Fos* (1.6 ± 0.02-fold, p=0.0018, unpaired two-tailed t-test, n=3) as seen after 30 min. Additionally, *Egr1* mRNA expression level was upregulated more with 60 min of NMDA treatment (1.5 ± 0.03-fold, p=0.0332, unpaired two-tailed t-test, n=3) than 30 min. In contrast to 30 min NMDA treatment, a slight increase in *c-Jun* mRNA expression was also detected (1.31 ± 0.01-fold, p=0.6631, unpaired two-tailed t-test, n=3, **Figure 9 c**). Further, we could not observe any upregulation in *Npas4* mRNA level (1.04 ± 0.18-fold, p>0.05, unpaired two-tailed t-test, n=3) after 60 min NMDA application.

These results indicate a time-dependent upregulation in certain IEGs expressions like *Egr1* and *c-Jun* after NMDAR activation, which could further affect neuronal function. In accordance with the qRT-PCR results, c-FOS expression analysis at the protein level by Western blot also showed a comparable increase by approximately (1.4 ± 0.12-fold, p=0.0265 and 1.2 ± 0.02-fold, p=0.0083, unpaired two-tailed t-test, n=3, **Figure 9 d**) after 30 and 60 min of NMDA treatment, respectively. To further detect if the NMDAR-mediated increase in IEGs expression relied exclusively on NMDAR activity, we examined the mRNA and protein levels of IEGs in the cultures pre-treated with 10 μM MK-801 for 1 hour followed by 30 min of constant 15 μM NMDA application. MK-801 treatment decreased *c-Fos* mRNA (0.17 ± 0.05-fold, p=0.0053, unpaired two-tailed t-test, n=3) and protein expression (0.7 ± 0.23-fold, p=0.3076, unpaired two-tailed t-test, n=3; **Figure 9 d, e**). *Egr1* mRNA expression also decreased relatively after treatment (0.47 ± 0.09, p=0.2476, unpaired two-tailed t-test, n=3), whereas *c-Jun* expression was slightly increased (1.13 ± 0.1-fold, p=0.5945, unpaired two-tailed t-test, n=3, **Figure 9 e**). As no increase in *c-Jun* expression was detected after 30 min of NMDA treatment (see **Figure 8 e**), any upregulation detected in this specific IEG expression with MK-801 pre-treatment is likely not linked directly to NMDAR mediated activity.

Therefore, our data strongly indicate a correlation between NMDAR activity-induced DSBs and the upregulation in specific IEGs expression in 14 DIV hippocampal cultures. Further, it hints toward a time-dependent change in the level of particular IEGs expression following NMDAR activation, which

could further influence neuronal activity or function.

5.1.2.2. CREB activation is essential for the induction of activity-induced DSBs and IEGs expression

An essential step in the induction of certain IEGs is the specific binding of the transcription factor CREB to the CRE of the promoters of its target IEGs following the activation of NMDAR.

As our previous results of Figures 8 and 9 suggest a correlation between activity-induced DSBs after 30 to 60 min of constant NMDA application and IEGs expression, we next investigated the specific influence of CREB on the generation of these physiological DSBs and further on specific IEGs expression. We, therefore, investigated if a disruption of CREB activity regulates the status of NMDAR-induced DSBs. The number of DSBs decreased in cultures pre-treated with the CREB antagonist-KG-501 (20 μM)- 3.76 ± 0.38 γH2AX foci per cell compared to 4.78 ± 0.33 foci detected in NMDA-only treatment (p=0.0047, Mann-Whitney U, n=3, **Figure 10 a, b**). Further, we analyzed the expression levels of *c-Fos* and *Egr1* by qRT-PCR in the presence of CREB antagonist-KG-501 (20 μM). A decrease in the expression levels of both IEGs up to *c-Fos*-(0.53 ± 0.03-fold, p=0.0012, unpaired two-tailed t-test, n=3) and *Egr1*-(0.51 ± 0.12-fold, p=0.0326, unpaired two-tailed t-test, n=3, **Figure 10 c**) was observed after the treatment. Thus, in 14 DIV hippocampal neurons, we can demonstrate that specific activation of NMDARs conditions a CREB-dependent synchronous increase in DSBs and expression of the IEGs-*c-Fos* and *Egr1*.

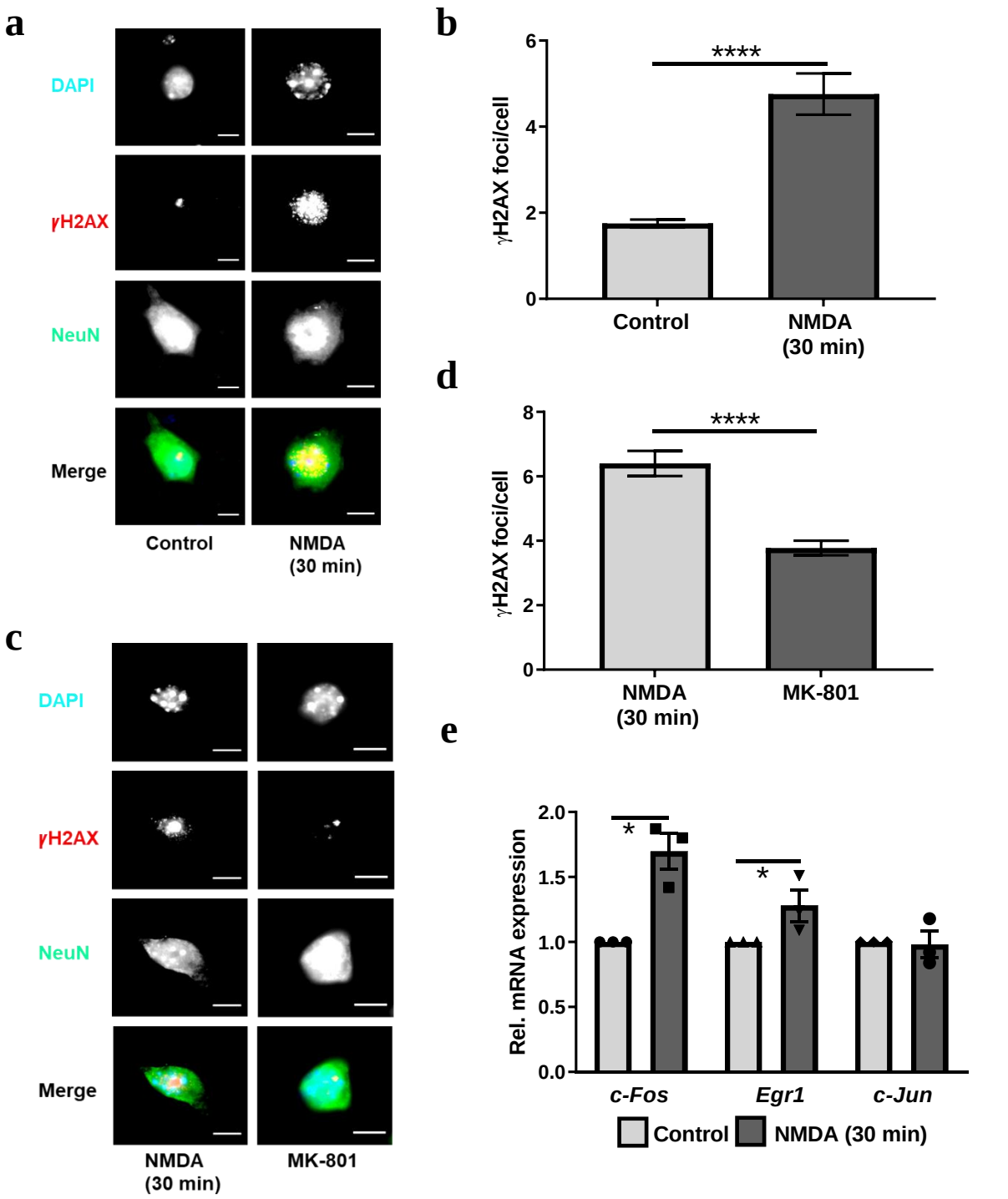

Figure 8: NMDA application (30 min) mediated DSBs induction and IEGs expression in 14 DIV HCs. (a) Primary cultures of hippocampal neurons stained against γH2AX after 30 min of NMDA (15 μM) treatment. DAPI staining for the nucleus and NeuN as a neuron-specific marker. (b) The number of DSBs (γH2AX foci per cell) analyzed after 30 min of NMDA treatment (Unpaired non-parametric T-test, Mann-Whitney test, $p<0.0001$, n=3). (c, d) Fluorescence images and quantitative analysis of γH2AX in response to 30 min of NMDA or after NMDAR blockage with 10 μM MK-801 followed by 30 min of 15 μM NMDA application (Unpaired non-parametric T-test, Mann-Whitney test, $p<0.0001$, n=3). Nucleus stained with DAPI and NeuN as a neuron-specific marker. (e) Scatter plot of relative mRNA levels of the IEGs (*c-Fos*, *Egr1*, and *c-Jun*) after 30 min NMDA treatment and control assessed by qRT-PCR. Both *c-Fos* ($p=0.0127$) and *Egr1* ($p=0.0421$) expression were upregulated after 30 min of treatment, whereas no change in *c-Jun* mRNA ($p=0.9672$) expression was detected.

Gapdh was used for qRT-PCR experiments as endogenous control. An unpaired two-tailed t-test on delta CT values was performed to assess the significance level (n=3, biologically independent experiments). Data is represented as the mean±sem. Scale bar-7μm.

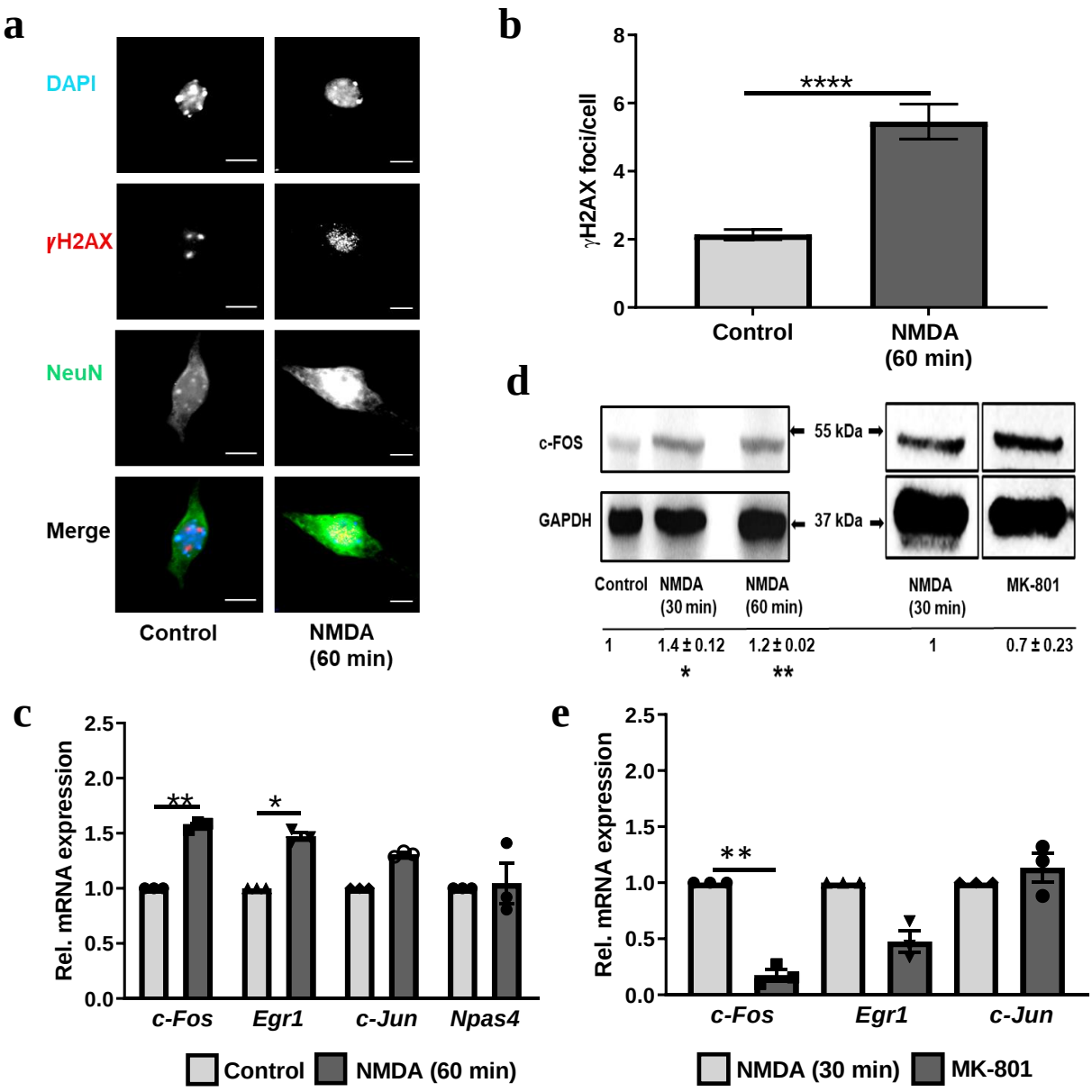

Figure 9: A 60 min NMDA application induced DSBs and IEGs expression is counteracted with pre-MK801 treatment. (a) Hippocampal cultures were stained against γH2AX after 60 min of NMDA treatment. DAPI staining for the nucleus and NeuN as a neuron-specific marker. (b) The γH2AX foci per cell were analyzed after 60 min of NMDA treatment (Unpaired non-parametric T-test, Mann-Whitney test, $p<0.0001$, $n=3$). (c) The bar graph represents the relative mRNA level of candidate IEGs (*c-Fos*, *Egr1*, and *c-Jun*) in control and 60 min NMDA treated cells assessed by qRT-PCR. Both *c-Fos* ($p=0.0018$) and *Egr1* ($p=0.0332$) expressions were upregulated after 60 min of NMDA treatment. Additionally, a slight increase in *c-Jun* ($p=0.6631$) mRNA and no change in *Npas4* gene ($p>0.05$) expression level were observed. (d, e) Quantitative analysis of c-FOS protein level after 30 ($p=0.0265$), 60 min ($p=0.0083$) of NMDA application, and in the pre-MK801 ($p=0.3076$) treated neuronal sample using western blotting. (f) Prior incubation of cultures with the NMDAR activity blocker- MK-801 decreased *c-Fos* ($p=0.0053$) and *Egr1* ($p=0.2476$) mRNA expression level, whereas no change in *c-Jun's* mRNA ($p=0.5945$) level was detected.

For qRT-PCR experiments, *Gapdh* was used as endogenous control, and the statistical test was performed on delta CT values to assess the significance level ($n=3$, biologically independent experiments). Data is represented as the mean±sem. Scale bar- 7 µm.

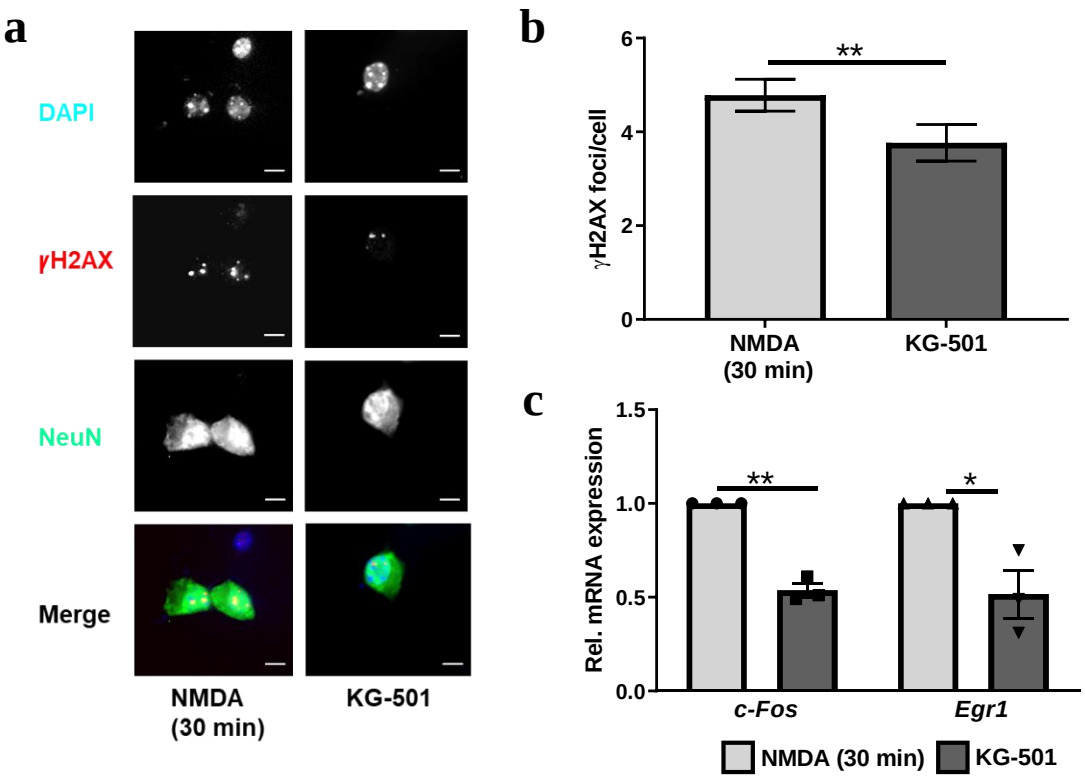

Figure 10: CREB influences DSBs generation and expression of IEGs following NMDAR activation. (a) Staining against γH2AX in neuronal cultures treated solely with NMDA for 30 min or pre-treated for an hour with KG-501, followed by 30 min NMDA incubation. DAPI staining for the nucleus and NeuN as a neuron-specific neuronal marker. (b) Number of DSBs analyzed in 60 cells by manual counting of γH2AX foci per cell following defined treatments (p=0.0047, unpaired non-parametric T-test, Mann-Whitney test, n=3). (c) The relative level of mRNA expression of candidate gene *c-Fos* (p=0.0012) and *Egr1* (p=0.0326) in the culture pre-treated with CREB antagonist- KG-501 compared to NMDA treatment only.

For qRT-PCR experiments, *Gapdh* was used as endogenous control, and the statistical test was performed on delta CT values to assess the significance level (n=3, biologically independent experiments). Data is represented as the mean±sem. Scale bar- 7 µm.

5.1.2.3. Temporal analysis of neuronal activity following NMDAR activation

In our previous results (**Figures 8 and 9**), we observed an upregulation in the DSBs status as well as *c-Fos* and *Egr1* mRNA expression levels- 30 and 60 min after NMDA treatment. Further, the slight upregulation observed in the *Egr1* expression and a detected increase in the *c-Jun* mRNA level after 60 min NMDA treatment compared to 30 min shows a time-dependent differential pattern of IEGs expression following initial NMDA stimulus (compare **figure 8e** and **9c)**. This differential IEGs expression pattern could further affect neuronal activity.

Therefore, we aimed to investigate the effect of such differential IEGs expression patterns observed after 30- and 60-min NMDA treatment on 14 DIV hippocampal cultures' neuronal network activity. As we observed a correlation between stimulation of DSBs and IEGs expression in our previous analysis, a repair of DSBs could also affect neuronal network activity. Therefore, we monitored the neuronal network activity for 2 hours with 30 min interval periods in an MEA following the initial NMDA stimulus, as according to previous observations, activity-induced DSBs are resolved within 2 hours of the initial stimulus [8]. We found that treatment with 15 µM NMDA induced a sustained increase in neuronal network activity as early as after 30 min of NMDA application (**Figure 11 a and b**; 1.35 ± 0.12-fold, p=0.0164, ANOVA, n=3), with a maximal firing rate observed after 60 min (1.76 ± 0.22-fold,

p=0.0034, ANOVA, n=3). Compared to 60 min, a reduction in neuronal network activity was observed after 80 until 120 min (reduction from 1.76 to 1.19 ± 0.12, p=0.0254, and 1.16 ± 0.14, p=0.0364, ANOVA, n=3**,** respectively). Incubation with the NMDAR-specific antagonist MK-801 (10µM) prevented the NMDA-induced increase in neuronal activity (0.51 ± 0.05-fold, p=0.0001, ANOVA, n=3), confirming that the observed changes in spike activity were mediated by NMDAR.

Taken together, our results in 14 DIV HCs show that NMDAR mediated increase in neuronal activity correlates with i) the expression of *c-Fos* and *Egr1* and ii) the CREB dependent induction of DSBs, supporting the notion that neuronal activity stimulates at least in part the expression of the IEGs *c-Fos* and *Egr1* within the first 60 min through the formation of DNA DSBs.

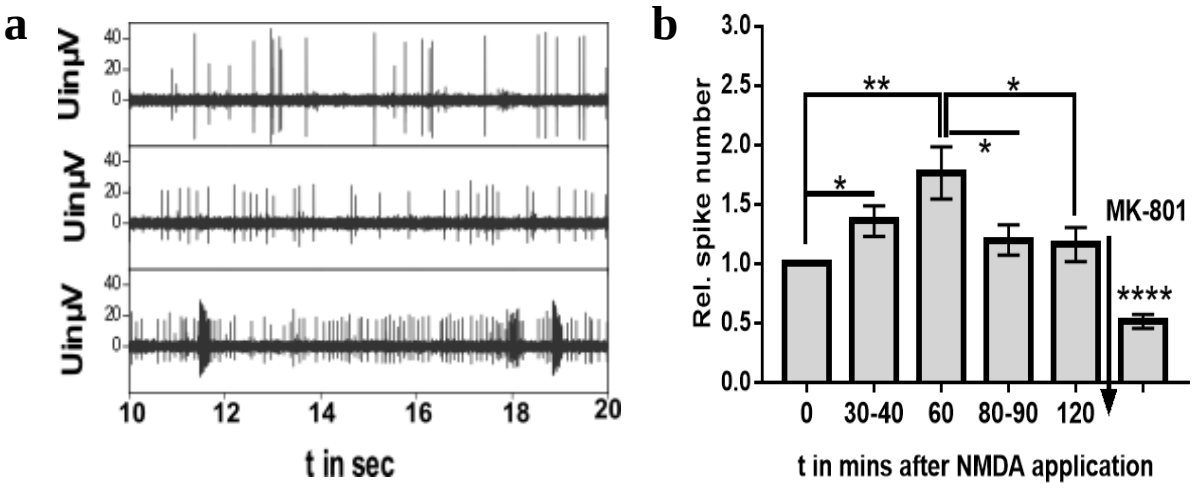

Figure 11: Analysis of 14 DIV HC neuronal network activity following initial NMDAR stimulus. (a) Representative 20-sec firing traces after 0-, 30- and 60-min NMDA application (15 µM) in 14 DIV HCs. (b) Analysis of relative spike number in the culture incubated for 2 hours with 15 µM NMDA concentration, with the spike activity recorded at each 30-min interval period. The activity's increase could be observed as early as 30 min after NMDA treatment (p=0.0164), with a peak at 60 min (p=0.0034). A significant decrease in the activity compared to 60 min treatment occurred after 80 min of NMDA application (p=0.0254), which persisted until 120 min (p=0.0364). MK-801 (p=0.0001) addition leads to a drastic decrease in the activity, validating the system measurement. Data are normalized to baseline activity (0 min after NMDA application) (One-way ANOVA test, 31 analyzed channels, n=3). Data is represented as the mean±sem.

5.1.3. GluN2B subunit of NMDAR mediates IEGs expression and regulates DNA DSBs status of the cell

To investigate the influence of NMDAR subunit composition on the expression of IEGs and induction of DSBs, we i) performed immunostaining with specific antibodies against the GluN1 and GluN2B subunits, ii) analyzed the mRNA level of *c-Fos*, *Egr1*, and *c-Jun*, and iii) analyzed the induction of DNA DSBs in the presence of a specific GluN2B-specific antagonist- Ro25-6981 maleate. Immunofluorescent staining results (**Figure 12 a**) showed predominant expression of GluN1 and GluN2B subunits in 14 DIV hippocampal neurons. Blocking of GluN2B subunit by pre-incubation of cultures with 10 µM Ro25-6981 maleate prior 30 min NMDA application resulted in downregulation of both *c-Fos* and *Egr1* at the mRNA level (0.56 ± 0.07-fold, p=0.0185 and 0.71 ± 0.007-fold, p=0.6544 unpaired two-tailed t-test, n=3, respectively, **Figure 12 b**) compared to NMDA treatment alone. Additionally, a decreased c-FOS protein expression was observed (0.63 ± 0.13-fold, p=0.0495, unpaired two-tailed t-test, n=3) upon treatment with Ro25-6981 maleate (**Figure 12 c**). In contrast, no change in

c-Jun mRNA expression was detected (0.98 ± 0.19-fold, p=0.9231, Figure 12 b). We observed a decrease in the number of γH2AX foci per cell from 8.4 ± 0.55 in NMDA treated cells to 5.9 ± 0.38 in pre-Ro25-6981 maleate treated cultures (**Figure 13 a and b**; p=0.0001, Mann-Whitney U, n=3). Thus, by specific GluN2B subunit antagonization, our data suggest that in hippocampal neurons, *c-Fos* and possibly *Egr1* expression is likely mediated by GluN2B-dependent DSB induction.

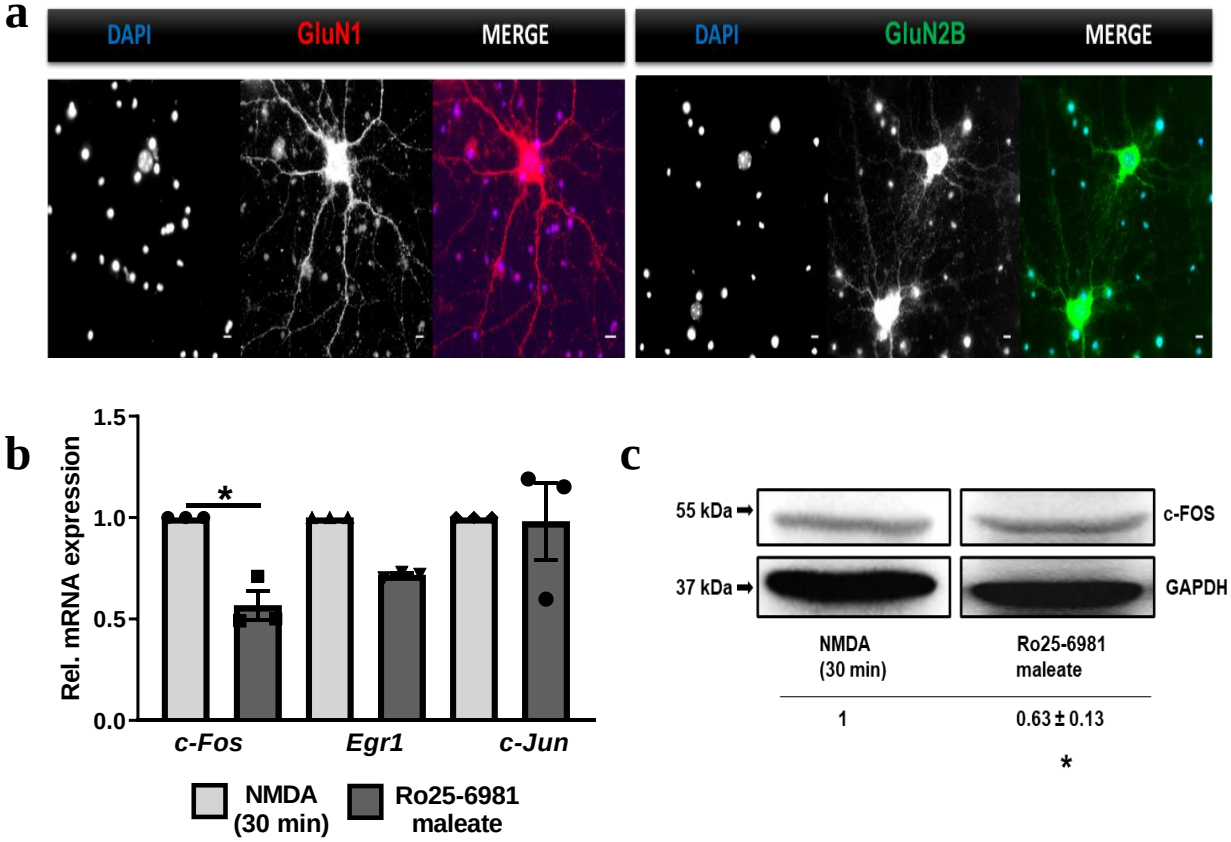

Figure 12: The GluN2B subunit is essential for *c-Fos* and *Egr1* mRNA expression. (a) Immunofluorescent staining against NMDAR subunits GluN1 and GluN2B. Confocal microscope analysis shows the localization of the two receptor subunits in the neuron. DAPI staining for the nucleus. (b) Prior incubation of HCs with GluN2B subunit blocker, Ro 25-6981 maleate, leads to the decreased mRNA expression level of *c-Fos* (p=0.0185) and *Egr1* (p=0.6544) compared to NMDA treatment alone. In contrast, no change in *c-Jun* mRNA (p=0.9231) was observed (Unpaired two-tailed t-test, n=3). (c) The relative c-FOS protein level (p=0.0495), assessed by Western blotting and its quantification (Unpaired two-tailed t-test, n=3).

For qRT-PCR experiments, *Gapdh* was used as endogenous control, and the statistical test was performed on delta CT values to assess the significance level. Data is represented as the mean±sem. Scale bar-50 µm.

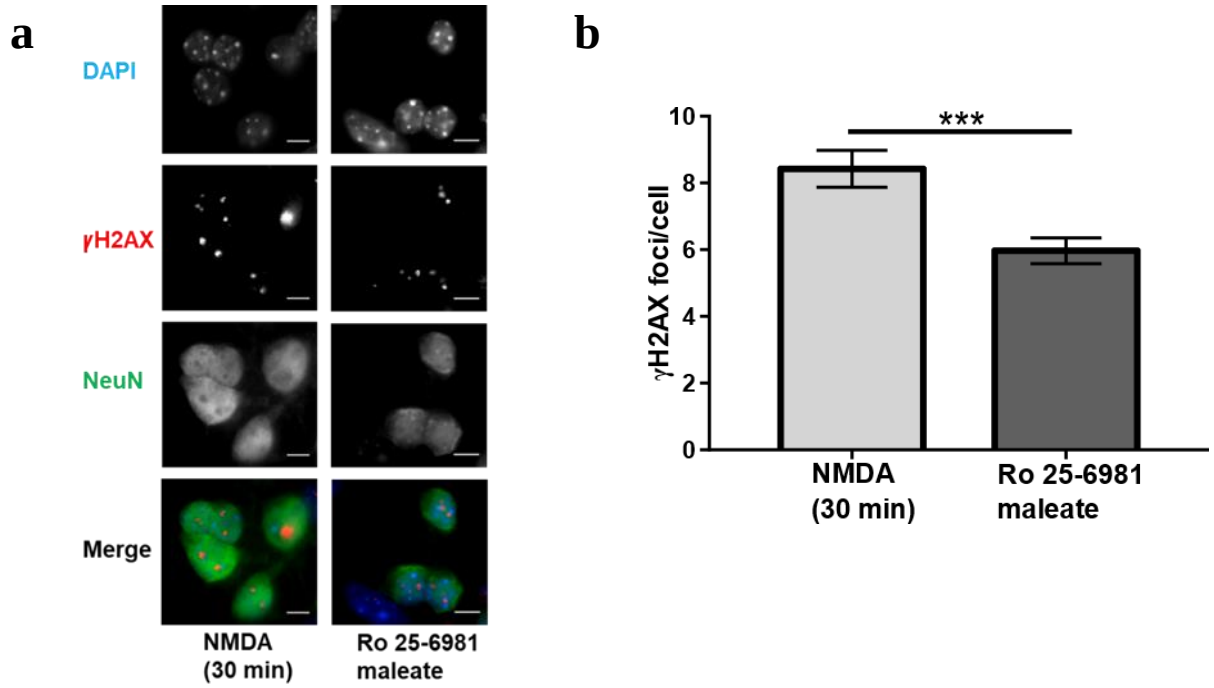

Figure 13: GluN2B subunit inhibition leads to decreased DNA DSBs status in 14 DIV neurons. (a) The γH2AX expression was detected by immunofluorescence staining in HCs either pre-incubated with Ro 25-6981 maleate for an hour followed by 30 min NMDA incubation or treated solely with NMDA for 30 min. DAPI staining for the nucleus and NeuN as a neuron-specific marker. (b) Foci analysis of 90 cells upon only NMDA or pre-Ro 25-6981 maleate treatment (Unpaired non-parametric T-test; Mann-Whitney test, n=3, p=0.001). Data is represented as the mean±sem. Scale bar-7 µm.

5.1.4. DSBs increase neuronal activity and stimulates *c-Fos* expression

Our previous analysis with NMDA incubation suggests that NMDAR activity-induced DSBs are involved in regulating IEGs expression (**Figures 8, 9** and **11**). Therefore, it seems likely that any change in DSBs status could lead to altering IEGs expression level and neuronal network activity. To investigate the DSBs involvement further in governing IEGs expression and evaluate the consequences of prolonged DSB on neuronal network activity, we analyzed the effects of etoposide treatment on the mRNA expression levels of *c-Fos*, *Egr1*, *c-Jun*, and *Npas4* and their implications on network activity.

First, the induction of DSBs with a 5 µM etoposide treatment was analyzed by staining against γH2AX. Addition of etoposide increased the mean γH2AX foci number from 2.2 ± 0.10 in untreated control to 12.47 ± 0.54 (**Figure 14 a and b**; $p<0.0001$, ANOVA, n=3).

To further investigate the role of NMDAR activity mediated DSBs on the number of etoposides mediated DSBs in the transcription of IEGs, the neuronal culture was incubated with NMDA and simultaneously treated with etoposide for 30 min, followed by staining against γH2AX. Simultaneous treatment of NMDA and etoposide showed no difference in the number of DSBs- 12.74 ± 0.68 to etoposide alone- 12.47 ± 0.54, as analyzed by manual counting of mean γH2AX foci per cell ($p=0.9693$, unpaired non-parametric T-test; Mann-Whitney test, n=3). This suggests that NMDA and etoposide-induced DSBs display a significant overlap.

Therefore, we next examined the effect of etoposide-induced DSBs on HCs network activity by measuring spike activity with the MEA system. Interestingly, 5 µM etoposide treatment also induced an increase in neuronal firing, with a slightly delayed but sustained increase after etoposide addition

compared to NMDAR-induced activity (**Figure 15 a**; 30-40 min etoposide- 1.05 ± 0.018-fold, p=0.0024, paired t-test, n=3 (73 channels); 50-60 min etoposide- 1.91 ± 0.10-fold, p<0.0001, paired t-test, n=3 (28 channels); 90-110 min etoposide- 1.35 ± 0.05-fold, p<0.0001, paired t-test, n=3 (78 channels); 120-140 min etoposide- 1.25 ± 0.09-fold, p=0.2685, all paired t-test, n=3 (73 channels)).

Next, to analyze whether the expression of IEGs is also affected by etoposide-induced DSBs, the mRNA levels of *c-Fos*, *Egr1*, and *c-Jun* were analyzed after 30 min of etoposide treatment. We observed a slight upregulation in the mRNA expression level of *c-Fos*, and *c-Jun* genes (*c-Fos*-1.23 ± 0.05-fold, p=0.9756; *c-Jun*-1.38 ± 0.19-fold, p=0.8274; ANOVA, n=4; **Figure 15 b**) with etoposide treatment whereas no change in *Egr1* mRNA (1.16 ± 0.04-fold, p=0.9864) expression level was detected. Additionally, c-FOS protein level analyzed with 30 min of etoposide treatment showed a comparable increase in protein level than mRNA expression (1.25 ± 0.28-fold, p=0.4411, unpaired two-tailed t-test, n=3; **Figure 15 c**).

Even though we did not observe upregulation in the mean γH2AX foci number in combined etoposide and NMDA treatment than the etoposide treatment alone, we next aimed to investigate if the combined treatment affects IEG´s expression level. Thus, cells were incubated simultaneously with NMDA and etoposide, and the IEGs mRNA expression levels were analyzed after 30 mins. The *c-Fos* expression increased with the combined treatment compared to the etoposide treatment alone (1.65 ± 0.14-fold, p=0.6434, unpaired two-tailed t-test, n=4). In contrast, no change in the mRNA expression of *Egr1* (1 ± 0.03-fold, p=0.8962, unpaired two-tailed t-test, n=4) and a slight decrease in *c-Jun* expression level (0.85 ± 0.08-fold, p= 0.8079, unpaired two-tailed t-test, n=4; **Figure 15 b**), was detected.

As previously, with 60 min of NMDA incubation, we detected an upregulation in *Egr1* and *c-Jun* mRNA expression and neuronal activity, compared to 30 min treatment (**Figure 8e and 9c**); therefore, we next aimed to determine whether a prolonged incubation with etoposide is also needed to lead to a significant increase in IEGs mRNA expression level. We now observed a statistically significant upregulation of *c-Fos* mRNA expression (1.36 ± 0.07-fold, p=0.0140, unpaired two-tailed t-test, n=3; **Figure 15 d**) after 60 min of etoposide treatment but no change in *Npas4* expression (1.06 ± 0.02-fold, p=0.0590, unpaired two-tailed t-test, n=3) compared to control treatment. We speculate that an increase in *c-Fos* expression observed after 60 min of etoposide treatment, compared to 30 min, may also increase network activity.

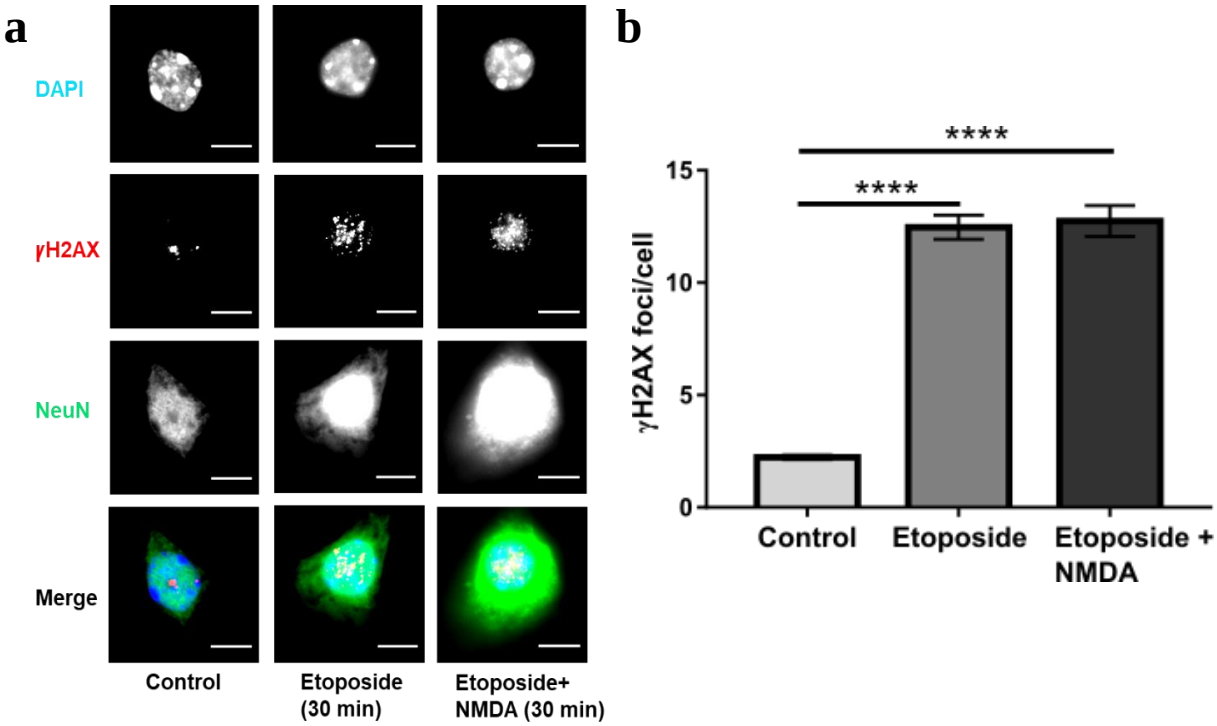

Figure 14: Etoposide incubation induces a significant amount of DNA DSBs in 14 DIV HC. (a) Fluorescence images demonstrate staining against γH2AX in the sample of control etoposide (30 min) and 30 min of simultaneous etoposide and NMDA treatment. DAPI staining for the nucleus and NeuN as a neuron-specific marker. (b) Quantitative foci analysis in the indicated samples (One-way ANOVA and unpaired non-parametric T-test, $p<0.0001$, Mann-Whitney test, 70 cells, n=3). Data is represented as the mean±sem. Scale bar-7μm.

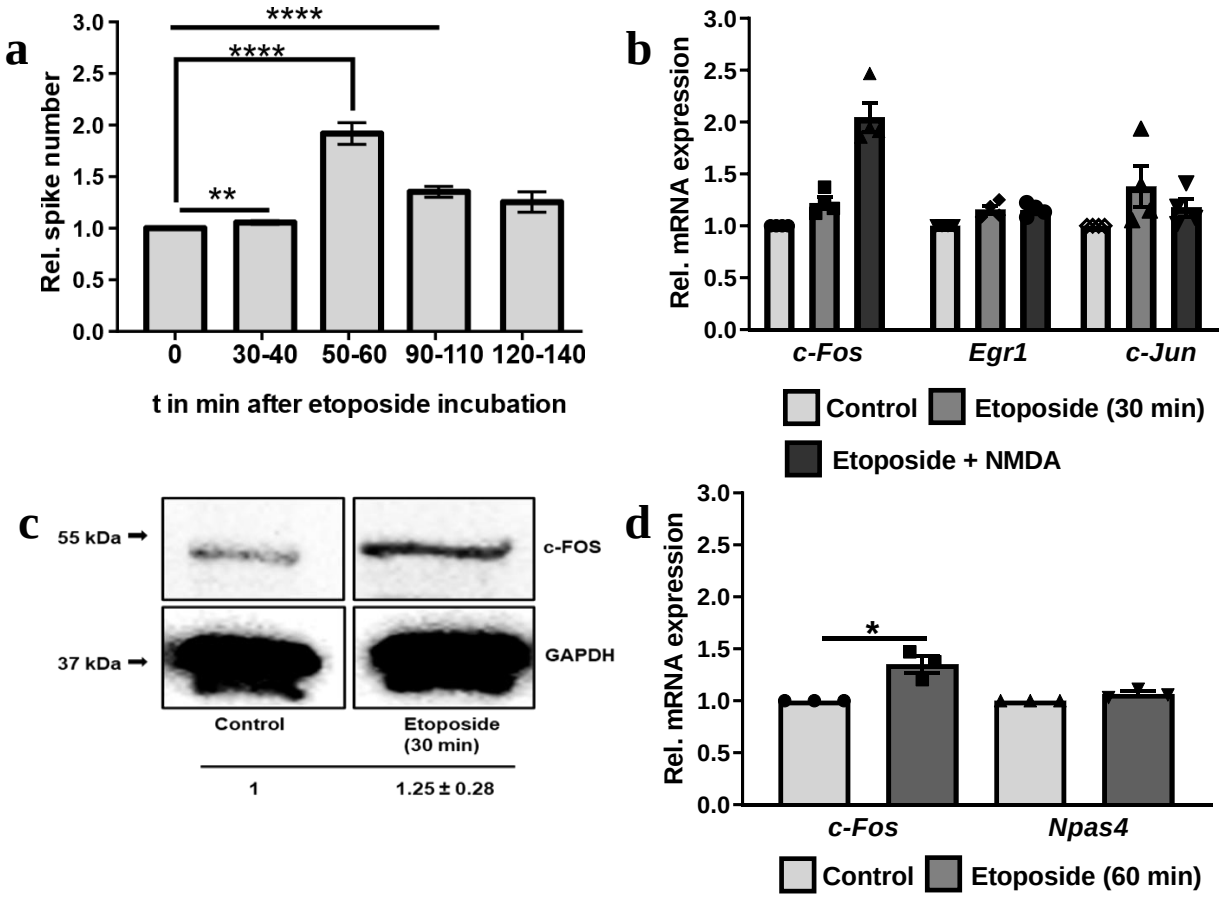

Figure 15: DNA DSB regulates neuronal firing and IEGs expression. (a) Relative firing rate measured by MEA system and analyzed over 2 hours under etoposide treatment. The firing rate increased just with 30 min of etoposide incubation (p=0.0024,73 channels); 50-60 min- p<0.0001 (28 channels); 90-110 min- p<0.0001 (78 channels); 120-140 min- p=0.2685 (73 channels). Data normalized to the baseline value (0 min of etoposide application) (Paired t-test, n=3). (b) The relative mRNA expression level of candidate IEGs (*c-Fos*, *Egr1*, and *c-Jun*) upon treatment solely with etoposide or simultaneous NMDA and etoposide for 30 min. *c-Fos* (p=0.9756) and *c-Jun* (p=0.8274) mRNA expression was upregulated with 30 min of etoposide treatment and increased *c-Fos* expression (p=0.6434) level detected with combined treatment of NMDA and etoposide hints to NMDA's additional effect on IEGs regulation (Unpaired two-tailed t-test and one-way ANOVA test, n=4). (c) The c-FOS (p=0.4411) protein level examined with Western blotting in etoposide treatment (Unpaired two-tailed t-test, n=3). (D) The graph depicts the *c-Fos* and *Npas4* mRNA expression levels assessed with qRT-PCR. Upregulated *c-Fos* expression level with 60 min (p=0.0140) of etoposide treatment indicates the time-dependent upregulation of certain IEGs. The mRNA level of *Npas4* (p=0.0590) remained unchanged with the treatment (Unpaired two-tailed t-test, n=3).

For qRT-PCR and Western blot experiments, Gapdh was used as endogenous control. For qRT-PCR, the statistical test was performed on delta CT values to assess the significance level. Data is represented as the mean±sem.

5.1.5. NMDA-promoted *c-Fos* expression and neuronal activity is governed by Top2β-induced DSBs

In our previous analysis with etoposide treatment, we demonstrated the importance of DSBs in the upregulation of hippocampal IEGs expression and activity (**Figure 15**). It is known that Top2β activity is crucial in DSBs formation and IEGs regulation in different brain areas like cortical culture [8]. To investigate if Top2β activity is also involved in HC DSBs formation, we abolished Top2β cleavage activity by pre-incubating the neuronal cultures for 1 hour with an in vitro inhibitor of the Top2β activity- ICRF-193 (10 μM) followed by 60 min incubation with NMDA (15 μM) and examined the effect on the DSBs status.

As shown by γH2AX staining, we observed statistically significantly less foci in the ICRF-193 samples

with 3.8 ± 0.20 foci per cell than in the NMDA-treated control experiments with 5.3 ± 0.26 foci per cell (**Figure 16 a, b**; p<0.0001, Mann-Whitney U, n=3).

To investigate if also the IEGs expression depends on Top2β activity, we assessed *c-Fos* expression level in culture pre-incubated for 72 hours with Accell siRNA targeting mice Top2β followed by 60 min incubation with NMDA (15 µM). As demonstrated by qRT-PCR analysis, downregulation of *Top2β* (0.16 ± 0.02-fold, p=0.0057, unpaired two-tailed t-test, n=3) mRNA was followed by a decrease in *c-Fos* (0.12 ± 0.006-fold, p=0.3880, unpaired two-tailed t-test, n=3; **Figure 16 c**) mRNA expression compared to NMDA control group. This result demonstrates the dependency of the *c-Fos* expression's on Top2β activity in also HCs.

Next, to analyze whether Top2β is additionally involved in regulating neuronal activity, the firing rate of Top2β-siRNA pre-treated cultures was compared to the cultures treated solely for 60 min with NMDA, as the upregulation in neuronal activity was detected with 60 min of NMDA treatment (**Figure 11 b**).

Our results show that the firing rate decreased dramatically when cells were exposed to Top2β siRNA compared to control siRNA (**Figure 16 d**; 0.18 ± 0.06-fold, Unpaired two-tailed t-test, p<0.0001, n=3), strongly indicating that the blocking of Top2β activity could hamper the increase in NMDA-induced neuronal activity and leads to downregulation of *c-Fos* expression by reducing Top2β-induced DSBs.

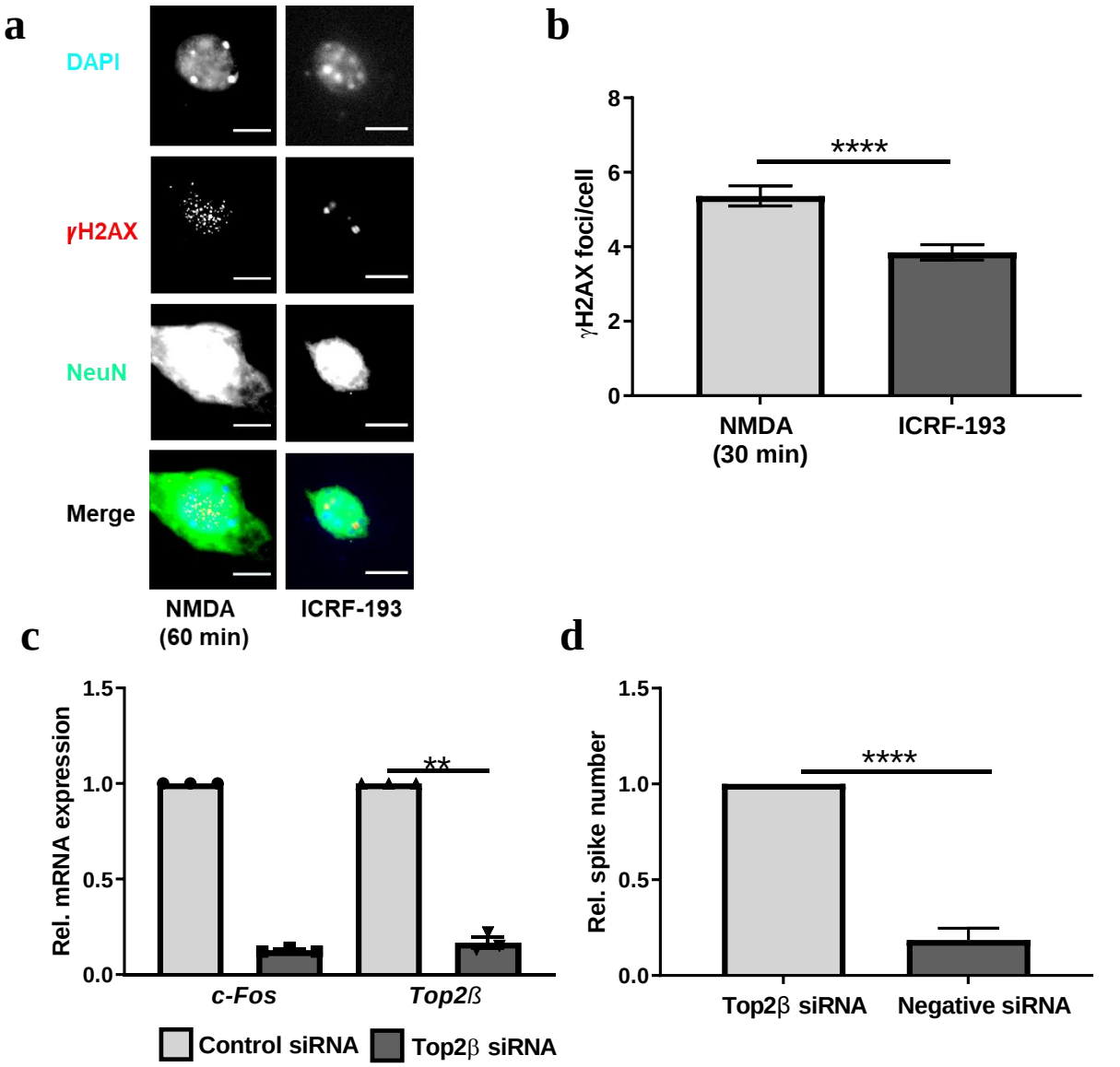

Figure 16: Top2β mediated DSBs stimulate IEGs expression and neuronal activity in HC. (a) Representative γH2AX staining after Top2β cleavage activity inhibition with ICRF-193 (10 μM) and subsequent NMDAR activation (15 μM NMDA), and in the only NMDA mock cultures. Nucleus stained with DAPI. Neurons were stained with the mature neuron marker, NeuN. (b) Quantitative γH2AX foci analysis in the indicated samples ($p<0.0001$, unpaired non-parametric T-test, Mann-Whitney test, n=3). (c) Relative downregulation in the mRNA level of *Top2β* ($p=0.0057$), and *c-Fos* ($p=0.3880$) after Top2β siRNA treatment compared to control siRNA treated neurons (Unpaired two-tailed t-test, n=3). (d) Quantification of average and relative spike numbers in Top2β and control siRNA cultures ($p<0.0001$, Unpaired two-tailed t-test,n=3).

For qRT-PCR experiments, *Gapdh* was used as endogenous control, and the statistical test was performed on delta CT values to assess the significance level. Data is represented as the mean±sem. Scale bar-7μm.

5.1.6. NHEJ mediated NMDAR induced DSBs repair control IEGs expression and activity

In our previous MEA analysis with NMDA treatment, we observed a decrease in the neuronal firing rate after 80 min compared to 60 min (**Figure 11 a and b**). The firing rate reduction suggests the possibility of a DSBs repair mechanism that could ultimately affect IEGs expression, which is critical for the mediation of firing rate. Therefore, to test the involvement of NHEJ, a central repair mechanism associated with both pathological and physiological repair of DSBs, in the regulation of IEGs expression

and neuronal activity, we evaluated the effect of a highly selective DNA-PK inhibitor-NU7441 (KU-57788).

First, we examined the effect of blocking the repair of NMDAR activity-induced DSBs in HC. For this, we assessed the number of DSBs in the cultures incubated with DNA-PK inhibitor (10 μM) for an hour followed by 80 min incubation with NMDA (15 μM). We assessed the DSBs in the respective treatment only at 80 min, as we observed a decrease in the firing rate after 80 min of prolonged NMDA treatment (**Figure 11 a and b**). Pre-treatment with NU7441 increased the mean number of foci to 9.1 ± 0.64 from 3.8 ± 0.23 detected in NMDA treatment alone (**Figure 17 a**, **b**; $p<0.0001$, Mann-Whitney U, n=3), suggesting a contribution of NHEJ repair in NMDA-induced DSBs.

Next, to check if the decrease in firing frequency observed after 80 min with NMDA is due to NHEJ mediated repair of DSBs, we measured the relative firing rate after 80 min in culture treated with NMDA alone or pre-incubated with NU7441. Spike rate analysis showed that the activity was higher in the sample treated with the DNA-PK inhibitor than in the samples treated with NMDA alone (**Figure 17 c**; 2.76 ± 1.0-fold, Unpaired two-tailed t-test, p=0.1257, 10 channels, n=3). This increase in spiking activity is coherent with the upregulation of DSBs in the cells, a co-relation also seen with previous MEA and DSBs analysis results with NMDA and etoposide treatment.

Next, we analyzed if the upregulation observed in neuronal activity with DSBs repair inhibition was reflected in the IEGs expression status. Therefore, we assessed the *c-Fos* and *Npas4* mRNA levels in pre NU7441 and only NMDA-treated cultures. We observed only a slight, nonsignificant upregulation in *c-Fos* expression (1.20 ± 0.06, unpaired two-tailed t-test, p=0.3534, n=3) after NU7441 treatment, compared with 80 min of NMDA treatment (**Figure 17 d**). Interestingly we also detected a significant upregulation in the *Npas4* mRNA level (1.32 ± 0.20, unpaired two-tailed t-test, p=0.0255, n=3).

To better understand the physiological impact of DSB repair on IEGs expression at the *in-vivo* level, we checked and evaluated the mRNA level of *c-Fos*, and *Npas4* in the neuronal cultures of an NHEJ-deficient mouse model (SCID). We observed significant upregulation in *c-Fos* expression in SCID mice (3.14 ± 0.31, p=0.0434, unpaired two-tailed t-test, n=3) and a very low mRNA expression level of *Npas4* (0.06 ± 0.01, p=0.0485, unpaired two-tailed t-test, n=3) 60 min after treatment with 15 μM NMDA compared to untreated WT control. Further, the expression of c-*Fos* was higher in NMDA-treated SCID- than in NMDA-treated WT cultures (compare **Figure 9 c and 17 e**).

These results of IEGS expression in repair-deficient cultures of SCID mice highlight the repair of NMDA-induced DSBs by NHEJ as a physiological mechanism regulating the differential expression of IEGs, e.g., *c-Fos* versus *Npas4*, and ultimately neuronal activity.

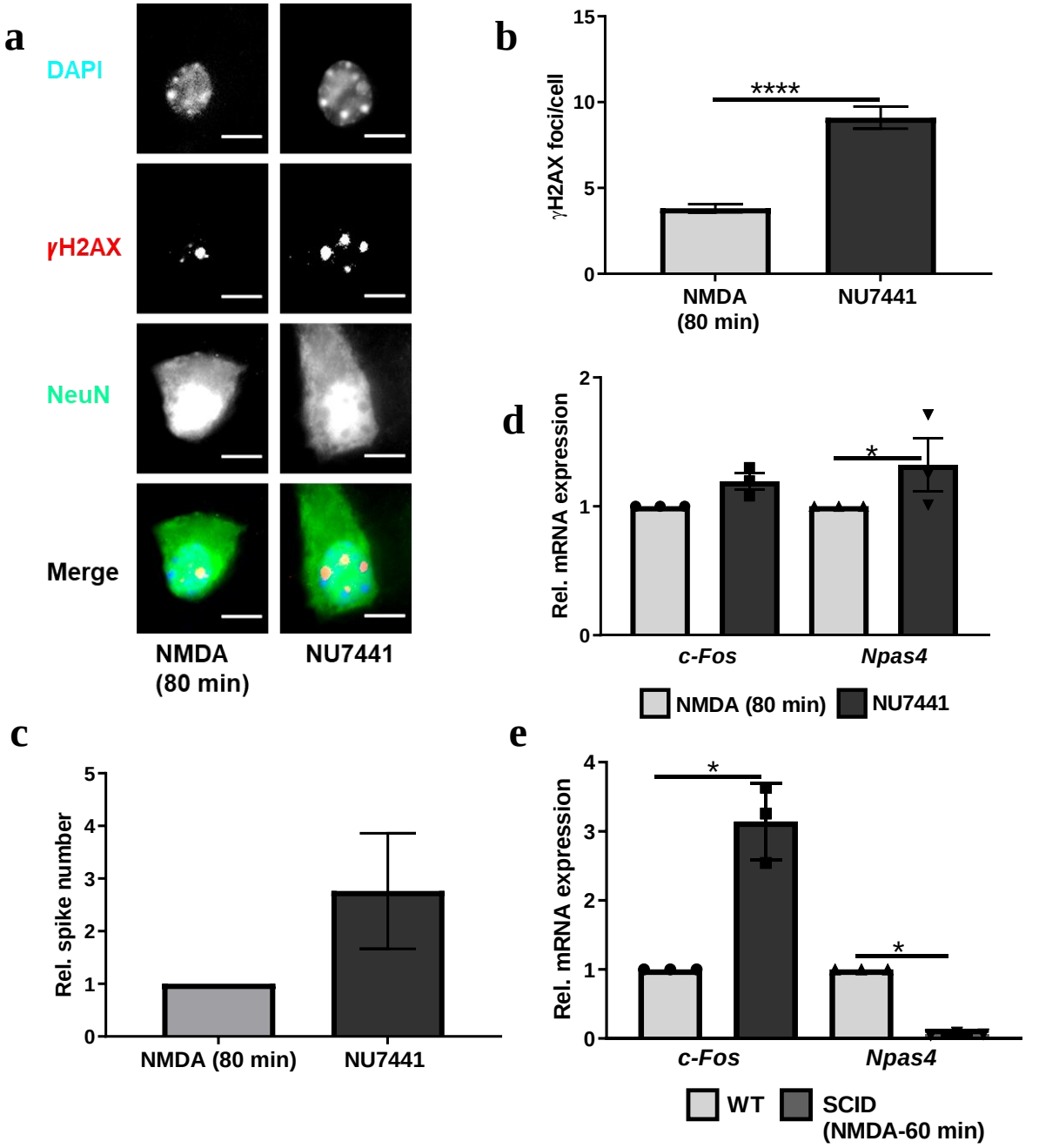

Figure 17: NHEJ mediated repair controls IEGs expression and neuronal activity. (a) DNA DSBs visualized with γH2AX staining in the culture of neurons pre-treated with NU7441 followed by 80 min of NMDA application and control sample, treated solely with NMDA for 80 min. DAPI staining for the nucleus and NeuN as a neuron-specific marker. (b) Quantitative γH2AX foci analysis in the indicated samples ($p<0.0001$, unpaired non-parametric T-test, Mann-Whitney U, n=3). (c) The relative firing rate measured by the MEA system in the culture pre-treated with NU7441 and the control sample treated only with NMDA for 80 min. The neuronal network activity was drastically higher in the sample treated with the NHEJ machinery blocker than in the NMDA-only treatment ($p=0.1257$, Unpaired two-tailed t-test, n=3). (d) The bar graph demonstrates relative upregulation in the mRNA expression level of *c-Fos* ($p=0.3534$), and *Npas4* ($p=0.0255$) in NU7441 treated cultures compared to only NMDA treated neurons (Unpaired two-tailed t-test,n=3). (e) The relative expression level of candidate IEGs (*c-Fos* and *Npas4)* was assessed by qRT-PCR in the neuronal cultures of SCID treated for 60 mins with 15 µM NMDA (*c-Fos*, $p=0.0434$; *Npas4*, $p=0.0485$) and in untreated WT control (Unpaired two-tailed t-test, n=3).

For qRT-PCR experiments, *Gapdh* was used as endogenous control, and the statistical test was performed on delta CT values to assess the significance level. Data is represented as the mean±sem. Scale bar-7µm.

5.1.7. Top2β expression level is upregulated with NMDA treatment

Since our data demonstrated that Top2β generated DNA DSBs are essential for certain IEGs expression (**Figure 15 and 16**), we next aimed to analyze whether the treatment with NMDA increases the mRNA expression level of Top2β as compared to basal condition, where NMDA is not provided in mice HCs. For this reason, we treated both SCID and WT mice 14 DIV HCs with NMDA and assessed the Top2β mRNA expression level after 60 min.

To evaluate if a correlation exists between Top2β expression status and mRNA level of certain IEGs, we in parallel evaluated the *c-Fos* and *Npas4* levels with the NMDA treatment of SCID and WT. As shown in **Figure 18 a**, the *Top2β* mRNA expression increases to 1.67 ± 0.32-fold after 60 min of NMDA treatment (unpaired two-sided t-test, p=0.0303, n=3). In parallel to the previous results (**Figure 9 c**), an upregulation in *c-Fos* mRNA expression of up to 1.45 ± 0.18-fold (unpaired two-sided t-test, p=0.1301, n=3), and no change in the mRNA expression level of *Npas4* 1.04 ± 0.18-fold (unpaired two-sided t-test, p=0.9766, n=3) was detected after NMDA treatment.

Next, we compared the *Top2β*, *c-Fos*, and *Npas4* expression levels in basal conditions in WT and SCID mice. Surprisingly, the mRNA expression level *Top2β*, *c-Fos* and *Npas4* detected in SCID mice was significantly lower compared to the WT control (0.04 ± 0.001-fold, 0.02 ± 0.0003-fold, 0.05 ± 0.08-fold; p=0.0020, p=0.0015, p=0.0004; unpaired two-sided t-test, n=3; **Figure 18 b**). With NMDA treatment of SCID mice culture, we observed a drastic upregulation of *Top2β* expression level and, in parallel to **Figure 17e** results, *c-Fos* mRNA expression level also increased whereas a significant decrease in *Npas4* level was seen in SCID mice neuronal culture compared to WT control after 60 min (2.87 ± 0.18-fold, 1.44 ± 0.08-fold, 0.07 ± 0.009-fold; p=0.0767, p=0.5092, p= 0.0017; unpaired two-sided t-test, n=3; **Figure 18 c**).

Hence, the data suggest that NMDA treatment leads to increased *Top2β* expression levels in neuronal culture. Further, the *Top2β* expression level dramatically upregulates with NMDA treatment, followed by *c-Fos* mRNA expression in SCID mice. Additionally, the results suggest the dependency of *c-Fos* expression on *Top2β* activity.

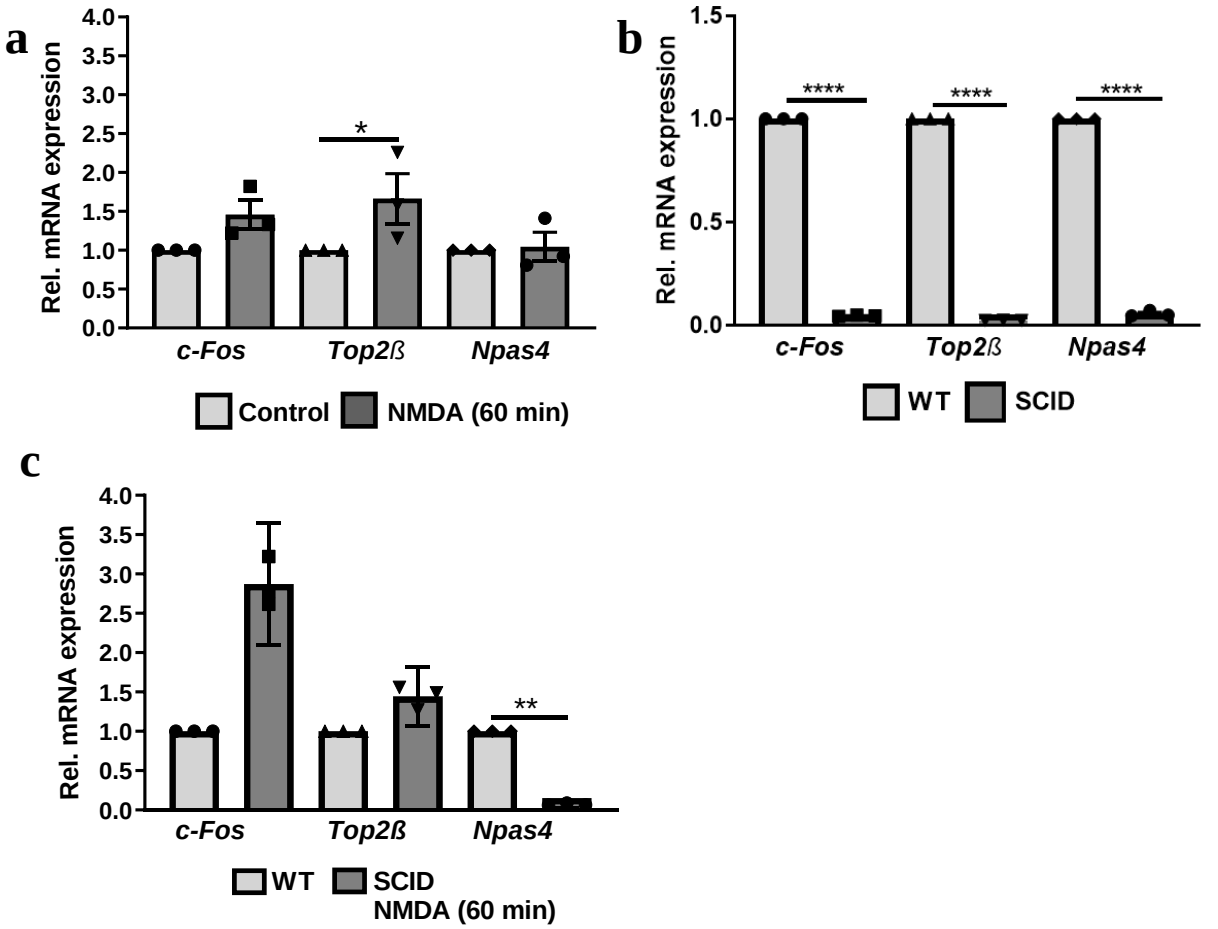

Figure 18: NMDA incubation upregulates *Top2β* mRNA expression level in HC. (a) Relative upregulation in the mRNA level of *Top2β* (p=0.0303) and, consequently, in *c-Fos* (p=0.1301) expression after 60 min of NMDA treatment compared to control. In contrast, no change in *Npas4* (p=0.9766) expression is detected after the treatment (Unpaired two-tailed t-test, n=3). (b) The graph depicts a significantly lower mRNA expression level of *Top2β* (p=0.0020), *c-Fos* (p=0.0015) and *Npas4* (p=0.0004) in SCID mice neuronal culture compared to neuronal cultures of WT (Unpaired two-tailed t-test, n=3). (c) The relative mRNA expression level of *Top2β* (p=0.0767) and candidate IEGs, *c-Fos* (p=0.5092) and *Npas4* (p=0.0017) assessed with qRT-PCR in the untreated neuronal cultures of WT control and SCID mice cultures treated for 60 mins with 15 µM NMDA (Unpaired two-tailed t-test, n=3).

For qRT-PCR experiments, *Gapdh* was used as endogenous control, and the statistical test was performed on delta CT values to assess the significance level. Data is represented as the mean±sem.

6. Discussion

In the first part of this work, using a 14 DIV HCs model system, we, i) for the first time demonstrate the effect of lower concentrations of NMDA and etoposide within 2 hours on neuronal network activity ii) shows the temporal coupling of neuronal activity with IEGs expression, suggesting the involvement of IEGs on the regulation of neuronal network activity iii) report the critical participation of CREB and GluN2B subunit of the NMDAR on IEGs expression. Additionally, from the results of Top2β siRNA, NHEJ inhibition and SCID mice, we show the crucial role of the formation and repair of Top2β mediated DSBs on IEGs expression and neuronal activity.

6.1. NMDAR mediated DNA DSBs govern IEGs expression and regulate neuronal spiking activity

Increasing evidence shows that physiological DSBs generated by Top2β complexes' following activity signal is involved in maintaining synaptic plasticity via promotion of plasticity-related IEGs [8]. As we observed the upregulation of DSBs and IEGs expression in HCs following NMDAR activation (**Figure 8** and **9**), our results support the assumptions of spatio-temporal control of immediate stimulus-coupled transcription in neurons by the formation of activity-dependent DNA breaks within promoters of specific genes. Therefore, DSBs regulated gene expression control seems to be a general mechanism for IEGs induction in neurons.

Previous studies have shown that IEGs show distinct temporal patterns and possess different activation kinetics [39,112]. Following NMDAR activation, we observed slight upregulation in *Egr1* and *c-Jun* expression only after 60 min of NMDA treatment (compare **Figure 8e** and **9c**). Hence, our results show the time-dependent regulation of IEGs expression with low-dose NMDA incubation in 14 DIV HCs.

It has been presented that controlled NMDARs activation could both lead to DSBs in nuclear DNA and cause an increase in neuronal activity in primary cultures without apparently causing significant cell death [113–115]. Following 30 and 60 min of NMDAR activation, we observed the correlation between the increase in DNA DSBs number and *c-Fos*, *Egr1* and *c-Jun* mRNA levels, whose expressions are involved in regulating the firing rate [44,47]. Therefore, we hypothesized that IEGs activation by DSBs induction following NMDARs activation might play a part in regulating prolonged neuronal activity, and the differential expression of these IEGs contributes to specific firing rates in neuronal culture. Hence, we employed an in vitro hippocampal model that allows correlation with functional changes in the neuronal network by MEA recordings and the temporal monitoring of DSBs and gene expression to understand how nuclear DNA lesions in the form of DSBs in response to non-pathological, subtoxic activation levels of NMDARs affect neuronal function. The increase in neuronal activity, as well as *Egr1* and *c-Jun* expression's upregulation, observed after 60 min of NMDA treatment, as compared to 30 min, hints towards the co-relation between dynamics transcription mechanism and neuronal activity (**Figure 8e, 9c and 11b**).

Various studies have shown how hypo and hyperfunction of synaptic-NMDARs contribute to altered

neuronal activity, which has severe implications for neuropathological conditions [116,117]. However, it has also been hinted that persistent NMDAR activity could potentially contribute to synaptic plasticity by altering the amount of metabotropic gamma-Aminobutyric acid (GABAB) receptors (GABABRs) [118]. Hence, continuous NMDAR activity can have both physiological and pathological consequences. While the bath application of NMDA in neurons is known to increase the spiking rate immediately, only a few have reported the impact on neuronal firing frequency in cultures with continuous exposure to NMDA [113]. To our knowledge, no study so far has investigated the changes in neuronal network activity for two or more hours with low-dose NMDA application. Our results are the first one (**Figure 11**) that depicts the changes that take place in spiking activity with low dose NMDA incubation for 2 hours with continuous low dose NMDA incubation of 14 DIV HCs.

Previous work did not observe cell death or CREB deactivation with NMDA concentrations at or below 15 µM [119]. Therefore, we exclude the possibility of NMDA-mediated neurotoxicity during the whole neuronal activity recording period.

6.1.1. CREB and GluN2B subunit regulates IEGs expression by controlling DSBs status following NMDAR activation

Our data from the results of γH2AX and qRT-PCR analysis with CREB inhibitor KG-501 further shows the involvement of CREB for the DSBs expression, ultimately deciding the fate of IEGs such as *c-Fos* and *Egr1* **(Figure 10)**. The role of CREB in neural plasticity is long known [120–123].

Viral transduction of CREB in neurons has been shown to increase the firing rate, thus playing a significant role in LTP [124–126]. With our results, we could provide evidence on how deficits in the CREB signaling pathway influence IEGs expression by DSBs expression, further explaining how CREB can influence neuronal firing.

GluN2B subunit of NMDAR is known to be involved in synaptic plasticity. However, to our knowledge, the molecular mechanism behind subunit conferred plasticity has not been investigated yet. Few studies have shown a link between IEGs and GluN2B activity [127]. However, here (i) using neuronal cell culture, we can clearly show the effect of downregulation of the specific subunit on particular IEGs expression, (ii) the possible influence of the subunit on DNA DSBs, which further control gene expression (**Figure 12** and **13**).

Therefore, our results might explain the possible mechanism why different disease-associated mutations or a differential blockade of NMDAR subunits could lead to further impairment of learning and memory processes [128,129]. The subunit composition of the NMDAR differs dependent on the brain area and developmental stage [130]. In our view, it could be assumed that different subunit compositions could have a varied effect on DSBs mediated IEGs expression and on the cell's electrophysiological activity. We also speculate that the GluN2B subunits and their various mutations could confer different functional properties due to the changes in calcium influx following receptor activation.

6.2. Physiological DNA DSBs are induced by Top2β activity following NMDAR activation

Etoposide hampers the activity of both Top2 isoforms- Top2α and Top2β, leading to the formation of un-ligated cleaved DNA DSBs at the site of Top2 activity. Top2β is involved in regulating the process of transcription in post-mitotic cells [21,23]. Therefore, in the culture of 14 DIV post-mitotic hippocampal neurons, Top2β is the dominant isoform mediating the effects of etoposide. With the observed upregulation in the DNA DSBs status as well as *c-Fos* and *c-Jun* mRNA expression level with etoposide treatment (**Figure 14b**, **15b** and **d**) and the detected downregulation in DSBs number and *c-Fos* expression with ICRF-193 and Top2β siRNA incubation in HCs (**Figure 16b** and **c**), our data confirm and extend the findings of the previous study in which a Top2β-induced formation of activity-induced DNA double-strand breaks within the promoter regions is required for the transcription of a subset of neuronal early response genes that may be crucial for experiential synaptic changes associated with learning and memory [8].

Recent shreds of evidence have shown the importance of Top1 and Top3β in mediating synaptic activity, as blocking these proteins' activity leads to a reduction in miniature excitatory postsynaptic currents (mEPSC) [131] and excitatory postsynaptic potential (EPSP) [132] in neuronal culture. However, how exactly the expression of Top1 and Top3β contributes to regulation in neuronal activity is not well understood. As *c-Fos* is involved in regulating the neuronal firing rate following its activation [44] and induction of temporary DNA DSBs in its promotor region by Top2β activity governs the expression [8] (**Figure 8**, **9, 15** and **16**). Therefore, we speculate that the observed downregulation in *c-Fos* expression with Top2β siRNA and its upregulation with 30 and 60 min of etoposide treatment is correlated with the increase or decrease in neuronal firing rate detected with etoposide and Top2β siRNA incubation (**Figure 15a** and **16d**). Hence, our study could provide new insights on how Top2β mediated DSBs could influence neuronal activity by regulating IEGs expression; however, how exactly IEGs modify neural circuits is still yet to be clear. Further, the increase in neuronal activity observed with continuous incubation of cultures with low dose etoposide for 2 hours also shows the influence of Top2β mediated DSBs on neuronal activity (**Figure 15a**). Our results are a few that give evidence on etoposide-mediated changes in firing rate [133].

Additionally, we also detected an increase in the *Top2β* mRNA expression level in HC cultures treated for 60 min with NMDA compared to cultures where NMDA was not provided (**Figure 18**). Therefore, it is tempting to speculate that the NMDAR activation mediated overall increase in the level of Top2β could further lead to a generation of the higher number of DNA DSBs in the various region of IEGs, consequently promoting the genes expression.

Previously, it has been shown that etoposide induces cell death, but before exerting the cytotoxic effect, there is an increase in AMPA-induced current [133]which further leads to NMDAR activation [134]. This indirect NMDAR activation by etoposide could serve as one of the reasons why a higher number of γH2AX foci was not detected with the combined NMDA and etoposide treatment, compared to etoposide treatment alone (**Figure 14b**). Prolonged exposure to a high etoposide concentration leads to

apoptosis. However, it has been shown that HC's treatment with a low concentration of etoposide for 2 hours does not activate caspase-3-like protease [133]. Therefore, we exclude the possibility of etoposide-mediated toxicity effects on neuronal activity and gene expressions.

The *Top2β* mRNA and IEGs expression level analysis in SCID mice demonstrated that the basal gene expression is downregulated in such a repair-deficient mice model with the absence of the repair. The downregulation in gene expression further could serve as one of the explanations of the cognitive defects associated with SCID mice.

6.3. NHEJ mediated repair of NMDAR induced DNA DSBs governs IEGs expression and neuronal activity

As NHEJ is also crucial for repairing Top2 poisons mediated DNA DSB [135]. This made us speculate on the role of NHEJ in also NMDAR induced DSBs. The DNA-PK complex is one of the main factors in NHEJ regulated repair [136,137]. Therefore, we used a highly selective DNA-PK inhibitor- NU7441 (KU-57788) to interfere in the DSBs repair. Our data suggest the involvement of DNA-PK_{cs} of the NHEJ pathway to repair NMDAR mediated Top2β induced DSBs (**Figure 17**). IEGs expression is quick and transient, such as after stimulation, expression of the *c-Fos* gene peaks at 30-60 min and returns to basal level after 90 min [138]. In the work of Madabhushi et al., 2015, it is shown that activity-induced DSBs are repaired within 2 hours of stimulation[8]. In our MEA analysis results of neuronal activity, we observed the drop-in activity after 60 min of NMDA treatment. Therefore, we speculate that the repair by NHEJ of DSBs at the promotor region of IEGs that mediate neuronal activity takes place after 60 min of initial stimulation in HC.

Npas4 expression is crucial for regulating neuronal firing responses to excitatory transmission by enhancing inhibition [50,139]. In our results, we observed an upregulation in *Npas4* mRNA expression (**Figure 17d**) and a decrease in neuronal firing activity with 80 min of NMDA incubation (**Figure 11**). Therefore, we further speculate that upregulation in *Npas4* expression could also be responsible for reducing spike activity. As we did not observe any upregulation in *Npas4* expression with etoposide treatment, it is tempting to speculate that this increase in *Npas4* mRNA expression is independent of DSBs induction.

Further, the observed upregulation of *c-Fos* expression in SCID mice HCs compared to NMDA-treated WT mice cultures is one of the significant results of our work. Therefore, one could assume that the absence of NHEJ in these mice contributes to the low basal expression of IEGs, and the expression is upregulated with NMDA treatment (**Figure 17e, 18b** and **c)**. Our approach may help to understand further the relationship between DNA repair and neurological defects and the pivotal role that receptor activation mediated transcriptional machinery plays in neurological disorders.

7. Conclusion and Outlook

The result presented in the first part of this work demonstrates that in 14 DIV HCs, NMDAR mediated DSBs are involved in the induction of IEGs expression. Our findings propose that CREB activation following NMDAR stimulation plays an essential role in regulating DSBs status and, consequently, *c-Fos* and *Egr1* mRNA expression level. Further, as suggested by our data, any modification or mutation in the GluN2B subunit of NMDAR could impact the DNA DSBs status and consequently alter the *c-Fos* and *Egr1* expression level, which ultimately can severely affect neuronal function and plasticity.

We further show that the formation and repair of the NMDAR induced DSBs rely on the activity of Top2β and NHEJ, and any perturbation in their activity could further modify the expression of IEGs. This alteration in IEGs expression status is further reflected in a change in the neuronal network activity of 14 DIV HCs. These results cannot be dismissed as a culture-dependent phenomenon since the IEGs expression analysis from SCID mice HCs indicates that changes in the ability to repair activity-induced DNA breaks may have significant pathophysiological effects. Only a few studies in pathological and non-pathological neurodegenerative conditions and disorders have investigated the role of DSBs that regulate neuronal activity. Our data could indicate a link between an impaired or missing DSBs repair with an alteration in IEGs expression and serve as an explanation of cognitive deficits seen in the SCID mice model. The link between induction of physiological DSBs, stimulation of IEGs expression and regulation of neuronal activity identified in this study by employing WT and SCID mice cultures could further be utilized in the therapies of the pathogenic conditions of the CNS.

Taken together, based on our results with HC cultures of WT and SCID mice, we shed light on the receptor-dependent control mechanism of neuronal activity and provide additional evidence for the role of induction and repair of DSBs in neuronal activity by the expression of IEGs. Therefore, our IEG regulation and neuronal activity results could contribute to a better understanding of synaptic plasticity.

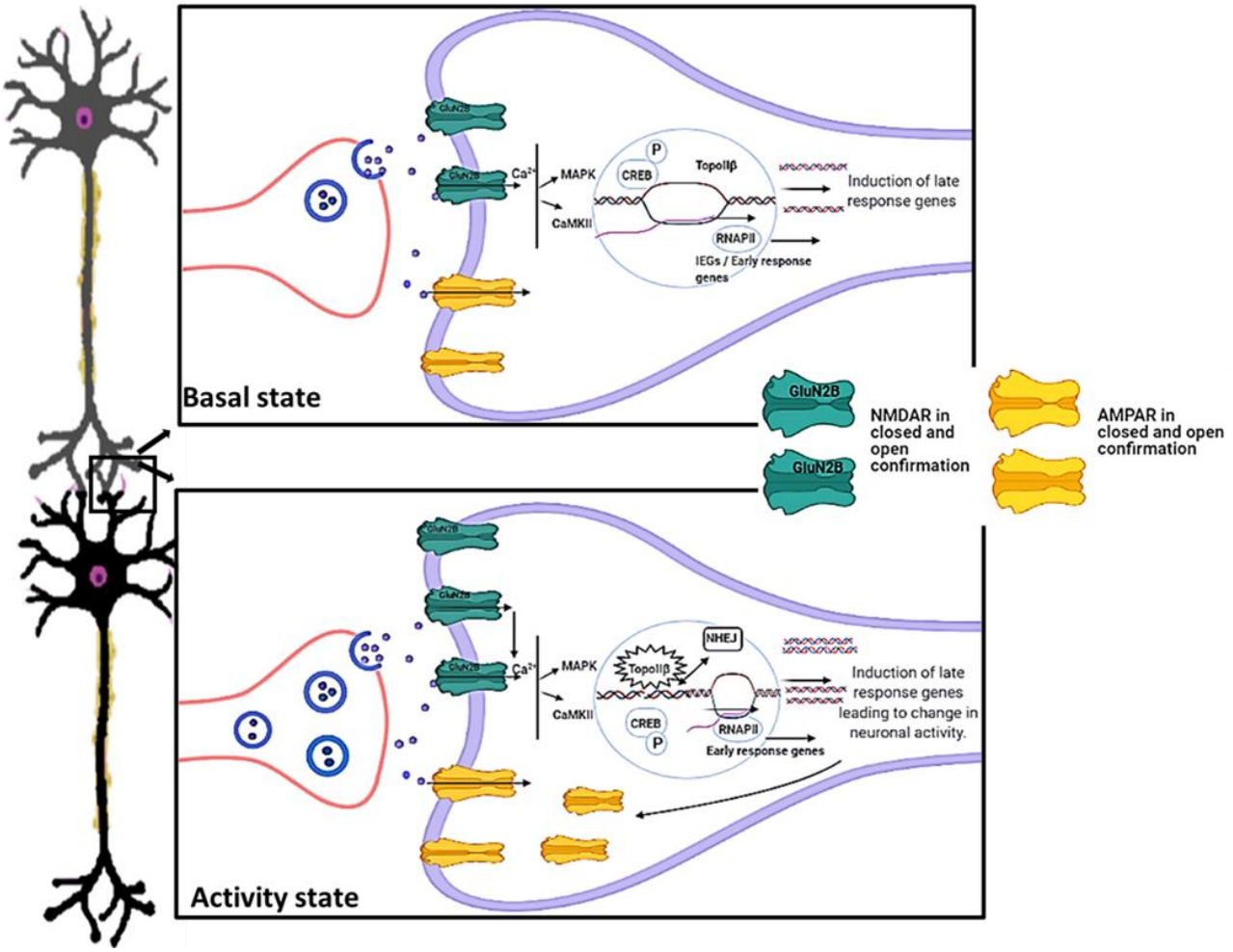

Figure 19: Schematic model of NMDAR generated DSBs mediated IEGs transcription in neurons. In the basal state, following the release of glutamate from the presynaptic receptor, the NMDAR channel opening allowed Ca^{2+} influx leads to the activation of MAPK and CaMKII, which phosphorylate CREB, leading to Top2β catalytic activity and transcription of IEGs or early response genes. In the basal state, the transcription of IEGs or early response genes are not regulated by DSBs; hence the transcription rate remains low. However, in the activity state, Top2β inflicts a DSB into the promoter region of the IEGs, which enables better promotor-enhancer interaction and this interaction, together with CREB activation, allows the paused RNA Pol II to initiate transcription. The activity of NHEJ mediates the repair of these Top2β induced DSBs. Due to the Top2β generated DSB, the transcription rate of the IEGs becomes higher. The IEGs can further lead to activation of different effector genes, ultimately leading to a change in synaptic or neuronal activity. IEGs could be involved in altering synaptic plasticity by the reorganization of the AMPARs on the surface. The GluN2B subunit of the NMDAR plays a role in Ca^{2+} regulation, and hence consequently, the subunit expression governs DSBs and IEGs expression status.

8. Results

8.1. Chapter 2: Investigation of the effect of low dose IR on the regulation of IEGs expression and neuronal activity of 14 DIV HCs

8.1.1. Effect on basal IEGs expression and neuronal activity of HCs after IR exposure

The immediate effect of clinically relevant IR doses, ranging between 0.5 and 2 Gy, on neurons' cellular and physiological status is not known or poorly understood. Therefore, we examined i) the impact of a single dose exposure of 0.5 and 2 Gy on the status of DNA DSBs ii) the effect of radiation on basal IEGs expression and neuronal activity of 14 DIV primary cultures of mice hippocampal neurons, 60 min post-irradiation.

To monitor the DNA DSBs status, the mean number of γH2AX foci per cell were analyzed 60 min-post irradiation in Sham (0 Gy irradiated), and 0.5 or 2 Gy exposed HCs. In general, unirradiated hippocampal neurons had 4.0 ± 0.19 foci per cell, which increased to 1.8 ± 0.15-fold after 0.5 Gy (**Figure 20 a, b**; $p<0.0001$, Mann-Whitney U, n=3;) and to 2.1 ± 0.13-fold after 2 Gy **(Figure 20 c, d**; $p<0.0001$, Mann-Whitney U, n=3). Next, to explore if the radiation exposure affects the basal transcriptional status of IEGs, the expression levels of *c-Fos*, *Egr1* and *c-Jun* mRNA 60 min post-exposure to doses of 0.5 and 2 Gy were analyzed by qRT-PCR. We detected only minor changes in the expression of *c-Fos* and *Egr1* after irradiation with 0.5 Gy (**Figure 21 a**; 0.94 ± 0.09-fold, p=0.95 and 0.93 ± 0.04-fold, p=0.94, unpaired two-sided t-test, n=3, respectively). However, a slight increase in the mRNA expression level of *c-Jun* by 1.14 ± 0.08-fold was found (unpaired two-sided t-test, p=0.9370, n=3). In contrast to 0.5, exposure to a single dose of 2 Gy resulted in a decreased *c-Fos* (0.46 ± 0.06-fold, unpaired two-tailed t-test, p=0.4079, n=3) and *Egr1* mRNA expression level (0.32± 0.03-fold, p=0.0051, unpaired two-tailed t-test, n=3; **Figure 21 b**). Similar to the qRT-PCR results, analysis of c-FOS expression by western blot with 2 Gy revealed a statistically significant and comparable decrease of the protein amount by (0.70 ± 0.07-fold, p=0.0061, unpaired two-tailed t-test, n=3; **Figure 21 c**). Hence, our results showed that only a higher 2 Gy dose exposure reduces the mRNA expression level of *Egr1, c-Fos* and lowers c-FOS protein levels, while a 0.5 exposure was insufficient to change IEG mRNA levels in14 DIV HCs.

As *c-Fos*, as well as *Egr1*, are regulators of neuronal excitability and activity, and we observed a drastic decrease in their mRNA expression level 60 mins post single 2 Gy dose exposure. Hence, we further assessed the mean firing activity in Sham and 2 Gy irradiated cultures. Our results show decreased neuronal network activity 60 min post-exposure in the irradiated group than Sham (0.57 ± 0.13-fold, p=0.0319, unpaired two-tailed t-test, 30 channels, n=3; **Figure 21 d, e**), that is consistent with the role of IEGs in determining neuronal activity. Therefore, our data show that exposure to a 2 Gy IR dose affects *c-Fos* and *Egr1* expression levels as early as 60 min post-exposure. This decrease in IEGs expression level could likely be associated with a reduction in the neuronal firing activity observed in 14 DIV HCs.

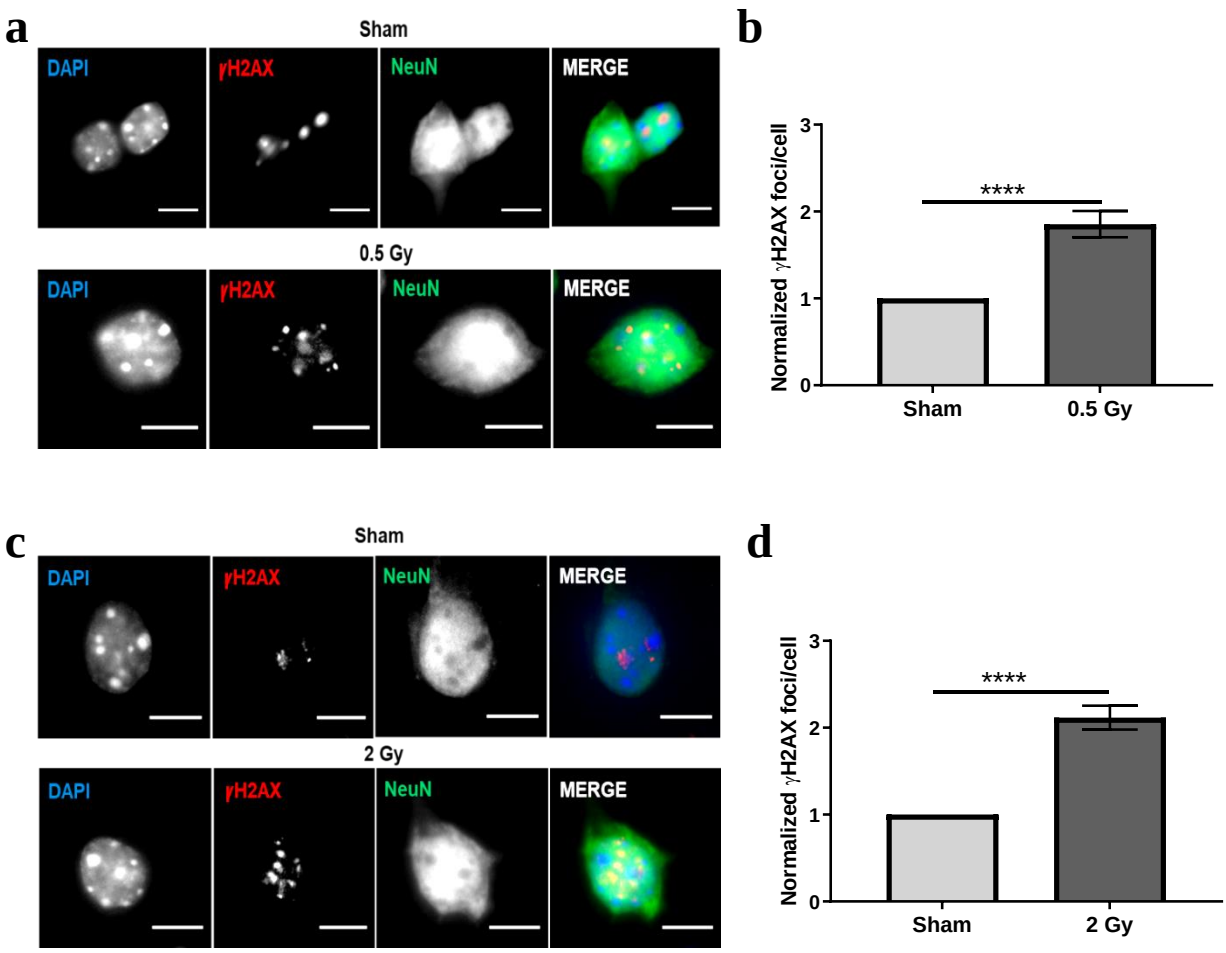

Figure 20: A single dose radiation exposure induced DNA DSBs in 14 DIV HCs. (a,c) DNA DSBs were visualized with γH2AX staining in Sham and 0.5 or 2 Gy irradiated neuronal culture 60 min post-exposure. Scale bar-7μm, DAPI staining for the nucleus, and NeuN as a specific neuronal marker. (b,d) Quantitative γH2AX foci analysis in the indicated samples (Unpaired non-parametric T-test, $p<0.0001$, Mann-Whitney U, n=3).

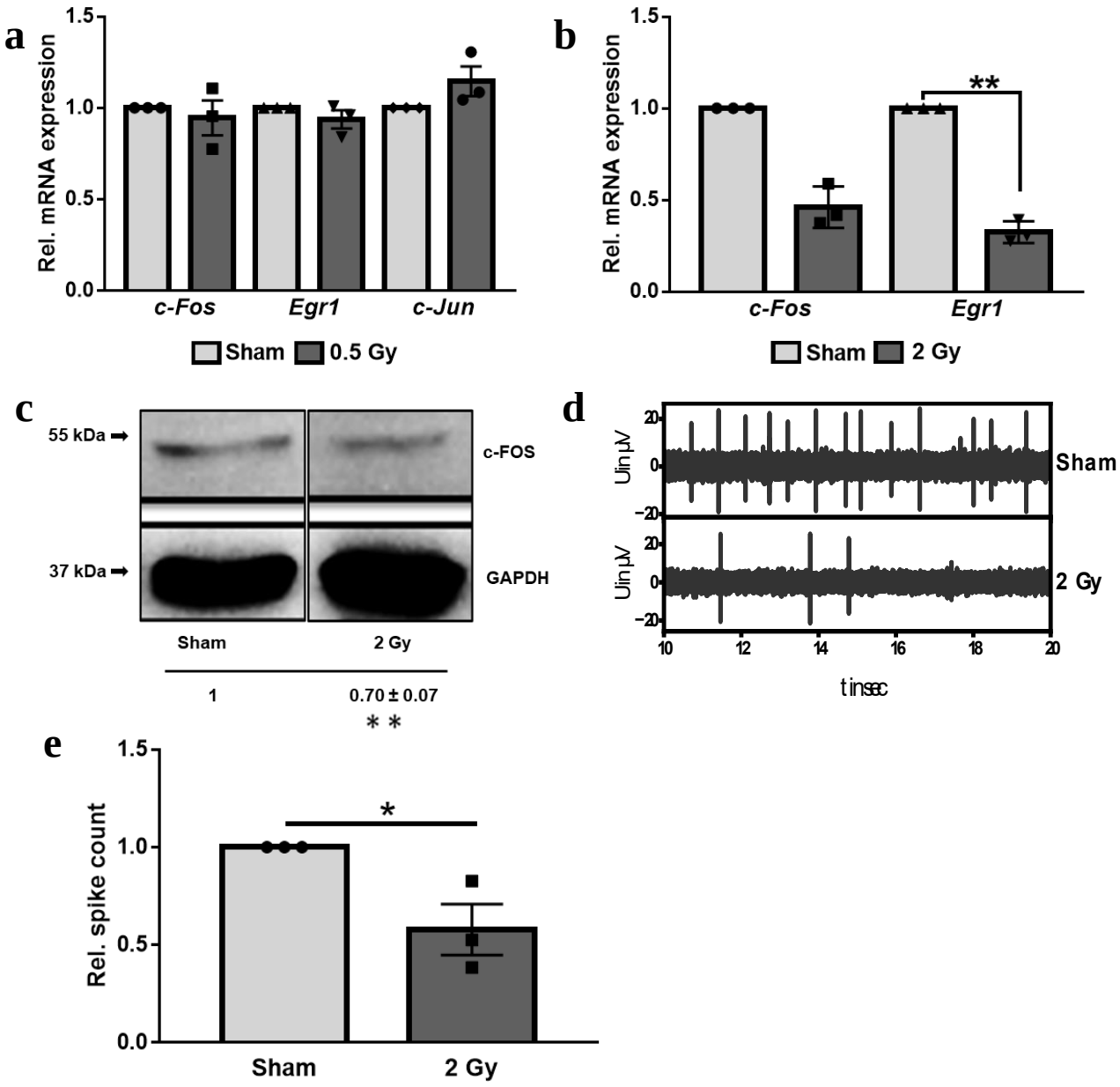

Figure 21: A single dose radiation exposure affects basal IEGs expression and activity of 14 DIV HCs. (a) The relative mRNA level of candidate IEGs (*c-Fos*, *Egr1*, and *c-Jun*) in unirradiated and 0.5 Gy irradiated cultures is represented using a scatter plot with a bar graph. No change in *c-Fos* (p=0.95) and *Egr1* (p=0.94) mRNA expression was detected with single-dose of 0.5 Gy post-60-min exposure; however, the expression level of *c-Jun* (p=0.93) mRNA seems to be upregulated (Unpaired two-tailed t-test, n=3) (b) Exposure to a single 2 Gy dose of radiation followed by analysis after 60 min shows relative low-level mRNA expression of *c-Fos* (p=0.4079) and *Egr1* (p=0.0051) compared to Sham culture (Unpaired two-tailed t-test, n=3). (c) c-FOS protein level assessed in unirradiated and 60 min post 2 Gy irradiated culture (p=0.0061) (Unpaired two-tailed t-test, n=3). (d) Representative, 20-sec firing traces recorded by MEA system in the unirradiated and 2 Gy irradiated cultures 60 min post-exposure. (e) Quantification of average and relative spike numbers recorded over 120 sec in the indicated samples shows how 2 Gy radiation dose leads to decreased neuronal network activity (p=0.0319, unpaired two-tailed t-test, n=3).

For qRT-PCR and Western blot experiments, Gapdh was used as endogenous control. For qRT-PCR result analysis, the statistical test was performed on delta CT values to assess the significance level. Data is represented as the mean±sem.

8.1.2. Effect of 0.5 and 2 Gy IR on NMDA-induced IEGs expression and neuronal activity

Our previous results show that a single 2 Gy dose of IR, in contrast to 0.5 Gy, decreased the basal expression of IEGs after 60 min (**Figure 21**). We now wanted to investigate whether a single 2 Gy IR dose exposure could also affect the IEGs expression induced via NMDA in the same way. Our previous results have shown that after 60 min of treatment with NMDA (15 µM), both *c-Fos* and *Egr1* expression and neuronal activity are increased (**Figure 9c and 11b**). Therefore, we next assessed the *c-Fos* and *Egr1* expression level in the neuronal culture simultaneously treated with 15 µM NMDA and irradiated with 0.5 and 2 Gy and compared the expression level to only NMDA treated culture. We could not detect significant changes in the mRNA expression level of *c-Fos* (1.0 ± 0.39-fold, p=0.8101) and *Egr1* (0.89 ± 0.05-fold, p=0.9192) after a simultaneous NMDA treatment and 0.5 Gy dose exposure (unpaired two-tailed t-test, n=3) (**Figure 22 a**). Thus, similar to the condition where NMDA was absent, the presence of NMDA also did not lead to any changes in IEGs expression in cultures exposed additionally to a 0.5 Gy dose.

Surprisingly, in contrast to the results with 2 Gy where NMDA was not present (**Figure 21 b**), irradiation with 2 Gy in the presence of NMDA did not result in a substantial decrease of *c-Fos* and *Egr1* expression, but in an additional increase of IEG expression by (1.54 ± 0.12-fold, 1.67 ± 0.14-fold; p=0.1087, p=0.0324; unpaired two-sided t-test, n=3) (compare **Figure 22 b** and **Figure 21 b**). These results hint toward an unexpected interaction between NMDAR signaling pathways and 2 Gy-mediated effects diametrically upregulating the expression level of IEGs compared with control conditions.

Recent evidence [8] and our previous results (**Figure 16 and 17**) show that following NMDAR activation, the induction and repair of Top2β-induced DSBs in the promotor region of IEGs, determine both their expression and activity in neurons. As we observed the upregulation in the *c-Fos* and *Egr1* mRNA expression level after 60 min in the cultures incubated simultaneous with NMDA and exposed to 2 Gy dose of IR, therefore, next, we aimed to investigate the status of DNA DSBs in combined treatment and compared the DSBs status to either 2 Gy or NMDA Sham treatment.

Compared to the Sham group, we observed an upregulation of the number of γH2AX foci per cell both in the cultures exposed to 2 Gy by 1.92 ± 0.18-fold (**Figure 23 a, b**; p=0.0003, Kruskal-Wallis one-way ANOVA, n=3) and in the cultures treated with NMDA by 1.86 ± 0.23-fold (**Figure 23 a, b**; p=0.0428, Kruskal-Wallis one-way ANOVA, n=3). However, although we observed a significant increase of 1.74 ± 0.14-fold in the number of γH2AX foci in the combined treatment of NMDA and 2 Gy, compared with only the NMDA-sham (**Figure 23 b**; p<0.0001, Mann-Whitney U, n=3), this was less than the addition of the increases in DSBs in 2 Gy and NMDA treatment alone. This result may suggest that i) NMDA's presence affects the repair of radiation-induced DSBs or ii) IR affects the induction or repair of NMDA-mediated DSBs.

To verify if the increase in DSBs number observed with NMDA incubation is indeed an NMDAR exerted effect, to assess the contribution of NMDAR in γH2AX foci count in cultures treated simultaneously with NMDA and irradiation, and to investigate if GluN2B subunit of NMDAR plays a

role in DSBs induction, cultures were pre-incubated for 60 min with 20 µM Ifenprodil- a GluN2B-selective antagonist followed by 60 min application with NMDA.

The 14 DIV cultures showed prominent GluN2B expression, as observed by immunostaining (**Figure 12 a**). We observed a decrease in DNA DSBs number in the culture pre-treated with Ifenprodil before combined NMDA application and irradiation exposure (0.81 ± 0.07-fold, p=0.0021, Kruskal-Wallis one-way ANOVA, 30 cells in n=3) and in cultures pre-treated with ifenprodil before NMDA application (0.47 ± 0.04-fold, p<0.0001, Kruskal-Wallis one-way ANOVA, 30 cells in n=3; **Figure 24 a, b**), compared to simultaneous NMDA and 2 Gy irradiated groups (values normalized to corresponding values of simultaneous NMDA and 2 Gy irradiated groups).

These results further confirm the finding of emphasizing the importance of the GluN2B subunit of NMDAR for DSBs induction, which may further contribute to altered IEG's expression status.

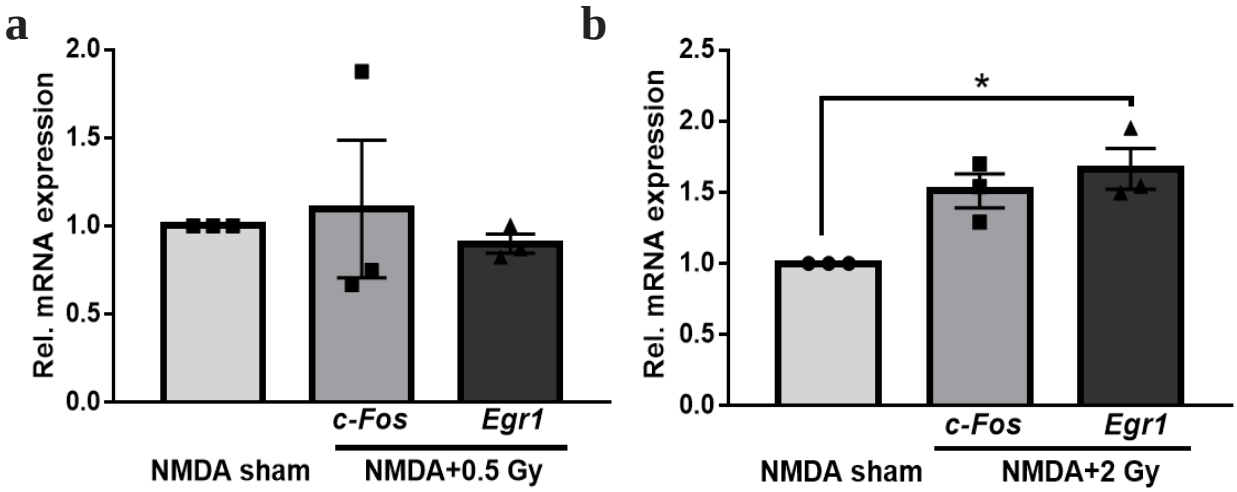

Figure 22: NMDA presence upregulates radiation alleviated IEGs expression level. (a) The graph depicts the relative mRNA expression level of candidate IEGs (*c-Fos* and *Egr1*) in the NMDA sham and combined NMDA, and 0.5 Gy radiated group, 60 min post-exposure. The data shows no to relatively lower changes in the mRNA expression level of *c-Fos* (p=0.8101) and *Egr1* (p=0.9192), indicating no difference exists in the indicated treatments at the gene expression level (unpaired two-tailed t-test, n=3). (b) Relative mRNA level of *c-Fos* (p=0.1087) and *Egr1* (p=0.0324) in the neuronal cultures of NMDA Sham, and in simultaneous NMDA and a single 2 Gy dose radiated culture followed by analysis after 60 min. The results hint toward an interaction between NMDAR mediated signaling pathway and radiation upregulating IEGs expression level (unpaired two-tailed t-test, n=3).

For qRT-PCR experiments, *Gapdh* was used as endogenous control, and the statistical test was performed on delta CT values to assess the significance level. Data is represented as the mean±sem.

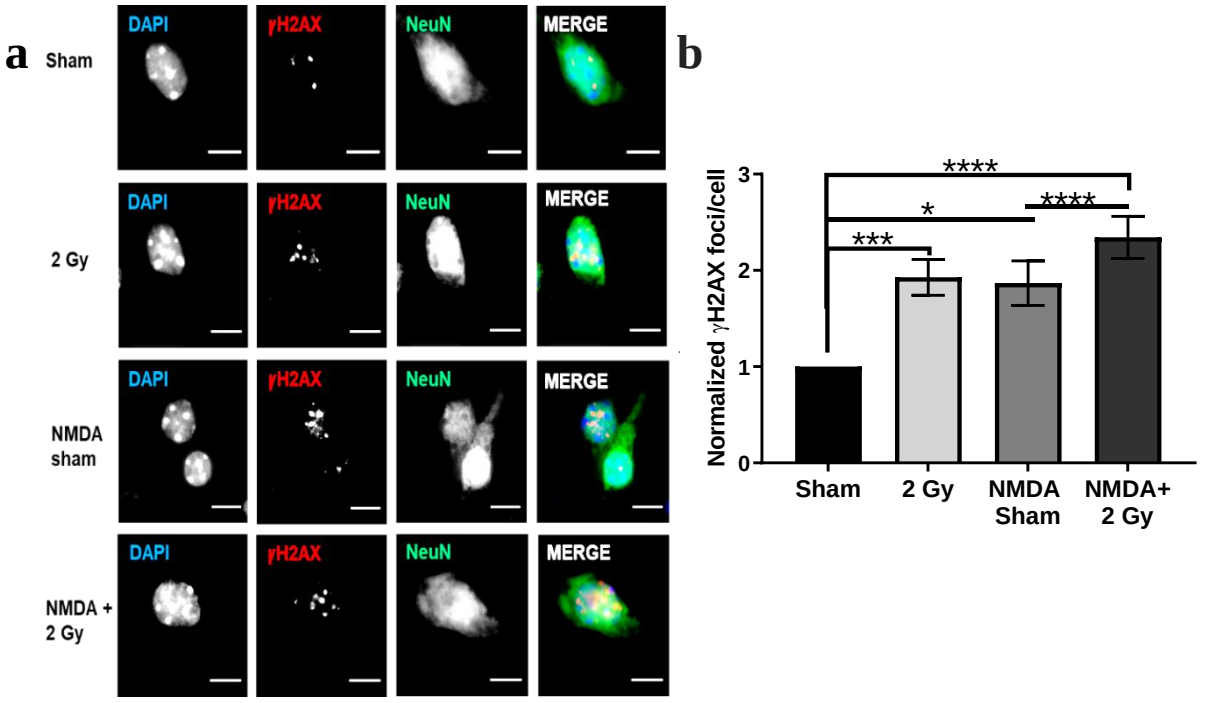

Figure 23: DNA DSBs analysis with NMDA treatment and radiation exposure. (a, b) Fluorescence images demonstrate staining against γH2AX in unirradiated, 2 Gy irradiated, NMDA unirradiated, and combined NMDA treated along with 2 Gy irradiated neuronal cultures. Nucleus stained for DAPI. Neurons stained with mature neuron marker NeuN. Scale bar-7μm. Quantitative foci analysis in the indicated samples (One way-ANOVA; Sham and 2 Gy, p value=0.0003; Sham and NMDA Sham, p value=0.0428; Sham and NMDA+2 Gy, p value<0.0001; unpaired non-parametric T-test, NMDA Sham and NMDA+2 Gy, p value<0.0001, 60 cells, n=3).
Data is represented as the mean±sem.

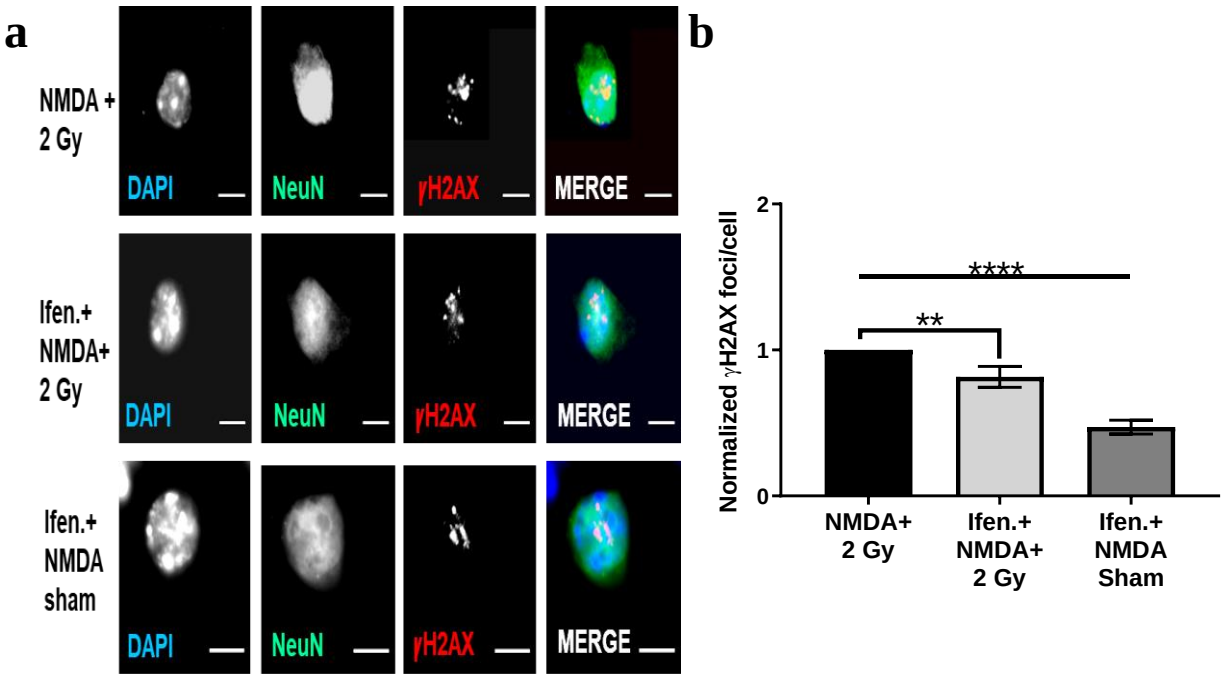

Figure 24: GluN2B subunit influences DNA DSBs status of 14 DIV HCs. (a, b) DNA DSBs visualized with γH2AX staining in combined NMDA and 2 Gy irradiated neuronal culture and in cultures pre-treated with Ifenprodil followed by 60 min post-exposure analysis. DAPI staining for the nucleus and NeuN as a neuron-specific marker. Quantitative γH2AX foci analysis in the indicated samples (One way-ANOVA; NMDA+ 2 Gy with Ifen. + NMDA+2 Gy, p value=0.0021; NMDA+2 Gy with Ifen. + NMDA Sham, p-value <0.0001, 30 cells, n=3).
Data is represented as the mean±sem. Scale bar-7μm.

9. Discussion

In the second part of the work, using a hippocampal neuron culture aged 14 DIV, we could show for the first time that i) exposure to a single 2 Gy dose of IR leads to a downregulation in *c-Fos* and *Egr1* expression level ii) a single dose of 2 Gy is sufficient to alter neuronal spiking rate as early as 60 min post-exposure iii) addition of NMDA alongside 2 Gy IR dose exposure leads to upregulation of radiation alleviated *c-Fos* and *Egr1* mRNA expression level iv) NMDA's presence influences the status of irradiation-induced DNA DSBs.

9.1. A single 2 Gy IR dose alters IEGs expression and neuronal activity of 14 DIV HC

Previous work has shown that a dose as low as 0.25 Gy could upregulate *c-Fos* expression level [94,140]. In contrast, others could not find any upregulation in *c-Fos* expression levels at such a low-radiation dose in their respective analyzed culture [141]. Therefore, the changes that occur in IEG's expression after irradiation are complex to define, as their expression level depends on factors such as examined tissue, irradiation dose, and the time after which the gene expression is monitored.

It has been shown that acute radiation exposure leads to alteration in synapse morphology [99]. Since *c-Fos* and *Egr1* expression are associated with synaptic plasticity [35], it becomes interesting to check these IEG's expression in neuronal culture with different radiation doses. However, till now, no study has analyzed the expression of these IEGs in mice neuronal culture. In our results, we could not detect any alteration in both basal *c-Fos* and *Egr1* expression levels with a single dose of 0.5 Gy (**Figure 21a**). As these genes' expression has been associated with stress-response [95] or synaptic plasticity [35], we assume that one single dose of 0.5 Gy is insufficient to induce in neuronal cultures alteration in any of the two processes. Additionally, the upregulation observed in *c-Jun* expression in the HCs with a 0.5 Gy dose, as reported by other previous work [94], suggests the critical involvement of such IEG in the early cellular event following radiation exposure. The association between ≤2.0 Gy radiation dose and alterations in cognitive functions has been shown by previous work[142,143].

As *c-Fos* and *Egr1* are critical for synaptic plasticity, a mechanism essential for cognitive function [40,47], we further analyzed the expression of these IEGs in mice HCs with a single 2 Gy dose exposure. In our study, we could observe a downregulatory effect of 2 Gy dose on basal mRNA expression levels of both *c-Fos* and *Egr1* (**Figure 21b**). Our results are consistent with the previous work, where a reduction in the *c-Fos* and *Egr1* expression level in mice brains was also observed with 1 and 10 Gy radiation dose exposure [99,144]. It is well-known that CREB activation and phosphorylation play an essential role in the initiation of *c-Fos* and *Egr1* expression [145–148]. Further, it has also been shown that radiation downregulates phosphorylated and total CREB expression levels [99,149]. Therefore, we hypothesize that the reduction observed in basal *c-Fos* and *Egr1* expression could be attributed to radiation-induced CREB downregulation. As these genes are essential for synaptic plasticity, reduction in these gene expressions, as seen with 2 Gy dose, could explain how radiation could be involved in

cognitive impairments. The *c-Fos* and *Egr1* gene expression are associated with neuronal activity and excitability[44,47,150]. Further, it has been shown that exposure to varying doses of IR creates acute alteration in CNS activity[151–153]. However, mechanisms underlying radiation-induced neuronal alterations are not well understood. Depending on the dose and time after which activity is analyzed, multiple factors might be responsible for neuronal activity alteration. As we observed a downregulation in both c-*Fos* and *Egr1* expression in our results with irradiation, we further analyzed the HCs neuronal network activity. Our results show that a single dose of 2 Gy is sufficient to alter the neuronal network activity post 60 min radiation exposure, hinting towards the role of IEGs in mediating neuronal excitability following radiation exposure (**Figure 21 e**). These findings also raise the critical question on the association between cumulative radiation dose and IEGs expression affecting neuronal activity.

9.2. NMDA presence upregulates radiation alleviated IEGs expression level

Our data show that in the presence of NMDA, exposure to 2 Gy radiation dose upregulates radiation alleviated IEGs expression level, and the expression level of *c-Fos* and *Egr1* mRNA is higher than in the only NMDA treated group (**Figure 22 b**). We speculate that decreased expression of *c-Fos* and *Egr1* mRNA observed with a single 2 Gy dose radiation exposure is an attribute of decreased CREB phosphorylation level, and the expression level is elevated following NMDA treatment.

We further hypothesize that increased IEGs expression observed with combined NMDA treatment and 2 Gy radiation exposure could be due to temporal modification in chromatin structure following NMDA treatment, further making the chromatin relaxed [154] and certain genes regions to become more accessible to radiation-induced DNA DSBs damage. The observed increase in the number of DNA DSBs with combined treatment and decrease in the number with Ifenprodil pre-incubation (**Figure 23 and 24**) further hints toward the association between NMDAR mediated remodeling and radiation-associated damage upregulation in *c-Fos* and *Egr1* expression.

10. Conclusion and outlook

In the second part of our work, we demonstrate for the first time that a single dose of 2 Gy in 14 DIV neuronal cultures is sufficient to cause downregulation in IEGs expression level and consequently the neuronal activity within 60 min post-radiation exposure. Until now, the immediate effect of low-dose IR on neuronal gene expression and function is not understood. As IEGs are involved in cognitive functions, our study hints at how acute IR at clinically relevant doses could be engaged in learning and memory impairment. Although *c-Fos* expression has been analyzed in various studies after exposure to different doses of radiation, only a few studies have dealt with alteration in *Egr1* expression level analysis with low dose IR exposure. This is the first report that presents the immediate effects of 0.5 and 2 Gy IR doses on the IEGs expression and neuronal spiking rate of HC cultures.

Further, our results from the combined NMDA treatment and 2 Gy radiation exposure suggest that an unexpected interaction occurs between NMDAR signaling pathways and 2 Gy-mediated effects diametrically upregulating the expression level of IEGs compared with control conditions. Our results are the first one that provides evidence on the interaction of NMDAR with low dose IR exposure, affecting IEGs expression level. No other data to our knowledge has reported this interaction; however, the future study of this interaction between receptor and irradiation signaling pathway could help develop potential strategies to manage radiation-induced brain injury.

Taken together, the results of our data help to elucidate the role of physiological and pathological induced DNA DSBs in neuronal gene expression and function, which could further have a significant effect on neuronal plasticity.

11. Literature

1. Thompson LH, Schild D. Homologous recombinational repair of DNA ensures mammalian chromosome stability. *Mutation Research - Fundamental and Molecular Mechanisms of Mutagenesis* 2001, DOI: 10.1016/S0027-5107(01)00115-4.
2. Lieber MR. The mechanism of human nonhomologous DNA End joining. *Journal of Biological Chemistry* 2008, DOI: 10.1074/jbc.R700039200.
3. Mao Z, Bozzella M, Seluanov A *et al.* DNA repair by nonhomologous end joining and homologous recombination during cell cycle in human cells. *Cell Cycle* 2008, DOI: 10.4161/cc.7.18.6679.
4. Katyal S, McKinnon PJ. DNA strand breaks, neurodegeneration and aging in the brain. *Mechanisms of Ageing and Development* 2008, DOI: 10.1016/j.mad.2008.03.008.
5. Oster S, Aqeilan RI. Programmed DNA Damage and Physiological DSBs: Mapping, Biological Significance and Perturbations in Disease States. *Cells* 2020, DOI: 10.3390/cells9081870.
6. Khan FA, Ali SO. Physiological Roles of DNA Double-Strand Breaks. *Journal of Nucleic Acids* 2017, DOI: 10.1155/2017/6439169.
7. van Gent DC, van der Burg M. Non-homologous end-joining, a sticky affair. *Oncogene* 2007, DOI: 10.1038/sj.onc.1210871.
8. Madabhushi R, Gao F, Pfenning AR *et al.* Activity-Induced DNA Breaks Govern the Expression of Neuronal Early-Response Genes. *Cell* 2015, DOI: 10.1016/j.cell.2015.05.032.
9. Bellesi M, Bushey D, Chini M *et al.* Contribution of sleep to the repair of neuronal DNA double-strand breaks: Evidence from flies and mice. *Scientific Reports* 2016, DOI: 10.1038/srep36804.
10. Shanbhag NM, Evans MD, Mao W *et al.* Early neuronal accumulation of DNA double strand breaks in Alzheimer's disease. *Acta Neuropathologica Communications* 2019, DOI: 10.1186/s40478-019-0723-5.
11. Alt FW, Schwer B. DNA double-strand breaks as drivers of neural genomic change, function, and disease. *DNA Repair* 2018, DOI: 10.1016/j.dnarep.2018.08.019.
12. Pommier Y, Sun Y, Huang SYN *et al.* Roles of eukaryotic topoisomerases in transcription, replication and genomic stability. *Nature Reviews Molecular Cell Biology* 2016, DOI: 10.1038/nrm.2016.111.
13. Austin CA, Lee KC, Swan RL *et al.* TOP2B: The first thirty years. *International Journal of Molecular Sciences* 2018, DOI: 10.3390/ijms19092765.
14. Jain C, Majumder H, Roychoudhury S. Natural Compounds as Anticancer Agents Targeting DNA Topoisomerases. *Current Genomics* 2016, DOI: 10.2174/1389202917666160808125213.
15. Nitiss JL. DNA topoisomerase II and its growing repertoire of biological functions. *Nature Reviews Cancer* 2009, DOI: 10.1038/nrc2608.
16. Deweese JE, Osheroff N. The DNA cleavage reaction of topoisomerase II: Wolf in sheep's clothing. *Nucleic Acids Research* 2009, DOI: 10.1093/nar/gkn937.
17. Nitiss JL. Targeting DNA topoisomerase II in cancer chemotherapy. *Nature Reviews Cancer* 2009, DOI: 10.1038/nrc2607.
18. Montecucco A, Zanetta F, Biamonti G. Molecular mechanisms of etoposide. *EXCLI Journal* 2015, DOI: 10.17179/excli2014-561.
19. Roca J, Ishida R, Berger JM *et al.* Antitumor bisdioxopiperazines inhibit yeast DNA topoisomerase II by trapping the enzyme in the form of a closed protein clamp. *Proceedings of the National Academy of Sciences of the United States of America* 1994, DOI: 10.1073/pnas.91.5.1781.
20. Capranico G, Tinelli S, Austin CA *et al.* Different patterns of gene expression of topoisomerase II isoforms in differentiated tissues during murine development. *BBA - Gene Structure and Expression* 1992, DOI: 10.1016/0167-4781(92)90050-A.
21. Tiwari VK, Burger L, Nikoletopoulou V *et al.* Target genes of Topoisomerase IIβ regulate neuronal survival and are defined by their chromatin state. *Proceedings of the National Academy of Sciences of the United States of America* 2012, DOI: 10.1073/pnas.1119798109.
22. Madabhushi R. The roles of DNA topoisomerase IIβ in transcription. *International Journal of Molecular Sciences* 2018, DOI: 10.3390/ijms19071917.
23. Lyu YL, Lin C-P, Azarova AM *et al.* Role of Topoisomerase IIβ in the Expression of Developmentally RegulatedGenes. *Molecular and Cellular Biology* 2006, DOI: 10.1128/mcb.00617-06.
24. Yang X. DNA topoisomerase IIβ and neural development. *Science* 2000, DOI:

10.1126/science.287.5450.131.
25. Lyu YL, Wang JC. Aberrant lamination in the cerebral cortex of mouse embryos lacking DNA topoisomerase IIβ. *Proceedings of the National Academy of Sciences of the United States of America* 2003, DOI: 10.1073/pnas.1232376100.
26. Morimoto S, Tsuda M, Bunch H *et al.* Type II DNA topoisomerases cause spontaneous double-strand breaks in genomic DNA. *Genes* 2019, DOI: 10.3390/genes10110868.
27. Haffner MC, Aryee MJ, Toubaji A *et al.* Androgen-induced TOP2B-mediated double-strand breaks and prostate cancer gene rearrangements. *Nature Genetics* 2010, DOI: 10.1038/ng.613.
28. Trotter KW, King HA, Archer TK. Glucocorticoid Receptor Transcriptional Activation via the BRG1-Dependent Recruitment of TOP2β and Ku70/86. *Molecular and Cellular Biology* 2015, DOI: 10.1128/mcb.00230-15.
29. Ju BG, Lunyak V v., Perissi V *et al.* A topoisomerase IIβ-mediated dsDNA break required for regulated transcription. *Science* 2006, DOI: 10.1126/science.1127196.
30. Bétermier M, Bertrand P, Lopez BS. Is Non-Homologous End-Joining Really an Inherently Error-Prone Process? *PLoS Genetics* 2014, DOI: 10.1371/journal.pgen.1004086.
31. Adachi N, Iiizumi S, So S *et al.* Genetic evidence for involvement of two distinct nonhomologous end-joining pathways in repair of topoisomerase II-mediated DNA damage. *Biochemical and Biophysical Research Communications* 2004, DOI: 10.1016/j.bbrc.2004.04.099.
32. Davis AJ, Chen DJ. DNA double strand break repair via non-homologous end-joining. *Translational Cancer Research* 2013, DOI: 10.3978/j.issn.2218-676X.2013.04.02.
33. Kinner A, Wu W, Staudt C *et al.* Gamma-H2AX in recognition and signaling of DNA double-strand breaks in the context of chromatin. *Nucleic acids research* 2008, DOI: 10.1093/nar/gkn550.
34. Cooke SF, Bliss TVP. Plasticity in the human central nervous system. *Brain* 2006, DOI: 10.1093/brain/awl082.
35. Minatohara K, Akiyoshi M, Okuno H. Role of immediate-early genes in synaptic plasticity and neuronal ensembles underlying the memory trace. *Frontiers in Molecular Neuroscience* 2016, DOI: 10.3389/fnmol.2015.00078.
36. Watson RJ, Clements JB. A herpes simplex virus type 1 function continuously required for early and late virus RNA synthesis. *Nature* 1980, DOI: 10.1038/285329a0.
37. Okuno H. Regulation and function of immediate-early genes in the brain: Beyond neuronal activity markers. *Neuroscience Research* 2011, DOI: 10.1016/j.neures.2010.12.007.
38. Akins PT, Liu PK, Hsu CY. Immediate early gene expression in response to cerebral ischemia: Friend or foe? *Stroke* 1996, DOI: 10.1161/01.STR.27.9.1682.
39. Kim S, Kim H, Um JW. Synapse development organized by neuronal activity-regulated immediate-early genes. *Experimental and Molecular Medicine* 2018, DOI: 10.1038/s12276-018-0025-1.
40. Gallo FT, Katche C, Morici JF *et al.* Immediate early genes, memory and psychiatric disorders: Focus on c-Fos, Egr1 and Arc. *Frontiers in Behavioral Neuroscience* 2018, DOI: 10.3389/fnbeh.2018.00079.
41. Sheng M, Greenberg ME. The regulation and function of c-fos and other immediate early genes in the nervous system. *Neuron* 1990, DOI: 10.1016/0896-6273(90)90106-P.
42. Kleim JA, Lussnig E, Schwarz ER *et al.* Synaptogenesis and FOS expression in the motor cortex of the adult rat after motor skill learning. *Journal of Neuroscience* 1996, DOI: 10.1523/jneurosci.16-14-04529.1996.
43. Cirelli C, Tononi G. On the functional significance of c-fos induction during the sleep- waking cycle. *Sleep* 2000, DOI: 10.1093/sleep/23.4.9.
44. Zhang J, Zhang D, McQuade JS *et al.* c-fos regulates neuronal excitability and survival. *Nature Genetics* 2002, DOI: 10.1038/ng859.
45. Han S, Hong S, Mo J *et al.* Impaired extinction of learned contextual fear memory in early growth response 1 knockout mice. *Molecules and Cells* 2014, DOI: 10.14348/molcells.2014.2206.
46. Maddox SA, Monsey MS, Schafe GE. Early growth response gene 1 (Egr-1) is required for new and reactivated fear memories in the lateral amygdala. *Learning and Memory* 2011, DOI: 10.1101/lm.1980211.
47. Duclot F, Kabbaj M. The role of early growth response 1 (EGR1) in brain plasticity and neuropsychiatric disorders. *Frontiers in Behavioral Neuroscience* 2017, DOI: 10.3389/fnbeh.2017.00035.
48. Adams KW, Kletsov S, Lamm RJ *et al.* Role for egr1 in the transcriptional program associated

with neuronal differentiation of pc12 cells. *PLoS ONE* 2017, DOI: 10.1371/journal.pone.0170076.
49. Datta R, Rubin E, Sukhatme V *et al.* Ionizing radiation activates transcription of the EGR1 gene via CArG elements. *Proceedings of the National Academy of Sciences of the United States of America* 1992, DOI: 10.1073/pnas.89.21.10149.
50. Lin Y, Bloodgood BL, Hauser JL *et al.* Activity-dependent regulation of inhibitory synapse development by Npas4. *Nature* 2008, DOI: 10.1038/nature07319.
51. Spiegel I, Mardinly AR, Gabel HW *et al.* Npas4 regulates excitatory-inhibitory balance within neural circuits through cell-type-specific gene programs. *Cell* 2014, DOI: 10.1016/j.cell.2014.03.058.
52. Sun X, Lin Y. Npas4: Linking Neuronal Activity to Memory. *Trends in Neurosciences* 2016, DOI: 10.1016/j.tins.2016.02.003.
53. Malik AN, Vierbuchen T, Hemberg M *et al.* Genome-wide identification and characterization of functional neuronal activity-dependent enhancers. *Nature Neuroscience* 2014, DOI: 10.1038/nn.3808.
54. Suberbielle E, Sanchez PE, Kravitz A v. *et al.* Physiologic brain activity causes DNA double-strand breaks in neurons, with exacerbation by amyloid-β. *Nature Neuroscience* 2013, DOI: 10.1038/nn.3356.
55. Bliss TVP, Collingridge GL. A synaptic model of memory: Long-term potentiation in the hippocampus. *Nature* 1993, DOI: 10.1038/361031a0.
56. Mayer ML. Glutamate receptor ion channels. *Current Opinion in Neurobiology* 2005, DOI: 10.1016/j.conb.2005.05.004.
57. Hansen KB, Yi F, Perszyk RE *et al.* Structure, function, and allosteric modulation of NMDA receptors. *Journal of General Physiology* 2018, DOI: 10.1085/jgp.201812032.
58. Gambrill AC, Barria A. NMDA receptor subunit composition controls synaptogenesis and synapse stabilization. *Proceedings of the National Academy of Sciences of the United States of America* 2011, DOI: 10.1073/pnas.1012676108.
59. Foster KA, McLaughlin N, Edbauer D *et al.* Distinct roles of NR2A and NR2B cytoplasmic tails in long-term potentiation. *Journal of Neuroscience* 2010, DOI: 10.1523/JNEUROSCI.4022-09.2010.
60. Sprengel R, Suchanek B, Amico C *et al.* Importance of the intracellular domain of NR2 subunits for NMDA receptor function in vivo. *Cell* 1998, DOI: 10.1016/S0092-8674(00)80921-6.
61. Cui Z, Feng R, Jacobs S *et al.* Increased NR2A:NR2B ratio compresses long-term depression range and constrains long-term memory. *Scientific Reports* 2013, DOI: 10.1038/srep01036.
62. Tajima N, Karakas E, Grant T *et al.* Activation of NMDA receptors and the mechanism of inhibition by ifenprodil. *Nature* 2016, DOI: 10.1038/nature17679.
63. Song X, Jensen MO, Jogini V *et al.* Mechanism of NMDA receptor channel block by MK-801 and memantine. *Nature* 2018, DOI: 10.1038/s41586-018-0039-9.
64. Wang JQ, Guo ML, Jin DZ *et al.* Roles of subunit phosphorylation in regulating glutamate receptor function. *European Journal of Pharmacology* 2014, DOI: 10.1016/j.ejphar.2013.11.019.
65. Regan MC, Romero-Hernandez A, Furukawa H. A structural biology perspective on NMDA receptor pharmacology and function. *Current Opinion in Structural Biology* 2015, DOI: 10.1016/j.sbi.2015.07.012.
66. Mayer ML, Westbrook GL, Guthrie PB. Voltage-dependent block by Mg2+ of NMDA responses in spinal cord neurones. *Nature* 1984, DOI: 10.1038/309261a0.
67. Blanke ML, VanDongen AMJ. Activation mechanisms of the NMDA receptor. *Biology of the NMDA Receptor*. 2008.
68. Kornhauser JM, Cowan CW, Shaywitz AJ *et al.* CREB transcriptional activity in neurons is regulated by multiple, calcium-specific phosphorylation events. *Neuron* 2002, DOI: 10.1016/S0896-6273(02)00655-4.
69. Petralia RS, Wang YX, Hua F *et al.* Organization of NMDA receptors at extrasynaptic locations. *Neuroscience* 2010, DOI: 10.1016/j.neuroscience.2010.01.022.
70. Tovar KR, Westbrook GL. The incorporation of NMDA receptors with a distinct subunit composition at nascent hippocampal synapses in vitro. *Journal of Neuroscience* 1999, DOI: 10.1523/jneurosci.19-10-04180.1999.
71. Hardingham GE, Fukunaga Y, Bading H. Extrasynaptic NMDARs oppose synaptic NMDARs by triggering CREB shut-off and cell death pathways. *Nature Neuroscience* 2002, DOI: 10.1038/nn835.
72. Levine MS, Cepeda C, André VM. Location, Location, Location: Contrasting Roles of Synaptic and Extrasynaptic NMDA Receptors in Huntington's Disease. *Neuron* 2010, DOI: 10.1016/j.neuron.2010.01.010.
73. Zhou X, Hollern D, Liao J *et al.* NMDA receptor-mediated excitotoxicity depends on the

coactivation of synaptic and extrasynaptic receptors. *Cell Death and Disease* 2013, DOI: 10.1038/cddis.2013.82.
74. Greenberg ME, Thompson MA, Sheng M. Calcium regulation of immediate early gene transcription. *Journal of Physiology - Paris* 1992, DOI: 10.1016/S0928-4257(05)80013-0.
75. Wang H, Peng RY. Basic roles of key molecules connected with NMDAR signaling pathway on regulating learning and memory and synaptic plasticity. *Military Medical Research* 2016, DOI: 10.1186/s40779-016-0095-0.
76. El-Husseini AE, Schnell E, Chetkovich DM *et al.* PSD-95 involvement in maturation of excitatory synapses. *Science (New York, NY)* 2000, DOI: 10.1126/science.290.5495.1364.
77. Gardoni F, Polli F, Cattabeni F *et al.* Calcium-calmodulin-dependent protein kinase II phosphorylation modulates PSD-95 binding to NMDA receptors. *European Journal of Neuroscience* 2006, DOI: 10.1111/j.1460-9568.2006.05140.x.
78. Fukunaga K, Miyamoto E. A working model of CaM kinase II activity in hippocampal long-term potentiation and memory. *Neuroscience Research* 2000, DOI: 10.1016/S0168-0102(00)00139-5.
79. Skeberdis VA, Chevaleyre V, Lau CG *et al.* Protein kinase A regulates calcium permeability of NMDA receptors. *Nature Neuroscience* 2006, DOI: 10.1038/nn1664.
80. Hickling S, Xiang L, Jones KC *et al.* Ionizing radiation-induced acoustics for radiotherapy and diagnostic radiology applications. *Medical Physics* 2018, DOI: 10.1002/mp.12929.
81. Do KH. General principles of radiation protection in fields of diagnostic medical exposure. *Journal of Korean Medical Science* 2016, DOI: 10.3346/jkms.2016.31.S1.S6.
82. Reisz JA, Bansal N, Qian J *et al.* Effects of ionizing radiation on biological molecules - mechanisms of damage and emerging methods of detection. *Antioxidants and Redox Signaling* 2014, DOI: 10.1089/ars.2013.5489.
83. Abbott A. Researchers pin down risks of low-dose radiation. *Nature* 2015, DOI: 10.1038/523017a.
84. Lindburg CA, Willey JS, Dean D. Effects of low dose X-ray irradiation on porcine articular cartilage explants. *Journal of Orthopaedic Research* 2013, DOI: 10.1002/jor.22406.
85. Cash H, Dean D. The effects of low-dose radiation on articular cartilage: A review. *Journal of Biological Engineering* 2019, DOI: 10.1186/s13036-018-0125-4.
86. Fry RJM, Hall EJ. Radiobiology for the Radiologist. *Radiation Research* 1995, DOI: 10.2307/3579017.
87. Azzam EI, Jay-Gerin JP, Pain D. Ionizing radiation-induced metabolic oxidative stress and prolonged cell injury. *Cancer Letters* 2012, DOI: 10.1016/j.canlet.2011.12.012.
88. Hall P, Adami HO, Trichopoulos D *et al.* Effect of low doses of ionising radiation in infancy on cognitive function in adulthood: Swedish population based cohort study. *British Medical Journal* 2004, DOI: 10.1136/bmj.328.7430.19.
89. Collett G, Craenen K, Young W *et al.* The psychological consequences of (perceived) ionizing radiation exposure: a review on its role in radiation-induced cognitive dysfunction. *International Journal of Radiation Biology* 2020, DOI: 10.1080/09553002.2020.1793017.
90. Lowe XR, Bhattacharya S, Marchetti F *et al.* Early brain response to low-dose radiation exposure involves molecular networks and pathways associated with cognitive functions, advanced aging and alzheimer's disease. *Radiation Research* 2009, DOI: 10.1667/RR1389.1.
91. Sherman ML, Datta R, Hallahan DE *et al.* Ionizing radiation regulates expression of the c-jun protooncogene. *Proceedings of the National Academy of Sciences of the United States of America* 1990, DOI: 10.1073/pnas.87.15.5663.
92. Calaf GM, Hei TK. Ionizing radiation induces alterations in cellular proliferation and c-myc, c-jun and c-fos protein expression in breast epithelial cells. *International journal of oncology* 2004, DOI: 10.3892/ijo.25.6.1859.
93. Woloschak GE, Chang-Liu CM, Jones PS *et al.* Modulation of Gene Expression in Syrian Hamster Embryo Cells following Ionizing Radiation. *Cancer Research* 1990.
94. Prasad A v., Mohan N, Chandrasekar B *et al.* Induction of transcription of "immediate early genes" by low-dose ionizing radiation. *Radiation Research* 1995, DOI: 10.2307/3579212.
95. Weichselbaum RR, Hallahan D, Fuks Z *et al.* Radiation induction of immediate early genes: Effectors of the radiation-stress response. *International Journal of Radiation Oncology, Biology, Physics* 1994, DOI: 10.1016/0360-3016(94)90539-8.
96. Martin M, Vozenin MC, Gault N *et al.* Coactivation of AP-1 activity and TGF-β1 gene expression in the stress response of normal skin cells to ionizing radiation. *Oncogene* 1997, DOI: 10.1038/sj.onc.1201433.

97. Meyer RG, Küpper JH, Kandolf R *et al.* Early growth response-1 gene (Egr-1) promoter induction by ionizing radiation in U87 malignant glioma cells in vitro. *European Journal of Biochemistry* 2002, DOI: 10.1046/j.0014-2956.2001.02658.x.
98. Usenius T, Tenhunen M, Koistinaho J. Ionizing radiation induces expression of immediate early genes in the rat brain. *Neuroreport* 1996;**7**:2559–63, DOI: 10.1097/00001756-199611040-00031
99. Kempf SJ, Casciati A, Buratovic S *et al.* The cognitive defects of neonatally irradiated mice are accompanied by changed synaptic plasticity, adult neurogenesis and neuroinflammation. *Molecular neurodegeneration* 2014, DOI: 10.1186/1750-1326-9-57.
100. Kempf SJ, Sepe S, von Toerne C *et al.* Neonatal irradiation leads to persistent proteome alterations involved in synaptic plasticity in the mouse hippocampus and cortex. *Journal of Proteome Research* 2015, DOI: 10.1021/acs.jproteome.5b00564.
101. Achanta P, Thompson KJ, Fuss M *et al.* Gene expression changes in the rodent hippocampus following whole brain irradiation. *Neuroscience Letters* 2007;418:143–8, DOI: 10.1016/j.neulet.2007.03.029
102. Rosi S, Andres-Mach M, Fishman KM *et al.* Cranial irradiation alters the behaviorally induced immediate-early gene Arc (activity-regulated cytoskeleton-associated protein). *Cancer Research* 2008, DOI: 10.1158/0008-5472.CAN-08-1861.
103. Van Loo KMJ, Rummel CK, Pitsch J *et al.* Calcium channel subunit α2σ4 is regulated by early growth response 1 and facilitates epileptogenesis. *Journal of Neuroscience* 2019, DOI: 10.1523/JNEUROSCI.1731-18.2019.
104. Löbrich M, Shibata A, Beucher A *et al.* γH2AX foci analysis for monitoring DNA double-strand break repair: Strengths, limitations and optimization. *Cell Cycle* 2010, DOI: 10.4161/cc.9.4.10764.
105. Corbett BF, You JC, Zhang X *et al.* ΔFosB Regulates Gene Expression and Cognitive Dysfunction in a Mouse Model of Alzheimer's Disease. *Cell Reports* 2017, DOI: 10.1016/j.celrep.2017.06.040.
106. Hendrickx A, Pierrot N, Tasiaux B *et al.* Epigenetic regulations of immediate early genes expression involved in memory formation by the amyloid precursor protein of alzheimer disease. *PLoS ONE* 2014, DOI: 10.1371/journal.pone.0099467.
107. Opsomer R, Contino S, Perrin F *et al.* Amyloid precursor protein (APP) controls the expression of the transcriptional activator neuronal PAS domain protein 4 (NPAS4) and synaptic GABA release. *eNeuro* 2020, DOI: 10.1523/ENEURO.0322-19.2020.
108. Choy FC, Klarić TS, Leong WK *et al.* Reduction of the neuroprotective transcription factor Npas4 results in increased neuronal necrosis, inflammation and brain lesion size following ischaemia. *Journal of Cerebral Blood Flow and Metabolism* 2016, DOI: 10.1177/0271678X15606146.
109. Köster J, Rahmann S. Snakemake-a scalable bioinformatics workflow engine. *Bioinformatics* 2012, DOI: 10.1093/bioinformatics/bts480.
110. Harris CR, Millman KJ, van der Walt SJ *et al.* Array programming with NumPy. *Nature* 2020, DOI: 10.1038/s41586-020-2649-2.
111. Virtanen P, Gommers R, Oliphant TE *et al.* SciPy 1.0: fundamental algorithms for scientific computing in Python. *Nature Methods* 2020, DOI: 10.1038/s41592-019-0686-2.
112. Cullingford TE, Markou T, Fuller SJ *et al.* Temporal regulation of expression of immediate early and second phase transcripts by endothelin-1 in cardiomyocytes. *Genome Biology* 2008, DOI: 10.1186/gb-2008-9-2-r32.
113. Soriano FX, Papadia S, Hofmann F *et al.* Preconditioning doses of NMDA promote neuroprotection by enhancing neuronal excitability. *Journal of Neuroscience* 2006, DOI: 10.1523/JNEUROSCI.0455-06.2006.
114. Amin H, Nieus T, Lonardoni D *et al.* High-resolution bioelectrical imaging of Aβ-induced network dysfunction on CMOS-MEAs for neurotoxicity and rescue studies. *Scientific Reports* 2017, DOI: 10.1038/s41598-017-02635-x.
115. Crowe SL, Movsesyan VA, Jorgensen TJ *et al.* Rapid phosphorylation of histone H2A.X following ionotropic glutamate receptor activation. *European Journal of Neuroscience* 2006, DOI: 10.1111/j.1460-9568.2006.04768.x.
116. Fan MMY, Raymond LA. N-Methyl-d-aspartate (NMDA) receptor function and excitotoxicity in Huntington's disease. *Progress in Neurobiology* 2007, DOI: 10.1016/j.pneurobio.2006.11.003.
117. Zhou Q, Sheng M. NMDA receptors in nervous system diseases. *Neuropharmacology* 2013, DOI: 10.1016/j.neuropharm.2013.03.030.
118. Terunuma M, Vargas KJ, Wilkins ME *et al.* Prolonged activation of NMDA receptors promotes

dephosphorylation and alters postendocytic sorting of GABAB receptors. *Proceedings of the National Academy of Sciences of the United States of America* 2010, DOI: 10.1073/pnas.1000853107.
119. Zhou X, Hollern D, Liao J *et al.* NMDA receptor-mediated excitotoxicity depends on the coactivation of synaptic and extrasynaptic receptors. *Cell Death and Disease* 2013, DOI: 10.1038/cddis.2013.82.
120. Dash PK, Hochner B, Kandel ER. Injection of the cAMP-responsive element into the nucleus of Aplysia sensory neurons blocks long-term facilitation. *Nature* 1990, DOI: 10.1038/345718a0.
121. Kaang BK, Kandel ER, Grant SGN. Activation of cAMP-Responsive genes by stimuli that produce long-term facilitation in aplysia sensory neurons. *Neuron* 1993, DOI: 10.1016/0896-6273(93)90331-K.
122. Kandel ER. The molecular biology of memory storage: A dialogue between genes and synapses. *Science* 2001, DOI: 10.1126/science.1067020.
123. Sakamoto K, Karelina K, Obrietan K. CREB: A multifaceted regulator of neuronal plasticity and protection. *Journal of Neurochemistry* 2011, DOI: 10.1111/j.1471-4159.2010.07080.x.
124. Dong Y, Green T, Saal D *et al.* CREB modulates excitability of nucleus accumbens neurons. *Nature Neuroscience* 2006, DOI: 10.1038/nn1661.
125. Zhou Y, Won J, Karlsson MG *et al.* CREB regulates excitability and the allocation of memory to subsets of neurons in the amygdala. *Nature Neuroscience* 2009, DOI: 10.1038/nn.2405.
126. Caracciolo L, Marosi M, Mazzitelli J *et al.* CREB controls cortical circuit plasticity and functional recovery after stroke. *Nature Communications* 2018, DOI: 10.1038/s41467-018-04445-9.
127. Lee J, Rajakumar N. Role of NR2B-containing N-methyl-D-aspartate receptors in haloperidol-induced c-Fos expression in the striatum and nucleus accumbens. *Neuroscience* 2003, DOI: 10.1016/j.neuroscience.2003.08.019.
128. Endele S, Rosenberger G, Geider K *et al.* Mutations in GRIN2A and GRIN2B encoding regulatory subunits of NMDA receptors cause variable neurodevelopmental phenotypes. *Nature Genetics* 2010, DOI: 10.1038/ng.677.
129. Lemke JR, Hendrickx R, Geider K *et al.* GRIN2B mutations in west syndrome and intellectual disability with focal epilepsy. *Annals of Neurology* 2014, DOI: 10.1002/ana.24073.
130. Sanz-Clemente A, Nicoll RA, Roche KW. Diversity in NMDA receptor composition: Many regulators, many consequences. *Neuroscientist* 2013, DOI: 10.1177/1073858411435129.
131. Mabb AM, Kullmann PHM, Twomey MA *et al.* Topoisomerase 1 inhibition reversibly impairs synaptic function. *Proceedings of the National Academy of Sciences of the United States of America* 2014, DOI: 10.1073/pnas.1413204111.
132. Joo Y, Xue Y, Wang Y *et al.* Topoisomerase 3β knockout mice show transcriptional and behavioural impairments associated with neurogenesis and synaptic plasticity. *Nature Communications* 2020, DOI: 10.1038/s41467-020-16884-4.
133. Lu C, Fu W, Zhao D *et al.* The DNA damaging agent etoposide activates a cell survival pathway involving α-amino-3-hydroxy-5-methylisoxazole-4-propionate receptors and mitogen-activated protein kinases in hippocampal neurons. *Journal of Neuroscience Research* 2002, DOI: 10.1002/jnr.10413.
134. Rajadhyaksha A, Barczak A, Macías W *et al.* L-type Ca2+ channels are essential for glutamate-mediated CREB phosphorylation and c-fos gene expression in striatal neurons. *Journal of Neuroscience* 1999, DOI: 10.1523/jneurosci.19-15-06348.1999.
135. de Campos-Nebel M, Larripa I, González-Cid M. Topoisomerase ii-mediated DNA damage is differently repaired during the cell cycle by non-homologous end joining and homologous recombination. *PLoS ONE* 2010, DOI: 10.1371/journal.pone.0012541.
136. Davis AJ, Chen BPC, Chen DJ. DNA-PK: A dynamic enzyme in a versatile DSB repair pathway. *DNA Repair* 2014, DOI: 10.1016/j.dnarep.2014.02.020.
137. Jette N, Lees-Miller SP. The DNA-dependent protein kinase: A multifunctional protein kinase with roles in DNA double strand break repair and mitosis. *Progress in Biophysics and Molecular Biology* 2015, DOI: 10.1016/j.pbiomolbio.2014.12.003.
138. Greenberg ME, Ziff EB. Stimulation of 3T3 cells induces transcription of the c-fos proto-oncogene. *Nature* 1984, DOI: 10.1038/311433a0.
139. Maya-Vetencourt JF. Activity-dependent NPAS4 expression and the regulation of gene programs underlying plasticity in the central nervous system. *Neural Plasticity* 2013, DOI: 10.1155/2013/683909.
140. Martin M, Pinton P, Crechet F *et al.* Preferential Induction of c-fos versus c-jun Protooncogene

during the Immediate Early Response of Pig Skin to γ-Rays. *Cancer Research* 1993.
141. Deloch L, Rückert M, Fietkau R *et al.* Low-dose radiotherapy has no harmful effects on key cells of healthy non-inflamed joints. *International Journal of Molecular Sciences* 2018, DOI: 10.3390/ijms19103197.
142. Tseng BP, Giedzinski E, Izadi A *et al.* Functional consequences of radiation-induced oxidative stress in cultured neural stem cells and the brain exposed to charged particle irradiation. *Antioxidants and Redox Signaling* 2014, DOI: 10.1089/ars.2012.5134.
143. Acharya MM, Patel NH, Craver BM *et al.* Consequences of low dose ionizing radiation exposure on the hippocampal microenvironment. *PLoS ONE* 2015, DOI: 10.1371/journal.pone.0128316.
144. Vollmann H, Wölfel S, Ohneseit P *et al.* Differential expression of Egr1 and activation of microglia following irradiation in the rat brain. *Strahlentherapie und Onkologie* 2007, DOI: 10.1007/s00066-007-1664-7.
145. Ginty DD, Bonni A, Greenberg ME. Nerve growth factor activates a Ras-dependent protein kinase that stimulates c-fos transcription via phosphorylation of CREB. *Cell* 1994, DOI: 10.1016/0092-8674(94)90055-8.
146. Sassone-Corsi P, Visvader J, Ferland L *et al.* Induction of proto-oncogene fos transcription through the adenylate cyclase pathway: characterization of a cAMP-responsive element. *Genes & development* 1988, DOI: 10.1101/gad.2.12a.1529.
147. Mayer SI, Willars GB, Nishida E *et al.* Elk-1, CREB, and MKP-1 regulate Egr-1 expression in gonadotropin-releasing hormone stimulated gonadotrophs. *Journal of Cellular Biochemistry* 2008, DOI: 10.1002/jcb.21927.
148. Bauer I, Hohl M, Al-Sarraj A *et al.* Transcriptional activation of the Egr-1 gene mediated by tetradecanoylphorbol acetate and extracellular signal-regulated protein kinase. *Archives of Biochemistry and Biophysics* 2005, DOI: 10.1016/j.abb.2005.03.016.
149. Kim JS, Yang M, Cho J *et al.* Promotion of cAMP responsive element-binding protein activity ameliorates radiation-induced suppression of hippocampal neurogenesis in adult mice. *Toxicological Research* 2013, DOI: 10.5487/TR.2010.26.3.177.
150. Yassin L, Benedetti BL, Jouhanneau JS *et al.* An Embedded Subnetwork of Highly Active Neurons in the Neocortex. *Neuron* 2010, DOI: 10.1016/j.neuron.2010.11.029.
151. Tolliver JM, Pellmar TC. Ionizing radiation alters neuronal excitability in hippocampal slices of the guinea pig. *Radiation Research* 1987, DOI: 10.2307/3577107.
152. Bassant MH, Court L. Effects of whole-body γ irradiation on the activity of rabbit hippocampal neurons. *Radiation Research* 1978, DOI: 10.2307/3574846.
153. Pellmar TC, Tolliver JM, Neel KL. Radiation-induced impairment of neuronal excitability. *Fundamental and applied toxicology : official journal of the Society of Toxicology* 1988.
154. Tian F, Hu XZ, Wu X *et al.* Dynamic chromatin remodeling events in hippocampal neurons are associated with NMDA receptor-mediated activation of Bdnf gene promoter 1. *Journal of Neurochemistry* 2009, DOI: 10.1111/j.1471-4159.2009.06058.x.

12. Figure and Table directory

List of Abbreviations

53BP1	**p53-binding protein 1**
ABD	**Agonist binding domain**
ADP	**Adenosine diphosphate**
AID	**Activation-induced cytidine deaminase**
AMPA	**α-amino-3-hydroxy-5-methyl-4-isoxazolepropionic acid**
AMPAR	**α-amino-3-hydroxy-5-methyl-4-isoxazole propionic acid receptor**
AP-1	**Activator protein 1**
APLF	**Aprataxin-and-PNK-like factor**
ARC	**Activity regulated cytoskeleton**
ATD	**Amino-terminal domain**
ATM	**Ataxia-telangiectasia mutated**
ATP	**Adenosine triphosphate**
BCA	**Bicinchoninic acid assay**
BDNF	**Brain-derived neurotrophic factor**
BRCA2	**Breast cancer type 2**
C2H2	**Cysteine2-Histidine2**
CaMK	**Calmodulin-dependent protein kinase**
cAMP	**Cyclic adenosine monophosphate**
CBP	**CREB-binding protein**
c-NHEJ	**Classical- non-homologous end joining**
CNS	**Central nervous system**
CREB	**cAMP response element-binding protein**
CSR	**Class switch recombination**

CTD	**Carboxyl-terminal domain**
DAPI	**4′,6-diamidino-2-phenylindole**
DEPC	**Diethyl pyrocarbonate**
DIV	**Days-in-vitro**
DMSO	**Dimethyl sulfoxide**
DNA	**Deoxyribonucleic acid**
DNA-PK	**DNA-dependent protein kinase**
DNA-PK$_{cs}$	**DNA-dependent protein kinase catalytic subunit**
DSB	**Double-strand break**
DTT	**Dithiothreitol**
EDTA	**Ethylenediaminetetraacetic acid**
EGR-1	**Early growth response-1**
EGTA	**Ethylene glycol-bis (β-aminoethyl ether)-N, N, N′, N′-tetraacetic acid**
ELK-1	**ETS Like-1 protein**
EPSP	**Excitatory postsynaptic potential**
ERK	**Extracellular signal-regulated kinases**
FBS	**Fetal bovine serum**
FU	**Fluorouracil**
GABA	**Gamma-aminobutyric acid**
GAPDH	**Glyceraldehyde 3-phosphate dehydrogenase**
Gly	**Glycine**
GluR6	**Glutamate receptor 6**
GS	**Goat serum**
HBSS	**Hank's buffered saline solution**
HCs	**Hippocampal cultures**

HD	**Huntington disease**
HDAC2	**Histone deacetylase 2**
HEPES	**4-(2-hydroxyethyl)-1-piperazineethanesulfonic acid**
HR	**Homologous recombination**
HRP	**Horseradish peroxidase**
ICRF-193	**meso-4,4-(2,3-butanediyl)-bis(2,6-piperazinedione)**
IEGs	**Immediate early genes**
Ifenprodil	**4-[2-(4-benzylpiperidin-1-yl)-1-hydroxypropyl]phenol**
IR	**Ionizing radiation**
JNK	**c-jun N-terminal kinase**
kDa	**Kilo Dalton**
KG-501	**2-naphthol-AS-E-phosphate**
LTD	**Long-term depression**
LTP	**Long-term potentiation**
MAP-2	**Microtubule-associated protein 2**
MAPK	**Mitogen-activated protein kinase**
MEA	**Microelectrode array**
mEPSC	**Miniature excitatory postsynaptic currents**
Min	**Minute**
MK801	**5R,10S)-(+)-5-methyl-10,11-dihydro-5H-dibenzo[a,d]cyclohepten-5,10-imine**
MMR	**Mismatch repair**
MRN	**Mre11-Rad50-Nbs1**
mRNA	**Messenger ribonucleic acid**
NeuN	**Neuronal nuclei**
NF	**Neurofilament**

NMDA	**N-Methyl-D-aspartate**
NMDAR	**N-Methyl-D-aspartate-receptor**
NPAS4	**Neuronal PAS domain protein 4**
NU7441	**8-(4-Dibenzothienyl)-2-(4-morpholinyl)-4H-1-benzopyran-4-one**
PARP	**Poly(ADPribose)polymerase**
PBS	**Phosphate-buffered saline**
Pen-Strep	**Penicillin-Streptomycin**
PK	**Protein kinase**
PP1	**Protein phosphatase 1**
PSD-95	**Postsynaptic density 95**
PVDF	**Polyvinylidene difluoride**
qPCR	**Quantitative polymerase chain reaction**
qRT-PCR	**Quantitative reverse-transcription polymerase chain reaction**
RAG	**Recombination activating genes**
RIF1	**Rap1-interacting factor 1**
RIPA	**Radio immunoprecipitation assay**
RNAPII	**RNA polymerase II**
RNS	**Reactive nitrogen species**
ROS	**Reactive oxygen species**
SCID	**Severe combined immunodeficiency**
SDS	**Sodium dodecyl sulfate**
Ser	**Serine**
SHM	**Somatic hypermutation**
siRNA	**Small interfering RNA**
SRF	**Serum response factor**

TBS	**Tris-buffered saline**
TMD	**Transmembrane domain**
TopI	**Topoisomerase I**
Top2 or Top II	**Topoisomerase II**
Top2cc	**Topoisomerase II cleavage complex**
Top2β	**Type 2 topoisomerase alpha**
Top2β	**Type 2 topoisomerase beta**
Tyr	**Tyrosine**
WT	**Wild type**
WT1	**Wilms' tumor 1**
XLF	**XRCC4-like factor**
XRCCP4	**X-ray cross-complementing protein 4**

Acknowledgment

First, I would like to thank my supervisor Prof. Dr. Laube, who gave me this exciting opportunity to work in his lab. I am very grateful that he guided me throughout my whole project, believed in my abilities and was humbly patient in results discussion and manuscript writing. Further, I am so thankful that he gave me the freedom as a researcher that helped me in my overall growth. Other than Prof. Dr. Laube, I am also grateful that I had the chance to present my work and take the guidance of Prof. Dr. Loewer and Dr. Alexander Rapp. Without their effective feedback and suggestions, this thesis would not have been reached its endpoint. I would also like to thank all the professors and students that were part of my GRK-1657 meetings. The suggestions and bits of advice provided in these meetings helped me go the extra mile for my Ph.D. project. I would also like to thanks Prof. Scherthan, who gave the idea of using SCID mice in the experiments and gave a new dimension to my thesis.

I would also like to express my sincere gratitude to all lab members who helped me directly and indirectly throughout my journey (Alex, Basti, Henrik, Axel, Michi, Kirsten, Gabi, Nina, Kai, Katja, Kiki). My special thanks go to Dr. Max Bernhard and Alexander Bausch. They guided me throughout my experiments and were so kind and patient enough to comment and help me edit my thesis. Without them, I still would have been lost many times in the writing of my thesis. I also would like to mention my sincere gratitude toward all the Bachelor students I assisted throughout my Ph.D. journey. The experiments done by them helped to move the pace of the thesis faster.

I want to mention the name of my Mom- Balbir kaur, who has always been the pillar of my strength, and without her blessing, I would not have even thought of starting my scientific journey. Then comes my whole family, who always had my back no matter how good or bad the days were or will be. Special thanks go to my brother Karan, who made sure that I smile during the challenging part of my Ph.D. journey.

I would also like to thanks my old friend- Aman Tannk, who always supported me and made sure that I do my best in life. Then, I would present my gratitude to Jan Wissmann, who helped in my MEA analysis and spent many hours discussing the project. Thank you, Jan, for guiding my assignment in the right direction and having an endless discussion about the thesis results.

I would also like to present my thanks to my partner Paul Trautmann, who might have met me in the last part of my journey, but I wrote my thesis in a calm mind because of his support. Furthermore, I would like to thank his parents, who provided fantastic food over the weekend and gave me moral and relaxing support to finish my thesis.

In the end, I would also like to thank the universe who made sure that I am present at the right time and at the right moment to make the miracles happen in my life.

So, overall thank you to all of you, and I apologize if I would have missed some names.

Curriculum vitae

Rajvinder Kaur

Palisadenstraße 64

64297 Darmstadt, Germany

Born on 22 January 1992 in India

EDUCATION	
Technical University, Darmstadt 04/2017-09/2021	• Ph.D. in Radiation biology and Neuroscience (Neurophysiology and Neurosensory systems lab, Prof. Dr. Laube, TU, Darmstadt, Germany). Scholarship in the DFG funded Graduate school (GRK 1657) "Molecular and cellular responses of ionizing radiation" (2017-2020)
Friedrich Schiller University, Jena 10/2013-12/2015	• Master in Molecular medicine • Thesis in the Department of Human Genetics: Expression of Prdm12 in sensory neurons and influence on neurite outgrowth.
Panjab University, Chandigarh (India) 04/2009-04/2012	• Bachelor's degree- Biotechnology (Hons.) • Bachelor Thesis in the Department of Plant Biotechnology: Allelochemical effect of aqueous extract of Tinospora cordifolia on in vitro mustard seed germination.
SCIENTIFIC ACTIVITIES	
Poster presentations	• Poster presentation of Ph.D. work at Society for Neuroscience Conference, Chicago 2019; and Gesellschaft fur Biologische Strahlenforschung meeting, Frankfurt, 2018.
Summer School, MPI, Cell Biology, Dresden 08/2019-09/2019	• Mouse Genome Engineering courses Self-designed the CRISPR plasmids for the Ph.D. project with the help of various academic experts in the field.
Summer School, University of Stockholm, Sweden, 04/2018-05/2018	• Introduction to Radiation biology course Hand-on-training in detecting cellular responses to high and low dose radiation effect